UNIVERSITAT DE BARCELONA

Unveiling the role of DXS-Interacting (DXI) proteins in the regulation of plastidial isoprenoid biosynthesis

Ernesto Llamas Pámanes

Aquesta tesi doctoral està subjecta a la llicència ***Reconeixement 3.0. Espanya de Creative Commons***.

Esta tesis doctoral está sujeta a la licencia ***Reconocimiento 3.0. España de Creative Commons***.

This doctoral thesis is licensed under the ***Creative Commons Attribution 3.0. Spain License***.

Unveling the role of DXS-Interacting (DXI) proteins in the regulation of plastidial isoprenoid biosynthesis

ERNESTO LLAMAS PAMANES

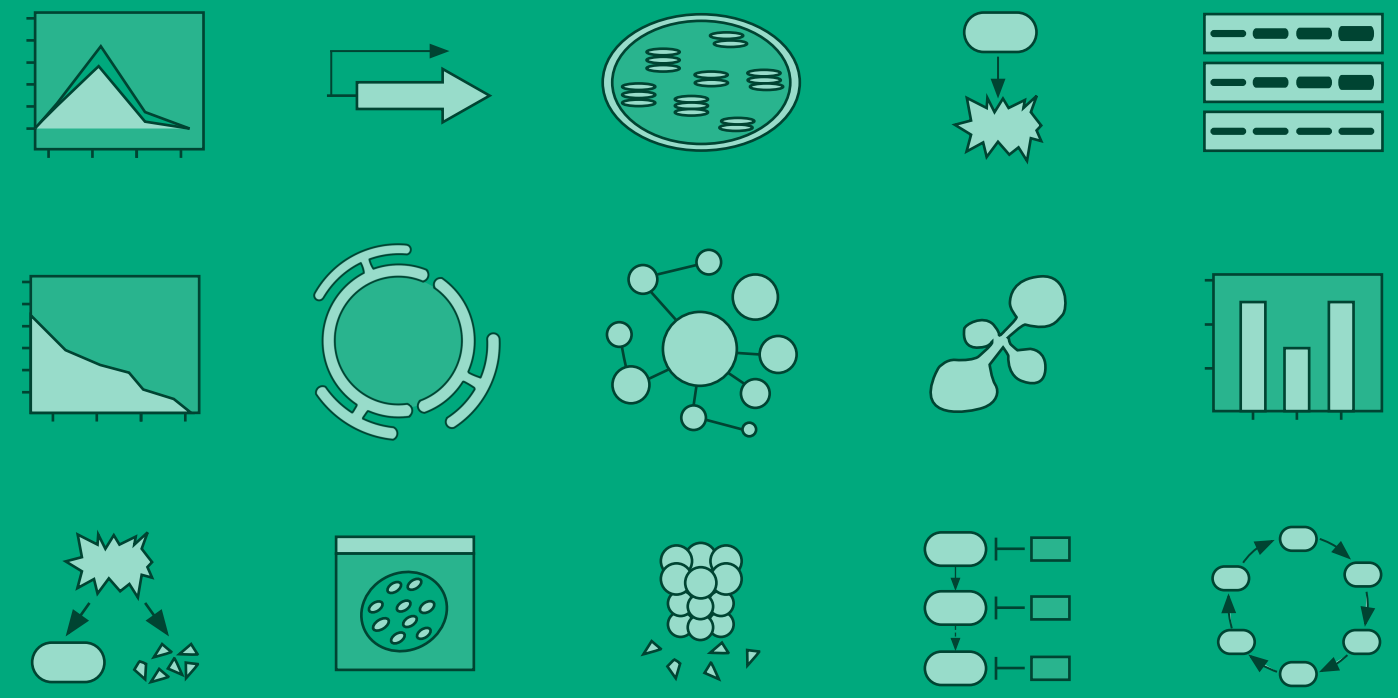

2017

UNIVERSITAT DE BARCELONA

UNIVERSITAT DE BARCELONA

FACULTAT DE FARMÀCIA I CIÈNCIES DE L'ALIMENTACIÒ

Unveiling the role of DXS-Interacting (DXI) proteins in the regulation of plastidial isoprenoid biosynthesis

ERNESTO LLAMAS PÁMANES

2017

UNIVERSITAT DE BARCELONA

FACULTAT DE FARMÀCIA I CIÈNCIES DE L'ALIMENTACIÒ

PROGRAMA DE DOCTORAT DE BIOTECNOLOGIA

Unveiling the role of DXS-Interacting (DXI) proteins in the regulation of plastidial isoprenoid biosynthesis

Memòria presentada per Ernesto Llamas Pámanes per optar al títol de doctor per la Universitat de Barcelona

Dr. Manuel Rodríguez Concepción
Director de la tesi

Ernesto Llamas Pámanes
Doctorand

Dr. Albert Ferrer Prats
Tutor

Ernesto Llamas Pámanes (2017)

Agradecimientos

La realización de esta tesis no hubiera sido posible sin en el apoyo de mi familia. A mi esposa Gabriela le agradezco el apoyo durante estos años, ambos hemos crecido profesional y personalmente. A mis padres, Ernesto y Patricia que sin su apoyo e inspiración esta logro no se hubiera cumplido. A mis hermanos Erick y Ricardo que a pesar de la distancia y de seguir distintos caminos, estamos unidos. Hacer un doctorado lejos de tus seres queridos es un gran sacrificio por ello, esta tesis va dedicada a mi familia. Mis logros son sus logros.

Al Dr. Manuel Rodríguez Concepción que me brindó la oportunidad de realizar esta tesis en su laboratorio. Gracias por su dirección, consejos y enseñanzas. Manuel ha sido un pilar importante en mi formación científica.

Estoy muy agradecido con todos los miembros del laboratorio 2.01. A Rosa por su constante apoyo personal y científico. A Pablo Pulido por su supervisión durante los primeros meses de la tesis. A Catalina Perelló, Águila Ruiz, Jordi Perez, Briardo Llorente, Miriam Ortiz, Lucio D'Andrea, Victoria Barja, David Manzano, Julia Emiliani, Miguel Simón, Sofía Hernández, Salvador Torres y a todas las personas que llegaron a formar parte del lab 2.01. También agradezco a todos mis amigos de otros laboratorios del CRAG. Todos ustedes son mi familia de Barcelona. Gracias por su ayuda y apoyo, han hecho de este período una experiencia increíble y divertida.

Gracias a todo el personal científico, de soporte y administrativo del CRAG, que también han contribuido enormemente al desarrollo de esta tesis.

Agradezco al Consejo Nacional de Ciencia y Tecnología (CONACyT) por la beca al extranjero que permitió mi estancia en Barcelona y a la Secretaría de Educación Pública (SEP) por la beca complemento.


Before PhD
2014
2015
2016
2017
Gabriela Hernández
Ernesto Llamas
Patricia Pámanes
Erick Llamas
Ricardo Llamas
Manuel Rodríguez
Catalina Perelló
Miriam Ortiz
Águila Ruiz
Pablo Pulido
Rosa Rodríguez
Briardo Llorente
Jordi Perez
Lucio D'Andrea
Victoria Barja
David Manzano
Julia Emiliani
Miguel Simón
Sofía Hernández
Salvador Torres

Summary

Chloroplasts provide plants with metabolic pathways that are unique among eukaroytes, including the methylerythritol 4-phosphate pathway (MEP) for the production of isoprenoids essential for photosynthesis and plant growth. The first reaction of the MEP pathway involves the synthesis of deoxyxylulose 5-phosphate (DXP) from the central metabolic intermediates glyceraldehyde 3-phosphate (GAP) and pyruvate catalyzed by DXP synthase (DXS). DXS has a major role in regulating the MEP pathway flux, but little is known about how its levels and activity are regulated. It has been shown that DXS stability and enzymatic activity can be modulated by interaction with other plastidial DXS-interacting (DXI) proteins. The goal of this thesis work has been to characterize the physiological role of DXS-DXI interactions and the molecular pathways leading from the interactions to the eventual biological effects in the model plant *Arabidopsis thaliana*.

To investigate whether loss of DXI function in mutants impacted DXS activity, we analyzed their resistance to clomazone (CLM), a DXS-specific inhibitor. Most of the loss-of-function mutants tested did not show resistance or sensitivity to this inhibitor. However, two mutant alleles for the gene *SBP*, which encodes the Calvin cycle enzyme sedoheptulose 1,7-bisphosphatase (SBPase), showed an increased resistance to CLM. In contrast, overproduction of SBPase in transgenic Arabidopsis plants resulted in reduced CLM resistance. Strikingly, we found that DXS protein levels or activity did not change when SBPase levels are altered in plants. Although co-immunoprecipitation assays were unable to confirm the interaction DXS-SBPase, our results do show a functional relationship between the Calvin cycle and the MEP pathway. We propose that excess GAP in the *sbp* mutant is diverted into the MEP pathway, preventing CLM binding to DXS.

The second part of the thesis continued previous work with DXI1, a DXS-interacting J-protein that facilitates the recognition of inactive DXS forms to deliver them to eventual reactivation or degradation pathways. In particular, we focused on investigating the molecular components involved in these two opposite pathways. By bioinformatic and experimental approaches, we confirmed that DXS is prone to aggregate in the chloroplast and associate to insoluble (membrane) fractions in an inactive form. These inactive forms of the enzyme were found to overaccumulate in plants defective in DXI1 (renamed J20). J20 is an adaptor of the Hsp70 chaperone. We demonstrated that the DXS-Hsp70 complex interacts with the Hsp100/ClpC1

chaperone to unfold DXS for delivery into the proteolytic chamber of the Clp proteolytic complex. On the other hand, correct folding of DXS is achieved with the contribution of Hsp100/ClpB3.

Our work suggests that degradation or activation of DXS might depend mostly on changes in ClpB3 levels. This disaggregase accumulates when the MEP pathway flux is decreased and in situations causing protein folding stress. Through molecular, genetic and pharmacological approaches, we demonstrated that this accumulation depends on a mechanism called chloroplast Unfolded Protein Response (cpUPR). Elicitation of this cpUPR by inhibition of protein synthesis in the chloroplast led to increased expression of nuclear genes encoding ClpB3 and other chloroplast chaperones, eventually causing a stress acclimation response. We further demonstrated that cpUPR is independent of GUN1, an integrator of retrograde signaling, since we observed that chaperones accumulate in both wild-type and *gun1* mutant plants. However, GUN1-defective plants were unable to develop the acclimation response. Our data therefore confirm that GUN1 is a central integrator of different pathways controlling chloroplast protein homeostasis beyond the control of nuclear gene expression.

Our results will contribute to taking more informed decisions on future approaches to manipulate levels of chloroplast isoprenoids of interest (such as vitamins, biofuels or drugs against cancer and malaria) in crop plants.

Resumen

Los cloroplastos tienen vías metabólicas únicas entre los eucariontes, incluyendo la vía del metileritritol 4-fosfato (vía MEP) para la producción de isoprenoides. La primera reacción de la vía MEP es la síntesis de desoxixilulosa 5-fosfato (DXP) a partir de gliceraldehído 3-fostato (GAP) y piruvato, catalizada por la enzima DXP sintasa (DXS). DXS tiene un papel central en regular el flujo de la vía MEP, pero aún se sabe relativamente poco acerca de cómo se regulan sus niveles y actividad enzimática. En esta tesis se ha estudiado cómo la interacción de DXS con otras proteínas regula su función en *Arabidopsis thaliana*. De entre estas proteínas interactoras, solo la pérdida de función de la enzima sedoheptulosa 1,7-bifosfatasa generó un fenotipo de resistencia a la inhibición de DXS. Los resultados de la tesis permiten concluir que existe un vínculo funcional entre el ciclo de Calvin y la vía MEP, seguramente mediado por la disponibilidad de GAP. Por otro lado, se ha observado que DXS es un enzima propenso a agregarse. Estas formas inactivas interaccionan con la proteína J20, un adaptador de la chaperona Hsp70. El complejo DXS-Hsp70 a su vez interactúa con ClpC1 para degradar DXS mediante la proteasa Clp. Por otro lado, la interacción del complejo con ClpB3 pliega correctamente y activa DXS. El destino de DXS podría depender mayoritariamente de los cambios en los niveles de ClpB3. Un menor flujo de vía MEP, la pérdida de la homeostasis proteica en el cloroplasto, o la expresión defectuosa del plastoma causan la acumulación de ClpB3 y de otras chaperonas mediante la activación de la expresión de los correspondientes genes nucleares. Esta respuesta no requiere de la actividad de GUN1, un nodo central en la comunicación cloroplasto-núcleo. Sin embargo, GUN1 es esencial para la posterior respuesta de aclimatación que permite a las plantas soportar mejor otros tipos de estrés como los causados por la inhibición de la síntesis de isoprenoides. Nuestros resultados pueden contribuir a tomar decisiones más informadas para manipular los niveles de isoprenoides cloroplastídicos de interés (como vitaminas, biocombustibles o fármacos contra el cáncer y la malaria) en plantas de cultivo.

Contents

List of Figures

List of Tables

List of Abbreviations

CAP	Chloramphenicol
CHL	Chlorophyll
CHX	Ciclohexamide
PQC	Protein Quality Control
Clp	Caseinolytic protease
cpUPR	chloroplast Unfolded Protein Response
CLM	Clomazone
KCLM	Keto-clomazone
co-IP	co-immunoprecipitation
DMAPP	Dimethylallyl diphosphate
DXI	DXS-interacting
GAP	Glyceraldehyde 3-phosphate
IPP	Isopentenyl diphosphate
MEP	Methylerythritol 4-phosphate
MEcPP	Methylerythritol 2,4-cyclodiphosphate
NFZ	Norflurazone
LIN	Lincomycin
RuP	Ribulose 5-phospahte
RuBP	Ribulose 1,5-biphosphate
RIF	Resistant to FSM
SBPase	Sedoheptulose-1,7-bisphosphatase
SE	Seedling establishment
UPR	Unfolded Protein Response

1. Introduction

Chloroplasts are cellular organelles found in plants that perform photosynthesis. Remarkably, photosynthesis is the most important process associated with plant life as it converts sunlight energy, captured by the pigment-containing light-harvesting antenna, into chemical energy that ultimately sustains plant growth. Besides performing photosynthesis chloroplasts are major chemical factories, synthesizing amino acids and lipids such as isoprenoids that provide plant cells with unique metabolites found in no other eukaryotic cells (Sakamoto et al., 2008).

In mature leaf cells, chloroplasts are usually lens-shaped, 5-10 μm in diameter and 2-4 μm in thickness. Each leaf cell typically contains 20 to 100 chloroplasts (Mullet, 1988; Lopez-Juez and Pyke, 2005). Chloroplasts and all other plastid types are surrounded by two membranes, the outer and the inner envelope membranes (Figure 1.1). In addition, chloroplasts have grana, which are stacks of thylakoid membranes where the photosystems (PSI and PSII) and the rest of the photosynthetic machinery is located. Also, lipoprotein particles called plastoglobules are associated with the thylakoid membranes (Brehelin et al., 2007). Thus, chloroplasts have three membrane systems and three aqueous compartments: the intermembrane space (between two envelopes), the stroma (surrounded by the inner envelope), and the thylakoid lumen (surrounded by thylakoid membrane) (Figure 1.1) (Sakamoto et al., 2008).

Chloroplasts are descendants of serial endosymbiotic events. They arose around 1-1.5 billion years ago from a cyanobacterial ancestor engulfed by a eukaryote in which mitochondria (originally αproteobacteria that had been engulfed and enslaved by a primitive eukaryotic host) had already been established. Most of the bacterial genes were transferred to the nuclear genome or lost, but modern organelles nevertheless retain metabolic activities, genetic mechanisms, and protein transport complexes that clearly reflect their prokaryotic origins (Reyes-Prieto et al., 2007; Cavalier-Smith, 2004).

Chloroplasts are a type of plastid, a term originated from the organelle's plasticity to activate or inactivate particular functions and adjust to the requirements of specialized tissues (Sakamoto et al., 2008). In vascular plants, all plastids are derived from small, non-green proplastids in meristematic cells. Proplastids normally originate maternally during the formation of plant zygotes, and are transmitted from

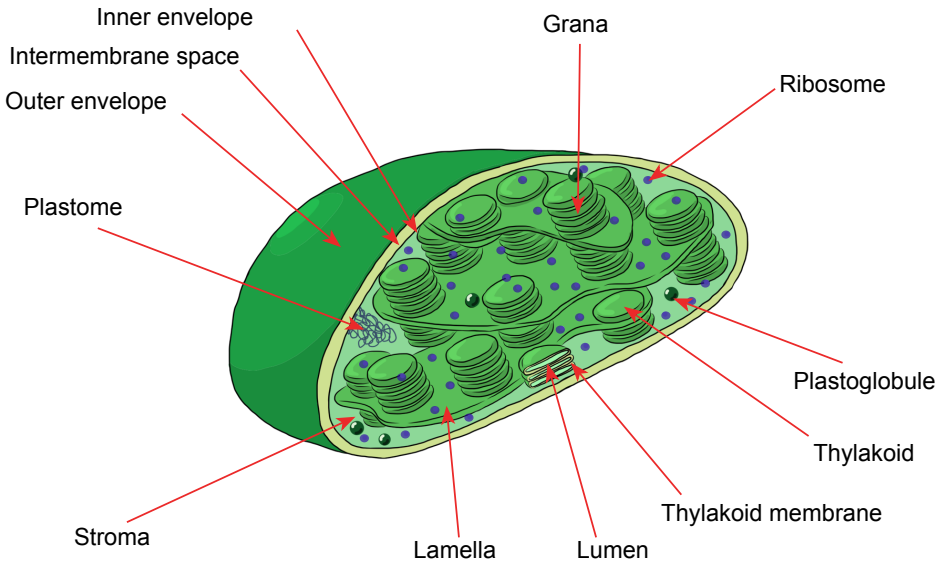

Figure 1.1: Chloroplast ultrastructure. Schematic representation of a chloroplast and its different structures.

generation to generation (Mullet, 1988; Lopez-Juez and Pyke, 2005). They then differentiate into diverse types of plastid depending on the functions which are needed in specific tissues (Sakamoto et al., 2008; Lopez-Juez and Pyke, 2005). Among the non-photosynthetic plastids, chromoplasts have been best studied due to their capacity to store massive levels of health-promoting carotenoid pigments in flowers and fruit tissues (Ruiz-Sola and Rodriguez-Concepcion, 2012; Cazzonelli and Pogson, 2010; Lu and Li, 2008). Other plastids specialized in the accumulation of particular groups of metabolites are elaioplasts (which store lipids to fuel seed germination) and amyloplasts (which accumulate starch in storage organs such as tubers). In plants germinated and grown in the dark, etioplasts are formed before chloroplasts differentiate as seedlings perceive the light and embark in a photosynthetic lifestyle (Sakamoto et al., 2008).

1.1 The chloroplast proteome

The vast majority of the *ca.* 3000 proteins required for normal chloroplast functions are encoded by the nuclear genome. However, some proteins are still encoded by the remnant genome found in present-day chloroplasts.

1.1.1 The plastid genome

In the model plant *Arabidopsis thaliana*, the plastid genome or plastome consists of a circular DNA of 154 kb in length and contains 45 RNA-coding genes and 87 protein-coding genes. The functional plastid gene products are principally involved in: transcription (RNA polymerase), translation (ribosomal and transfer RNAs, ribosomal proteins), photosynthetic electron transfer (subunits of PSI, PSII, the cytochrome b_6f complex and NAD(P)H dehydrogenase [NDH]), and photosynthetic metabolism (subunits of ATP synthase and RubisCO). Additionally, two photosynthesis-unrelated housekeeping genes, *accD* and *clpP1*, encode subunits of acetyl-CoA carboxylase and the Clp (Caseinolytic protease) protease, respectively (Sakamoto et al., 2008).

1.1.2 Chloroplast gene expression

Despite more than a billion years of separate evolution, the gene expression machinery of plastids still shares substantial similarities with its cyanobacterial ancestor, but it has also acquired some novel organelle-specific features, components, and regulatory mechanisms (Tiller and Bock, 2014). Plastome-encoded genes are transcribed by two types of RNA polymerases, both of which are necessary for the biogenesis of photosynthetically active chloroplasts (Allison et al., 1996; Swiatecka-Hagenbruch et al., 2008). The plastome itself encodes a bacterial-type multi-subunit RNA polymerase (plastid-encoded RNA polymerase, PEP) that requires nucleus-encoded sigma factors to facilitate promoter recognition. Additionally, a single subunit of a nucleus-encoded RNA polymerase (NEP) related to the RNA-synthesizing enzymes of T-type bacteriophages and mitochondria is present in plastids (Hedtke et al., 2002).

Primary transcripts produced by both polymerases are usually polycistronic and undergo extensive post-transcriptional processing steps, including intron removal by splicing, processing of primary polycistronic RNA molecules into mature monocistronic or oligocistronic mRNAs, trimming of the 5′ and 3′ ends, and RNA editing (Stern et al., 2010; Barkan, 2011). Members of the RNA-binding pentatricopeptide repeat protein (PPR) family have been shown to play crucial roles in many of these post-transcriptional processes (Schmitz-Linneweber and Small, 2008).

1.1.3 Chloroplast translation

Translation in chloroplasts relies on bacterial-type 70S ribosomes utilizing a set of tRNAs that is entirely encoded in the plastid genome. These chloroplast ribosomes consist of two multi-component subunits: the large (50S) and the small (30S) ribosomal subunit. Both subunits are ribonucleoprotein complexes comprising one or

more ribosomal RNA species (rRNAs) and many proteins. The chloroplast 30S ribosomal subunit comprises a total of 24 proteins of which 21 are orthologs of *Escherichia coli* 30S ribosomal proteins (S1-S21), and three are unique to chloroplast ribosomes (PSPR2, PSRP3, PSRP4). In the 50S subunit, 31 out of 33 ribosomal proteins have orthologs in *E. coli* (L1-L6, L9-L24, L27-L29, and L31-L36) and two proteins are specific to chloroplasts (PSRP5 and PSRP6) (Tiller and Bock, 2014).

Chloroplast translation can be blocked by several inhibitors. Lincomycin (LIN) and erythromycin specifically block translation in the chloroplast without any direct effects on cytoplasmic or mitochondrial protein synthesis. LIN prevents elongation of short peptide chains by inhibiting peptidyl transferase and erythromycin inhibits translocation of the ribosome. On the other hand, streptomycin inhibits chloroplast protein synthesis, but cytosolic protein synthesis is also inhibited. Chloramphenicol (CAP), inhibits both plastid and mitochondrial protein synthesis (Mulo et al., 2003). At high enough concentrations, these inhibitors completely block chloroplast development.

1.1.4 Chloroplast protein import

Typically, nucleus-encoded chloroplast proteins are synthesized in a precursor form having an amino-terminal targeting signal called a transit peptide. These precursors, or preproteins, are transported into the chloroplast post-translationally (in an unfolded state), in an energy-consuming process (Figure 1.2). Import is mediated by hetero-oligomeric protein complexes in the outer and inner envelope membranes; these complexes are termed, respectively, TOC and TIC (Translocon at the Outer/Inner envelope membrane of Chloroplasts) (Figure 1.2). The import system is comprised by multiple preprotein receptors that project large domains into the cytosol. ATP hydrolysis powers the channel components in the outer and inner membranes. The core elements of the TOC complexes are Toc159, Toc34, and Toc75. The first two are receptor components that mediate transit peptide recognition via their cytosolically oriented GTPase domains, while Toc75 forms a barrel channel for preprotein conductance. On the other hand, Tic110 and Tic40 are critical components of the TIC apparatus. Molecular chaperones (some of them discussed in section 1.2.1) participate throughout the process of chloroplast protein import, performing a diversity of roles that include guidance, maintenance of basic competence for transport, and provision of an import driving force (Flores-Perez and Jarvis, 2013).

1.2 Protein Quality Control in chloroplasts

Once a preprotein arrives in the chloroplast interior (the stroma), the transit peptide is removed and the mature unfolded protein adopts its functional (*i.e.* correctly

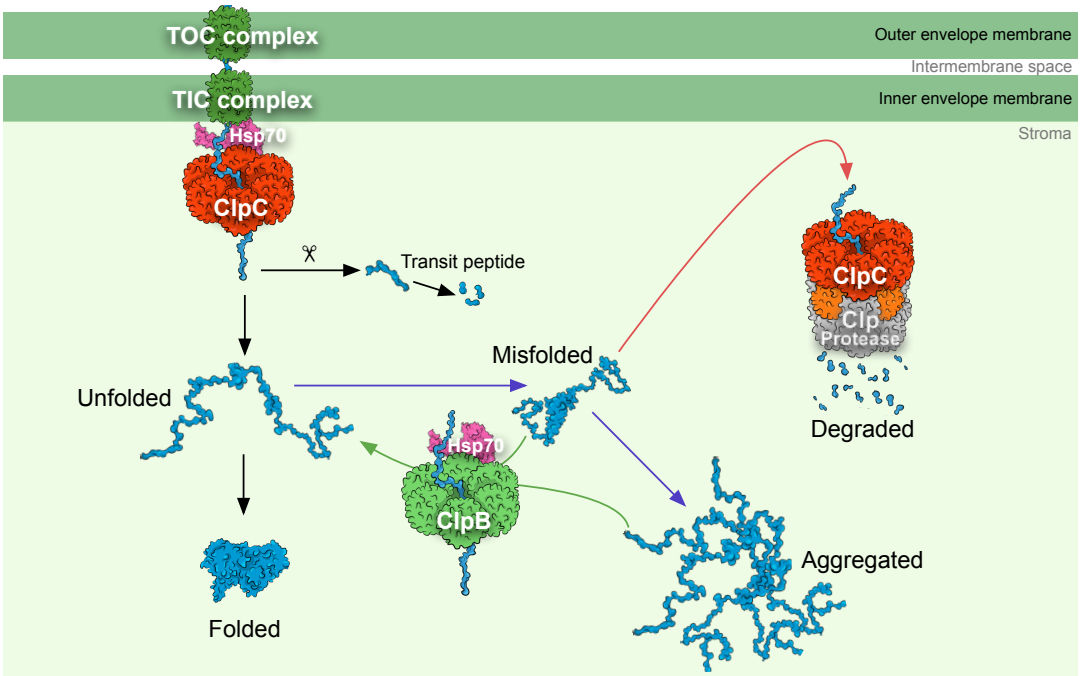

Figure 1.2: Chloroplast protein import and quality control systems. Preproteins are imported in an unfolded state to the chloroplast through TOC and TIC complexes and then the transit peptide is removed. Unfolded proteins tend to acquire its active/folded conformation spontaneously. Misfolded proteins, many of which can form toxic protein aggregates, are refolded or degraded by the indicated components of the protein quality control system.

folded) conformation (Figure 1.2) or engage one of the several internal sorting pathways if its final location is not the stroma (Flores-Perez and Jarvis, 2013). However, protein misfolding is an inevitable process affecting both imported and plastome-encoded proteins that can be aggravated by environmental stresses, such as heat shock. When misfolded, proteins tend to aggregate and become insoluble, eventually forming toxic aggregates (Figure 1.2). In response to this problem, protein quality control (PQC) systems composed of molecular chaperones and proteases have evolved to remove protein aggregates and either refold or eliminate misfolded proteins to maintain protein homeostasis (Figure 1.2). Several groups of prokaryotic-like chaperones (such as Hsp70 and Hsp100) and protease systems (including Clp, Lon, Deg, and FstH) are found in chloroplasts, but their specific targets and PQC-related roles remain little studied (Boston et al., 1996; Kato and Sakamoto, 2010; Nordhues et al., 2010; Nishimura et al., 2016)

1.2.1 Chloroplast chaperones

Molecular chaperones guide almost all cellular proteins through their life cycle. They (1) protect the nascent chains from the crowded cellular environment as they emerge from the ribosome; (2) help folding multidomain proteins to their native state and mediate assembly and disassembly of protein complexes; (3) facilitate protein transport across membranes; (4) participate in disassembling protein aggregates

and folding denatured and misfolded proteins back to their native state; and (5) unfold proteins prior to their proteolytic degradation (Nordhues et al., 2010).

Although chaperones are frequently referred to as heat shock proteins (Hsp), some of them are not induced by stress as they carry essential housekeeping functions under all growth conditions, as indicated above (Nordhues et al., 2010). In chloroplasts, several families of chaperones with a potential role on PQC are found. They include the following (eukaryotic/*E. coli* nomenclature): Hsp100/Clp, Hsp90/HtpG, Hsp70/DnaK, Hsp60/GroEL and small Hsp (sHsp) proteins (Kotak et al., 2007). Work in this thesis has focused on the chloroplast chaperones belonging to the Hsp-100 and Hsp70 families.

The Hsp70s are involved in a variety of cellular processes including protein folding, protein disaggregation, protein degradation, and protein transport across membranes (Su and Li, 2008). It is well established that Hsp70s invariably require a J-domain protein adaptor (Hsp40/DnaJ) and, almost always, a nucleotide exchange factor (GrpE) as partners to be completely functional (Kampinga and Craig, 2010a). In Arabidopsis, there are two nuclear-encoded Hsp70 proteins in the chloroplast (cpHsp70-1 and cpHsp70-2) having overlapped and distinct functions. Both chaperones are important for plant development under normal and heat stress conditions, and they are also necessary for chloroplast protein import (Su and Li, 2008; Su and Li, 2010). For simplicity, these plastidial chaperones will be named just Hsp70-1 and Hsp70-2 in this thesis.

The Hsp100/Clp proteins, from now on Clp, are chaperones that act to unfold, remodel or disassemble protein complexes and aggregates using the energy of ATP (Lee et al., 2007). Chloroplast members of this family in Arabidopsis include one member of class B (ClpB3) and three members of class C (ClpC1, ClpC2, and ClpD) (Clarke et al., 2005; Peltier et al., 2004). ClpB3 (also named APG6) participates in proplastid differentiation into chloroplasts or amyloplasts, mediates assembly of chloroplast proteins, and promotes efficient translation regulating certain mRNAs that are essential for chloroplast development (Myouga et al., 2006). Work in different systems has shown that ClpB type chaperones can assist Hsp70 in the solubilization of toxic aggregates of damaged proteins (Figure 1.2) (Rosenzweig et al., 2013; Seyffer et al., 2012; Goloubinoff et al., 1999; Glover and Lindquist, 1998; Miot et al., 2011; Kampinga and Craig, 2010b; Haslberger et al., 2007; Zolkiewski, 1999; Doyle et al., 2007; Kim et al., 2001). Unlike ClpB3, the three chloroplast chaperones of the ClpC type lack the conserved domain responsible for the interaction with Hsp70 chaperones (Levchenko et al., 2000; Kim et al., 2001; Doyle et al., 2007) but contain the IGF motif (or ClpP-loop) that allows them to interact with the catalytic domain of the Clp protease complex (Figure 1.2). Similar to Hsp70, ClpC chaperones have also been involved in chloroplast protein import (Figure 1.2) (Flores-Perez and Jarvis, 2013).

1.2.2 Chloroplast proteases

Protein-degrading machineries play key roles in chloroplast proteome biogenesis, remodeling, and maintenance. More than 20 proteases have been identified in chloroplasts through biochemical, genetic, bioinformatics, and proteomic approaches during the last two decades (Van Wijk, 2015). They include processing peptidases, proteases, and aminopeptidases with a broad range of functions: (a) removal of transit peptides from nucleus-encoded organellar proteins; (b) N-terminal methionine cleavage of organelle-encoded proteins; (c) additional N- or C-terminal cleavages for the maturation, stabilization, and possibly activation of proteins; (d) removal of misfolded, damaged, or aggregated proteins; (e) removal of unwanted proteins in response to environmental or developmental transitions (*e.g.*, from chloroplast to chromoplast); (f) release of membrane-bound proteins (*e.g.* transcription factors); and (g) generation of protein degradation products as a respiratory substrate for stressed plants (Van Wijk, 2015).

Most chloroplast proteases originated from several bacterial prototypes and have been duplicated and diversified regarding its structure and function. Many are metalloproteases or Ser proteases, and a few are Asp proteases (Nishimura et al., 2016). Based on the physiological roles, they can be classified into two functional categories: (1) protein biogenesis and (2) protein remodeling/maintenance. The remaining proteases await further characterization of their precise roles and are therefore categorized as unknown function (Nishimura et al., 2017). In this work, we will make emphasis on the Clp protease, providing detailed structural information.

1.2.3 The Clp protease

The Caseinolytic protease (Clp) is the stromal ATP-dependent multiheteromeric Ser-type protein degradation machinery of the chloroplast (Figure 1.2 and 1.3). The Clp protease system has two separate functional units. 1) A hexameric ring formed by ClpC chaperones (ClpC1, ClpC2 and ClpD) that contributes to substrate recognition, unfolding, and translocation into the proteolytic chamber. And 2) a tetradecameric barrel-like proteolytic core that contains Ser-His-Asp triads for degradation. Additionally, the chloroplast Clp system has acquired two accessory proteins (ClpT1 and ClpT2) for core assembly, stabilization, and activation. The Clp protease also has a binary adaptor (ClpS/ClpF) for substrate recognition and delivery (Figure 1.3) (Nishimura et al., 2017).

In Arabidopsis, the proteolytic (ClpPR) core complex is composed of two heptameric rings with a molecular weight of 300 kDa. ClpP subunits have proteolytic activity, while ClpR (ClpP-related) subunits appear to lack catalytic activity. The heptameric P-ring is formed by ClpP3, ClpP4, ClpP5, and ClpP6 subunits (in 1:2:3:1 stoichiometry). The R-ring is composed of ClpR subunits and ClpP1, the only subunit encoded

in the plastid genome and the only catalytic subunit within the R-ring (Figure 1.3) (Olinares et al., 2011b). The P-ring contains seven catalytic sites, and whereas R-ring contains only three catalytic sites (Nishimura and Van Wijk, 2015). The main function of the R-ring may lie in the stabilization of the core complex (Peltier et al., 2004; Sjogren et al., 2006; Olinares et al., 2011b).

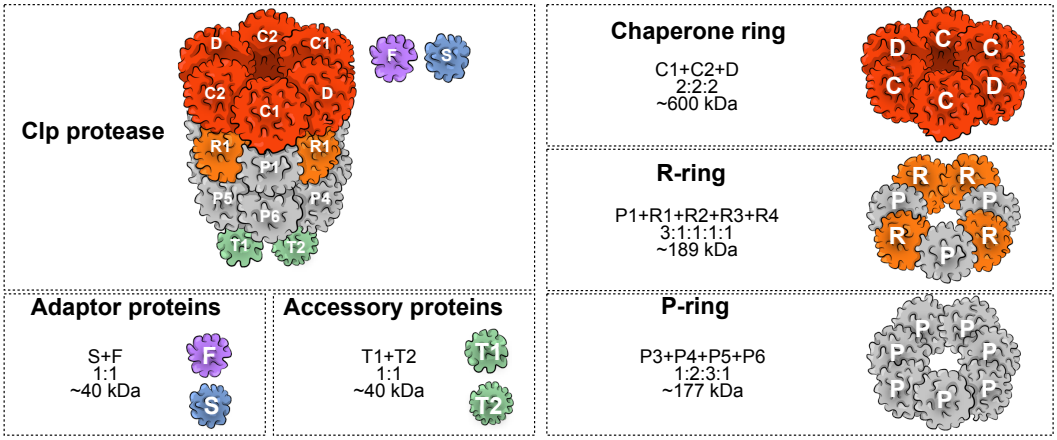

Figure 1.3: Schematic representation of the Clp protease complex. The complex composition with all subunits identified to date is shown. ClpP proteolytic subunits (P subunits) are indicated in gray and ClpP-related subunits (R subunits) lacking proteolytic acitivity are in orange. The chaperone ring subunits are in red. Accesory proteins (ClpT1 and ClpT2) are indicated in green, and adaptor proteins of the complex are shown in purple (ClpF) and blue (ClpS). The subunit stoichiometry and size (in kDa) of the three rings and the other constituents of the complex are also given. Image modified from Moreno et al., 2017.

Primary sequence comparison shows that ClpP subunits share sequence identities between 24 to 48%, whereas ClpR proteins have 28% to 38% identities to each other, suggesting both structural and functional divergence even within the ClpP and ClpR subfamilies (Kim et al., 2009). However, which ClpP and ClpR subunits interact with each other within each ring is unknown and extensive homology modeling did not suggest any preferential orientation within ClpPR rings (Peltier et al., 2004). All four ClpR subunits have plant-specific extended C-termini (up to 52 aa in length) which are not proteolytically cleaved during the core assembly (Olinares et al., 2011a). These C-terminal extensions are predicted to fold over the top of the core structure, potentially affecting the interaction with the chaperones (Peltier et al., 2004). Also, a short (9-10 aa) insertion sequence (named L1 insertion) is found in ClpR1, ClpR3 and ClpR4, but not in ClpR2 and ClpP subunits, and was proposed to influence substrate entry in the catalytic cavity (Peltier et al., 2004).

The chaperone ring is composed of two copies of the AAA^+ family Hsp100 chaperones ClpC1, ClpPC2, and ClpD. Capable of triggering conformational changes in substrate proteins (Diemand and Lupas, 2006; Hanson and Whiteheart, 2005). The typical domain architecture of proteins in this superfamily consists of an N-terminal domain (N-domain), which serves as a binding site for adaptor proteins and substrates, followed by one or two characteristic conserved modules, namely

AAA domains or nucleotide binding domains (NBDS), each of which contains the well-known Walker A and B motifs required for ATP binding and hydrolysis (Hanson and Whiteheart, 2005; Erbse et al., 2003; Lupas and Martin, 2002; Dougan et al., 2002; Chowdhury et al., 2010).

Binding of the Clp chaperones to the proteolytic core is crucial for protein degradation in plastids. ClpC1 and ClpC2 possess a conserved short hydrophobic motif in the C-terminus, the IGF/L motif or P-loop, which binds to the hydrophobic residues on the apical surface of the Clp protease core; this IGF is essential for the chaperone-core association (Kress et al., 2009; Kim et al., 2001; Singh et al., 2001). An additional short 8 amino acid sequence (rich in basic residues) called the R-motif, located just a few residues immediately downstream of the IGF loop, confers specific interaction between ClpC and R-ring protein subunits. Notably, ClpD lacks the R-motif and uvrB/C motif (of unknown function) contrasting to ClpC1 and ClpC2 (Tryggvesson et al., 2012; Nishimura and Van Wijk, 2015).

The ClpT1 and ClpT2 subunits are unique in land plants. They show high homology to the N-terminal domain of ClpC chaperones (Kim et al., 2015). ClpT proteins have been proposed to facilitate the association between the P-ring and R-ring (Sjogren and Clarke, 2011). Particularly, monomeric ClpT1 binds to the P ring, forming a stable P7/T1-ring complex, which interacts with the ClpT2 monomer to form P/T1/T2 ring (Sjogren and Clarke, 2011; Clarke, 2012). This mechanism enables R-ring docking and stabilization of the assembled core complex for proteolysis (Peltier et al., 2004; Sjogren and Clarke, 2011; Clarke, 2012; Kim et al., 2015).

1.2.4 Consequences of the loss of Clp subunits

Genetic and phenotypic analysis of various *clp* mutants in Arabidopsis showed defects in embryogenesis, seedling development and chloroplast biogenesis. Interestingly, the severity of the phenotypes differs greatly among the various *clp* null mutants (Kim et al., 2013). In the case of ClpP3, ClpP4 and ClpP5, the severity of the phenotype correlates with the copy number in the Clp core. Complete loss of ClpP5 (three copies) or ClpP4 (two copies) is embryo lethal, whereas null mutants for ClpP3 (1 copy) can germinate, grow under heterotrophic (but not autotrophic) conditions, and even produce viable seeds (Kim et al., 2013). Complete loss of ClpR2 or ClpR4 delayed embryogenesis and resulted in developmental arrest in the cotyledon stage. This arrest could be broken by growth on sucrose, but mutants remained sterile (Kim et al., 2009). By contrast, the Arabidopsis ClpR1-defective *clpr1-1* null mutant has only a weak virescent phenotype because ClpR1 is partially redundant with ClpR3. On the other hand, the null mutants of ClpP1, the only plastid-encoded subunit (of the R-ring) could not be recovered, indicating that ClpP1 is essential for viability (Shikanai et al., 2001).

The *ClpC1* null allele shows a pale green phenotype throughout all developmental stages (Sjogren et al., 2004; Kovacheva et al., 2005), while *ClpC2* and *ClpD* null alleles have no visible phenotype (Nishimura et al., 2013; Park and Rodermel, 2004). On the other hand, complete loss of ClpC proteins results in embryo lethality (Kovacheva et al., 2007). In contrast, single mutants for the adaptor proteins ClpS and ClpF as well the *clps clpf* double mutant display WT phenotypes (Nishimura et al., 2013; Nishimura et al., 2015).

Reduced Clp proteolytic activity causes 1) a significant decrease in photosystem complexes resulting in loss of energetics, a possible compensatory increase in levels of nucleoside triphosphate transporters involved in ATP import, and elevated plastoglobule proteins indicative of membrane stresses, 2) decreased levels of Calvin cycle enzymes and increased levels of enzymes in shikimate pathway for amino acids, MEP pathway for isoprenoid, thiamine biosynthesis for vitamin B1, fatty acid synthesis, starch and other carbohydrate metabolism, 3) imbalanced protein homeostasis including inefficient protein import, unprocessed protein accumulation, upregulation of import machinery, sorting machinery, processing peptidases, chaperones (*e.g.* HSP70s, HSP90, CPN60s, CPN21 and CPN10) and proteases (*e.g.* FtsH2/5), 4) overaccumulation of nucleoid proteins, ribosomal RNA (rRNA) precursors, ribosome biogenesis regulators and translation factors without a significant loss of translation (Nishimura and Van Wijk, 2015).

1.2.5 The chloroplast unfolded protein response

When damaged or misfolded proteins accumulate and aggregate in mitochondria, an adaptive transcriptional response known as the unfolded protein response (UPR) is activated, sending a signal to the nucleus to induce the expression of nuclear genes encoding mitochondria-targeted PQC components (Arnould et al., 2015; Lin and Haynes, 2016; Fiorese and Haynes, 2017). The existence of a chloroplast UPR (cpUPR) has only recently been proposed (Ramundo and Rochaix, 2014; Colombo et al., 2016). Specifically, gradual depletion of the catalytic capacity of the stromal Clp protease in *Chlamydomonas reinhardtii* by down-regulation of ClpP1 expression was found to trigger the accumulation, both at the RNA and protein level, of small heat shock proteins, chaperones, and proteases (Ramundo and Rochaix, 2014).

The existence of a cpUPR in higher plants has not been demonstrated. However, Arabidopsis mutants with constitutively decreased Clp proteolytic activity show highly increased levels of chaperones like Cpn60, Hsp70, Hsp90 and ClpB3 (Sjogren et al., 2004; Rudella et al., 2006; Kim et al., 2009; Stanne et al., 2009; Zybailov et al., 2009; Kim et al., 2013; Nishimura et al., 2013). Interestingly, work in non-plant systems has shown that the mitochondrial Clp protease is a key component of the UPR mechanism in this organelle (Haynes et al., 2007; Arnould et al., 2015). While these observations suggest that a UPR conceptually like that observed in mitochondria

might operate in the chloroplast, the physiological signal(s) triggering the putative cpUPR and the specific consequences for chloroplast function remain unexplored.

1.2.6 Retrograde signaling: GUN1

Development of functional chloroplasts and adaptation of plants to stress conditions causing chloroplast malfunctioning (including protein folding stress) requires an active exchange of information with the nucleus. This coordination between plastidial and nuclear gene expression is key for chloroplast function. Signaling from the chloroplast to the nucleus is referred to as retrograde signaling (Chan et al., 2016; Kleine and Leister, 2016).

Several retrograde signals and pathways have been reported in the literature. A major integrator of multiple retrograde signals is the chloroplast-localized pentatricopeptide repeat protein encoded by the *GENOMES UNCOUPLED 1* (*GUN1*) gene. The molecular mechanism underlying signal integration by GUN1 has remained elusive. However, the recent identification of a set of GUN1-interacting proteins by co-immunoprecipitation and mass-spectrometric analyses as well as protein-protein interaction assays (Koussevitzky et al., 2007b; Colombo et al., 2016) has opened a new perspective. According to these results, GUN1 appears to have roles in translation, protein import and degradation in plastids. Almost a quarter of the GUN1 interactors are chaperones, including ClpC1, ClpC2, Hsp70-1, and Hsp70-2 (Figure 1.2) (Tadini et al., 2016; Colombo et al., 2016), suggesting that GUN1 might somehow participate in a putative cpUPR. This possibility will be further investigated in this work.

1.3 The MEP pathway in the context of chloroplast metabolism

Chloroplasts are involved in a range of metabolic processes including photosynthesis, fatty acid synthesis, isoprenoid synthesis, starch synthesis, nitrogen assimilation, and amino acid biosynthesis among others (Bowsher and Tobin, 2001). Nonetheless, in this thesis we will focus on the methylerythritol 4-phosphate (MEP) pathway (Figure 1.4). The MEP pathway uses carbon fixed by the Calvin cycle as glyceraldehyde 3-phosphate (GAP) using the energy provided by photosynthesis to produce the universal precursors of isoprenoids isopentenyl diphosphate (IPP) and dimethylallyl diphosphate (DMAPP). Some MEP-derived isoprenoids function in photosynthesis (chlorophylls, carotenoids, tocopherols, phylloquinones, and plastoquinone) and regulate growth (hormones such as cytokinins, gibberellins, abscisic acid, and strigolactones). Others participate in the communication of plants with their environment (*e.g.* monoterpenes). Many of these metabolites are also useful for humans as drugs, phytochemicals, and health-promoting nutrients (Pulido et al., 2012). This

section will first cover the photosynthesis, Calvin cycle and isoprenoid biosynthesis to eventually describe the MEP pathway and its regulation.

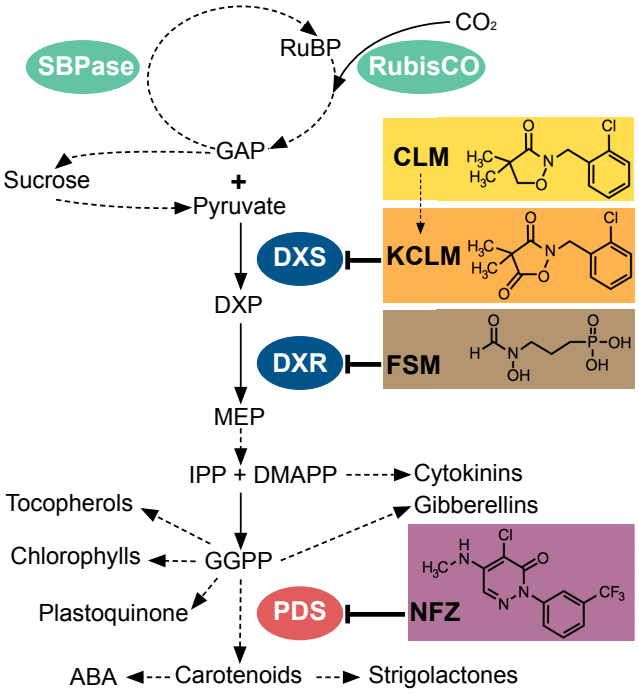

Figure 1.4: The MEP pathway in the context of chloroplast metabolism. The MEP pathway produces the universal isoprenoid precursors IPP and DMAPP. DXP production from pyruvate and GAP is catalyzed by DXS. In plants, the herbicide clomazone (CLM) is converted into keto-clomazone (KCLM) to inhibit DXS activity. The production of MEP is catalyzed by DXR and can be inhibited by fosmidomycin (FSM). On the other hand, carotenoid production can be inhibited by using the herbicide norflurazon (NFZ). The Calvin Cycle, MEP pathway and carotenoid pathway enzymes are shown in green, blue and red colors, respectively. Enzyme acronyms: RubisCo, Ribulose-1,5-biphosphate (RuBP) carboxylase/oxygenase; SBPase, Sedoheptulose-1,7-bisphosphatase; DXS, Deoxyxylulose 5-phosphate synthase; DXR, Deoxyxylulose 5-phosphate reductoisomerase; PDS, Phytoene Desaturase. Dashed arrows indicate multiple steps.

1.3.1 Photosynthesis

Photosynthesis is an integrated process. We can group the many reactions that occur during photosynthesis in plants in two broad categories. In the photosynthetic electron-transfer reactions (also called the "light reactions"), energy derived from sunlight energizes an electron in the chlorophyll molecule, enabling the electron to move along an electron-transport chain in the thylakoid membrane (Figure 1.5). The chlorophyll obtains its electrons from water (H_2O), producing oxygen (O_2) as a by-product. During the electron-transport process, H^+ is pumped across the thylakoid membrane, and the resulting electrochemical proton gradient drives the synthesis of ATP in the stroma. As the final step in this series of reactions, high-energy electrons are loaded (together with H^+) into $NADP^+$, converting it to NADPH. Notably, chlorophylls, plastoquinone and phylloquinones are MEP-derived isoprenoids with

direct roles in this phase (Figure 1.5). Other photosynthesis-related isoprenoids such as carotenoids and tocopherols are most relevant for photoprotection, as they prevent reactive oxygen species (ROS) damage that might result from excess excitation energy (DellaPenna and Pogson, 2006).

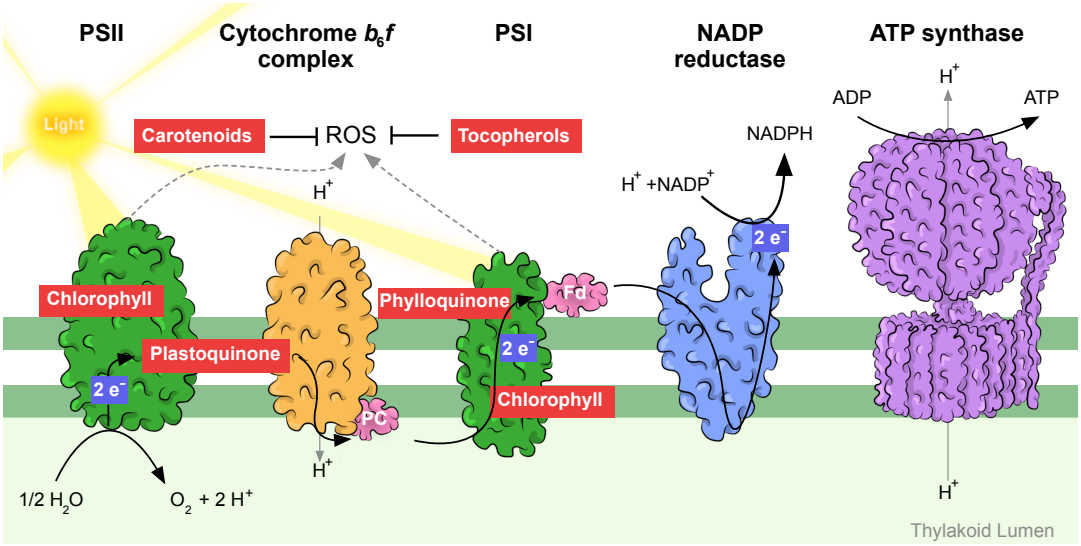

Figure 1.5: Isoprenoids and the light reactions of photosynthesis. Protein complexes responsible for the electron transfer reactions in photosynthesis: photosystem II (PSII), cytochrome b_6f, photosystem I (PSI), NADP reductase and ATP synthase. MEP-derived metabolites involved in this process are boxed in red. PC, plastocianine; Fd, ferredoxine.

In the carbon-fixation reactions (also called the "dark reactions"), the ATP and the NADPH produced by the photosynthetic electron-transfer reactions serve as the source of energy and reducing power, respectively, to drive the conversion of CO_2 to carbohydrates ($[CO_2H]_n$). The carbon-fixation reactions, which begin in the chloroplast stroma and continue in the cytosol, eventually produce sucrose and many other organic molecules in the leaves (*i.e.* source tissues) of the plant. Sucrose is then exported to other tissues such as roots, flowers, and fruits (*i.e.* sink tissues) as the source of both organic molecules and energy for growth (Alberts et al., 2008).

While the formation of ATP, NAPDH, and O_2 (which requires light energy directly) and the fixation of CO_2 to carbohydrates (which requires light energy only indirectly) are separate processes, elaborate feedback mechanisms interconnect them. Several chloroplast enzymes needed for carbon fixation, for example, are inactivated in the dark and reactivated by light-stimulated electron-transport processes (Alberts et al., 2008).

1.3.2 The Calvin cycle

Most plants produce a three-carbon (C_3) compound, 3-phosphoglycerate (3-PGA), as the first stable product in the multistep conversion of CO_2 into carbohydrates. This process is known as the C_3 carbon fixation pathway or Calvin Cycle. The cycle

proceeds through several steps in three phases: carboxylation, reduction, and regeneration (Figure 1.6). The one-step carboxylation phase consists on the carboxylation of ribulose 1,5-biphosphate (RuBP) to produce two molecules of 3-PGA. The two-step reductive phase converts 3-PGA into the triose phosphate GAP. Part of GAP is then used for the production of other metabolites (such as MEP-derived isoprenoids) or used in the next phase of the cycle (Figure 1.6). ATP and NADPH are used in this phase of the cycle. The last and largest set of reactions regenerates RuBP; in this process, an additional ATP is consumed during the conversion of ribulose 5-phosphate (RuP) to RuBP. All the enzymes required in the Calvin cycle are in the stroma. In addition to RubisCo, the enzymes that are unique to the cycle are sedoheptulose-1,7-biphosphatase (SBPase, which dephosphorylates a diphosphosugar to yield a monophosphosugar) and phosphoribulokinase (PRK, which phosphorylates RuP to RuBP) (Malkin and Krishna, 2000).

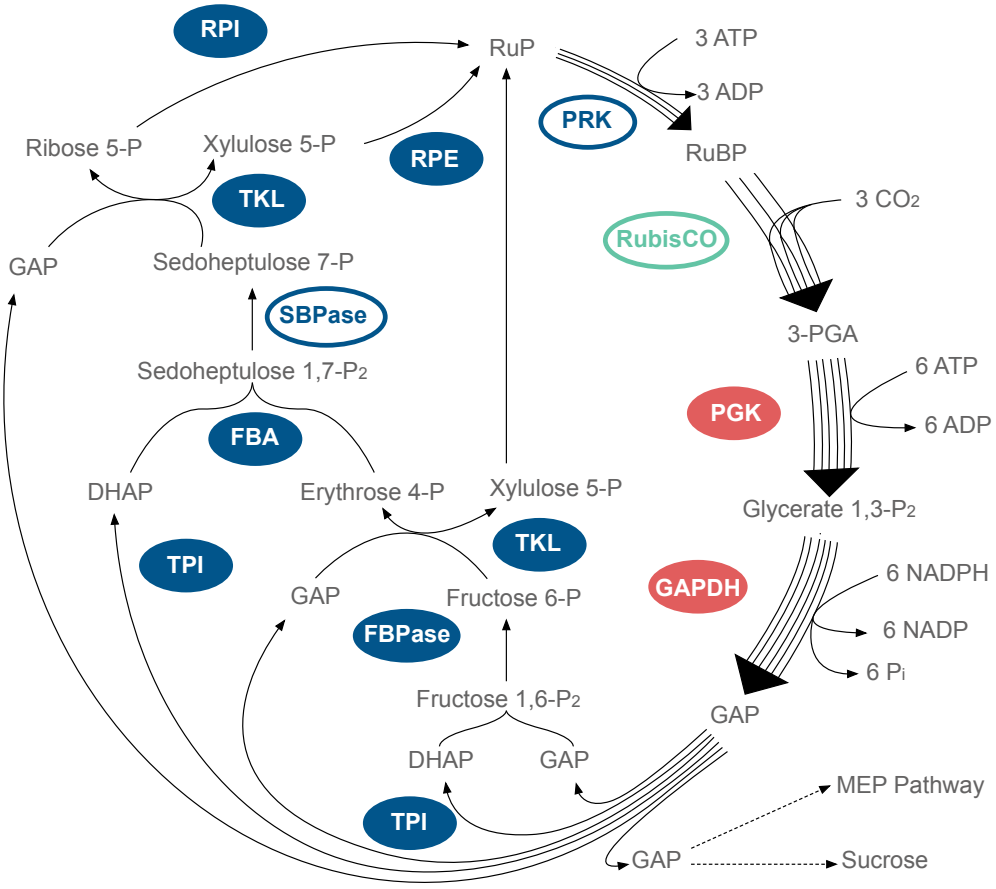

Figure 1.6: Schematic representation of the Calvin cycle. The Calvin cycle is divided into in three phases: carboxylation, reduction, and regeneration. Green, red and blue colors represent enzymes participating in such phases respectively. Those unique to the Calvin cycle are shown in white background. Enzyme acronyms: PRK, Phosphoribulokinase; RubisCo, Ribulose-1,5-bisphosphate carboxylase/oxygenase; PGK, Phosphoglycerate kinase; GAPDH, Glyceraldehyde-3-phosphate dehydrogenase; TPI, Triose-phosphate isomerase; FBA, Fructose-biphosphate aldolase; FBPase, Fructose-1,6-bis-phosphatase; TKL, Transketolase; SBPase, Sedoheptulose-1,7-bisphosphatase; RPI, Ribose 5-phosphate isomerase; RPE, ribulose-phosphate 3-epimerase.

The addition of three molecules of CO_2 to three molecules of the C_5 sugar RuBP yields six molecules of C_3 3-PGA, each of which is phosphorylated and reduced to generate GAP that together with ATP are used to regenerate RuBP molecules. A remaining GAP molecule, the net product of carbon fixation can be used to build carbohydrates, isoprenoids, or other cellular constituents (Malkin and Krishna, 2000).

1.3.3 Isoprenoid biosynthesis

Isoprenoids are a hugely diverse family of compounds derived from the C_5 precursors IPP and DMAPP. All free-living organisms produced isoprenoids, but their abundance and variety in plants is unparalleled. Some plant isoprenoids play primary (*i.e.* essential) functions in photosynthesis (carotenoids, chlorophylls, tocopherols, phyloquinones, plastoquinone), respiration (ubiquinone), membrane architecture (sterols), and growth regulation (brassinosteroids, cytokinins, gibberellins, abscisic acid, strigolactones), whereas others have secondary (*i.e.* specialized) roles as pigments, volatiles, and defense compounds, many of which have applications in industry and agriculture (Pulido et al., 2012). Unlike most organisms, plants use two independent pathways to produce IPP and DMAPP in different cell compartments (Pulido et al., 2012; Vranova et al., 2012). The plastidial MEP pathway simultaneously produces both IPP and DMAPP from pyruvate and GAP (Figure 1.7). In the cytosol, the mevalonic acid (MVA) pathway converts acetyl-CoA into IPP, which is then isomerized to DMAPP by specific isomerases. MVA-derived isoprenoids play roles as primary (*e.g.* ubiquinone, sterols, brassinosteroids) and secondary (*e.g.* triterpenes, sesquiterpenes, polyterpenes) metabolites. Despite the compartmentalization of IPP and DMAPP synthesis in plant cells, multiple studies using inhibitors, mutants, and labeled precursors in feeding experiments have shown that an exchange of isoprenoid precursors takes place among different subcellular locations (Flores-Perez et al., 2010; Paetzold et al., 2010). However, the genetic block of either the MVA pathway or the MEP pathway in null mutants or the complete inhibition of single pathway enzymes in wild-type (WT) plants treated with specific inhibitors results in a developmental block and a seedling-lethal phenotype, indicating that the loss of one of the two pathways cannot be compensated by the remaining pathway (Pulido et al., 2012). The advantages for plants of retaining two pathways (MVA and MEP) in separate compartments are not fully understood. Likely the physical separation of the pathways facilitates the optimal supply of the metabolic precursors required in each cell compartment. For example, many plastidial isoprenoids are required for photosynthesis and therefore a chloroplast-based control of their production might be more effective.

1.3.4 The MEP Pathway

The two substrates of the MEP pathway are GAP, originated from the Calvin cycle, and pyruvate, derived from glycolysis and likely imported to chloroplasts from the cytosol (Furumoto et al., 2011; Trowbridge et al., 2012; Seemann et al., 2006).

The first reaction of the pathway (Figure 1.4) is the condensation of (hydroxyethyl) thiamin derived from pyruvate with the C_1 aldehyde group of GAP to produce deoxyxylulose 5-phosphate (DXP), catalyzed by DXP synthase (DXS). The intramolecular rearrangements and reduction of DXP catalyzed by DXP reductoisomerase (DXR) yields MEP in the next step of the pathway. MEP is afterwards converted via cytidine 5'-diphosphomethylerythritol (CDP-ME) and CDP-ME 2-phosphate (CDP-MEP) into methylerythritol 2,4-cyclodiphosphate (MEcPP) by the enzymes MEP cytidylytransferase (MCT), CDP-ME kinase (CMK) and MEcPP synthase (MDS), respectively. In the last two steps of the pathway, the enzyme hydroxymethylbutenyl diphosphate (HMBPP) synthase (HDS) transforms ME-cPP into HMBPP, whereas HMBPP reductase (HDR) converts HMBPP into a *ca.* 5:1 mixture of IPP and DMAPP (Rodriguez-Concepcion and Boronat, 2002; Phillips et al., 2008) (Figure 1.7).

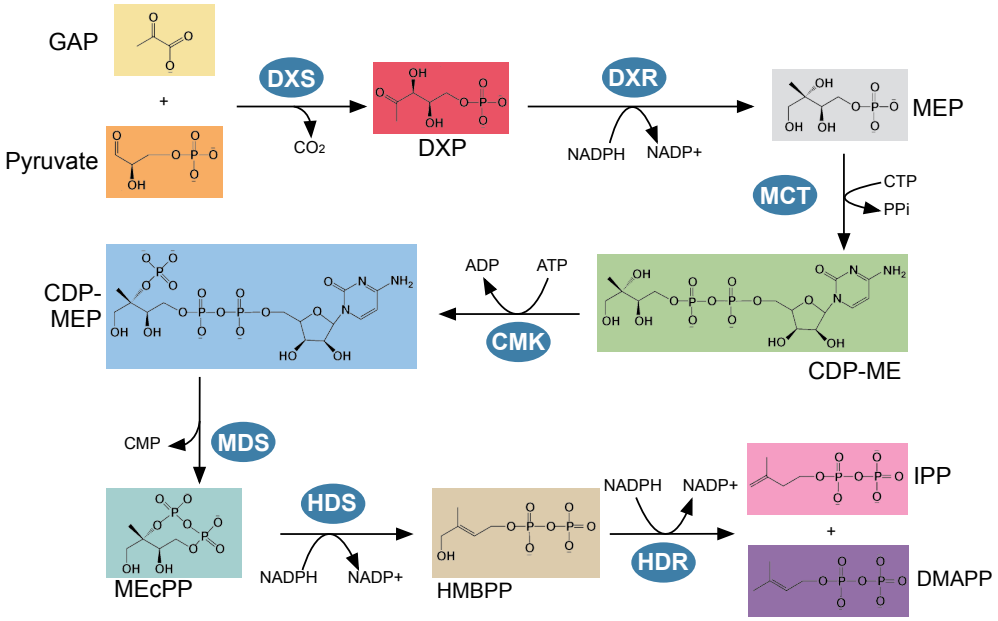

Step	Enzyme	Acronym	AGI code
1	Deoxyxylulose 5-phosphate synthase	DXS	AT4G15560
2	Deoxyxylulose 5-phosphate reductoisomerase	DXR	AT5G62790
3	Methylerythritol 4-phosphate cytidylyltransferase	MCT	AT2G02500
4	Cytidine 5'-diphosphomethylerythritol kinase	CMK	AT2G26930
5	Methylerythritol 2,4-cyclodiphosphate synthase	MDS	AT1G63970
6	Hydroxymethylbutenyl diphosphate synthase	HDS	AT5G60600
7	Hydroxymethylbutenyl diphosphate reductase	HDR	AT4G34350

Figure 1.7: The MEP pathway. See table for acronyms and AGI codes. Modified from Phillips et al., 2008

It is well established that all the MEP pathway enzymes are encoded by the nuclear genome and are imported into plastids. Recent proteomics approaches have detected all the Arabidopsis MEP pathway enzymes in the stroma (Joyard et al., 2009). MEP pathways enzymes and genes are summarized in Figure 1.7.

IPP and DMAPP can be interconverted in a reversible reaction catalyzed by isoforms of the enzyme IPP/DMAPP isomerase targeted to different cell compartments, including chloroplasts. Condensation of these C_5 units by downstream enzymes generates prenyl diphosphate molecules of increasing chain length which serve as the starting points for the production of all the variety of isoprenoids. They include C_{10} geranyl diphosphate (GPP, precursor of monoterpenes), C_{15} farnesyl diphosphate (FPP, mostly produced in the cytosol and mitochondria for the synthesis of ubiquinone, sterols, triterpenes, and sesquiterpenes), and C_{20} geranylgeranyl diphosphate (GGPP, the precursor of most plastidial isoprenoids; Figure 1.4).

1.3.5 Resources for MEP pathway research

Knockout mutants are available for all the MEP pathway genes in Arabidopsis. All these null mutants show a very similar albino phenotype and developmental arrest (Phillips et al., 2008). Electron microscopy analyses have shown that chloroplast development is arrested at early stages in these mutants, resulting in organelles with incipient internal oppressed membrane and vesicle structures but no organized thylakoid membranes or grana (Hsieh and Goodman, 2005; Estevez et al., 2000; Hsieh et al., 2008). On the other hand, the identification of partial loss-of-function mutants resulting from single mutations in two of the MEP pathway genes, *DXS* and *HDS*, has allowed the identification of important regions for the enzymatic activity of the corresponding enzymes and has uncovered new regulatory aspects of the MEP pathway (Phillips et al., 2008). In particular, defective HDS activity and subsequent accumulation of MEcPP in Arabidopsis mutants unveiled a role for this MEP pathway intermediate in retrograde signaling (Xiao et al., 2012).

The characteristic pale/albino phenotype and developmental delay of Arabidopsis MEP pathway mutants can be phenocopied using specific chemical inhibitors of the pathway (Figure 1.4). Such inhibitors have been used as tools for better understanding the control and flux of the MEP pathway. Although methods for the determination of DXS and DXR activities are available, they are time-consuming, require specialized equipment, and cannot be used for genetic screenings. An inexpensive and high-throughput alternative to enzymatic assays that has the added advantage of estimating MEP pathway enzyme activity *in vivo* is to quantify the resistance to competitive inhibitors specifically targeting these enzymes (Perello et al., 2014).

Low concentrations of the MEP pathway inhibitors clomazone (CLM, an inhibitor of DXS) and fosmidomycin (FSM, an inhibitor of DXR) cause an arrest of seedling establishment (SE) and a pale phenotype (Perello et al., 2014). SE is defined as the

production of true leaves that can support further plant development (Rodriguez-Concepcion et al., 2004; Kasahara et al., 2002). In the case of CLM, it is converted by plant tissues to keto-clomazone (KCLM), the biologically active inhibitor (Figure 1.4) (Zeidler et al., 2000; Matsue et al., 2010; Ferhatoglu and Barrett, 2006). Plants germinated and grown in the presence of CLM, KCLM or FSM cause a concentration-dependent inhibition of SE. Therefore, a quantification of SE rates can be used as a common estimator of resistance to inhibition of the MEP pathway and hence as a proxy for *in vivo* DXS and DXR activities (Perello et al., 2014). The pale phenotype, caused by reduced production of chlorophylls and photoprotective carotenoids, can also be quantified by measuring the levels of these photosynthetic pigments (Zeidler et al., 2000; Matsue et al., 2010; Kuzuyama et al., 1998; Steinbacher et al., 2003; Pulido et al., 2013; Rodriguez-Concepcion et al., 2004; Carretero-Paulet et al., 2006; Perello et al., 2014). But an important difference between the phenotype of plants grown in media supplemented with CLM or FSM is that the former only causes bleaching of true leaves (but not cotyledons) at low concentrations of the inhibitor, whereas FSM causes a similar reduction in the levels of photosynthetic pigments in both cotyledons and true leaves. The molecular basis of the differential phenotype of CLM and FSM-treated plants has not been explored.

Downstream the MEP pathway, the production of carotenoids can also be specifically blocked with norflurazon (NFZ), a non-competitive inhibitor of the enzyme phytoene desaturase (Jung, 2004) (Figure 1.4). NFZ has been extensively used in retrograde signaling studies. In particular, suppressor screens for Arabidopsis mutants able to de-repress the inhibition of photosynthesis-related nuclear genes in NFZ-treated seedlings led to the identification of GUN1 and other components of the chloroplast-nucleus communication network (Susek et al., 1993; Koussevitzky et al., 2007b).

1.4 Regulation of the MEP pathway flux: The pivotal role of DXS

Based on the competitive nature of CLM and FSM mode of action, resistance to these inhibitors (*i.e.* increased SE rates or reduced bleaching) can be accomplished by increasing the activity of DXS or DXR in plants. Lines overexpressing DXS show resistance to both CLM and FSM (due to a higher production of DXP, which competes with FSM for the active site of DXR) and those overexpressing DXR are resistant to FSM but not to CLM (Rodriguez-Concepcion et al., 2004; Carretero-Paulet et al., 2006). In our laboratory, screening for Arabidopsis mutants with increased or reduced resistance to CLM or FSM led to the identification of unanticipated mechanisms controlling the levels or/and activity of the target enzymes but also other MEP pathway enzymes. These studies unveiled that, besides the coarse control derived

from changes in gene expression (*i.e.* transcriptional regulation), a fine control of enzyme levels and their activity occurs at several post-translational levels (Guevara-Garcia et al., 2005; Laule et al., 2003; Sauret-Gueto et al., 2006; Flores-Perez et al., 2008a; Flores-Perez et al., 2010; Pulido et al., 2012; Hemmerlin, 2013). This is particularly relevant for DXS, the main regulatory enzyme of the pathway.

1.4.1 Transcriptional regulation of the MEP pathway

Comparative expression analysis of the genes encoding MEP pathway enzymes under various growing conditions showed that transcript accumulation is modulated by multiple internal (*i.e.* developmental) and external (*i.e.* environmental) signals in a coordinated manner in plants (Guevara-Garcia et al., 2005; Carretero-Paulet et al., 2002; Hsieh et al., 2008; Cordoba et al., 2009). The existence of regulatory factors responsible for these responses has been suggested (Cordoba et al., 2009). By contrast, gene coexpression networks have revealed that there is no global transcriptional regulation of all genes encoding MVA and MEP pathway enzymes. Isoprenoids synthesized via MVA and MEP pathways are controlled by independent regulatory networks with restricted connectivity (Vranova et al., 2013). MEP pathway genes are expressed in all plant organs and developmental stages. In particular, *DXS* gene is maximally expressed in the apical meristem and least in the roots (Vranova et al., 2013). Nonetheless, transcripts for all MEP pathway genes fluctuate following the same 24 h phase, reaching their highest transcript levels in the morning (Cordoba et al., 2009; Covington et al., 2008). Also, circadian regulation has been demonstrated for the Arabidopsis genes encoding DXS and HDR using clock-defective mutants (Pokhilko et al., 2015).

Regarding environmental regulation, light has a major impact on the transcript accumulation of several MEP pathway genes. Expression analysis in Arabidopsis showed that all genes from the pathway are up-regulated upon exposure to light (Guevara-Garcia et al., 2005; Carretero-Paulet et al., 2002; Hsieh et al., 2008; Cordoba et al., 2009). Positive regulation of MEP pathway genes by light provides an advantage during early seedling development following deetiolation, due to the high demand for photosynthesis-related metabolites (Cordoba et al., 2009). In agreement, synthesis of phytyl chains and carotenoids is increased after illumination, concomitant with the light-dependent accumulation of transcripts from MEP pathway genes (Cordoba et al., 2009; Ghassemian et al., 2006; Rodríguez-Concepción, 2006). On the other hand, transcription of all MEP-pathway genes in *A. thaliana* seedlings are repressed in the dark except for *HDR*, whose transcript levels remain high (Hsieh and Goodman, 2005).

Additionally, sugars (sucrose) have the capacity to increase the accumulation of several of the MEP pathway gene transcripts in dark-grown plants (Hsieh and Goodman, 2005). Since the two precursor molecules of the MEP pathway, GAP, and pyruvate, are derived directly from photosynthesis or glycolysis, it is not surprising that sugar levels regulate this pathway by altering the expression of the corresponding genes (Cordoba et al., 2009). Transcription of MEP pathway genes is also regulated by several other environmental signals and conditions, such as osmotic stress, dehydration, high and low temperature, UV irradiation, bacterial pathogens, herbivory, fungal elicitors, wounding, and mycorrhiza (Vranova et al., 2013). In any case, changes in gene expression do not always lead to similar changes in MEP pathway protein levels and, most importantly, enzyme activities and metabolite production (Rodríguez-Concepción, 2006).

1.4.2 Post-transcriptional regulation of the MEP pathway

Despite the intense efforts to understand the regulation of the MEP pathway, strict correlation between gene expression, protein levels and enzyme activity has been not observed. Allosteric regulation, structural regulation, secondary post-translational regulation and redox regulations are some of the post-translational events that regulate MEP pathway enzymes (Hemmerlin, 2013).

The final two reactions of the MEP pathway catalyzed by HDS and HDR are redox regulated. HDS and HDR are iron-sulfur reductases that require a reduced [4Fe-4S]1^{+} cluster for enzyme activity (Vranova et al., 2013). Ferredoxin, can directly transfer electors to the iron-sulfur cluster of HDS in the light and reduce it in the absence of any reducing cofactor. In the dark, and particularly in nonphotosynthetic tissues such as roots, the regulation of HDS activity also requires ferredoxin $NADP^{+}$/ferredoxin oxidoreductase and NADPH as an electron shuttle (Seemann et al., 2006). The oxygen sensitivity property of HDS and HDR may play a pivotal role in the pathway regulation (Hemmerlin, 2013).

In the case of DXS, several phosphopeptides have been identified in its structure. Phosphorylation could promote conformational changes that would directly interfere with enzyme activity, or affect subcellular localization, or alternatively initiate protein degradation (Seo and Lee, 2004). DXS seems to be phosphorylated *in vivo*, but the functional meaning of this modification still remains unclear (Dale et al., 1995; Hemmerlin, 2013).

In addition, DXS enzymatic activity is inhibited by the MEP pathway products IPP and DMAPP to control the carbon flux through the pathway. It was observed that IPP and DMAPP compete with the cofactor thiamin diphosphate for binding with DXS (Ghirardo et al., 2014; Banerjee et al., 2013; Pokhilko et al., 2015). Low IPP and DMAPP level also induce a post-transcriptional accumulation of DXS protein (Guevara-Garcia et al., 2005; Cordoba et al., 2009). DXS (and HDR) accumulate at

high levels in all the MEP pathway mutants, once again highlighting the role of IPP and DMAPP as a feedback mechanism controlling MEP pathway flux (Guevara-Garcia et al., 2005; Cordoba et al., 2009; Pokhilko et al., 2015).

During the last years, our laboratory has identified Arabidopsis mutants that are resistant to FSM (*rif* mutants), unveiling several mechanisms for the post-translational control of the MEP pathway flux (Sauret-Gueto et al., 2006; Flores-Perez et al., 2008a; Flores-Perez et al., 2010). For instance, *rif18* was characterized as a loss-of-function allele of the *PRL1* (*Pleiotropic Regulatory Locus 1*) gene encoding a WD-40 protein required to produce miRNAs and siRNAs, which are key regulators on sugar and hormone responses (Zhang et al., 2014; Flores-Perez et al., 2010). This mutant revealed a strong influence of sugar availability for MEP-derived isoprenoid production (Flores-Perez et al., 2010). In fact, it was recently shown that the availability of GAP coming from photosynthesis can be a useful diagnostic marker for MEP pathway flux (Pokhilko et al., 2015).

On the other hand, the characterization of the *rif1* and *rif10* mutants showed that their FSM resistance phenotype was the result of higher DXS and DXR protein levels but not transcripts. RIF1 and RIF10 are both required for the proper expression of the plastome. *RIF10* encodes a plastid-targeted exoribonuclease polyribonucleotide phosphorylase (PNPase), implicated in the processing of a variety of plastid transcripts (Flores-Perez et al., 2008a). *RIF1* encodes a plastid-targeted protein homolog of the *Bacillus subtilis* YqeH protein, a GTPase required for proper ribosome assembly (Flores-Perez et al., 2008a; Gas et al., 2009). Their loss of function in *rif1* and *rif10* lines causes a reduction in the production of plastome-encoded proteins linked to the post-transcriptional accumulation of DXS, DXR, HDS, and HDR in mutant plastids. An enhanced post-transcriptional accumulation of MEP pathway enzyme levels was also observed upon pharmacological inhibition of plastome gene expression in WT seedlings grown in the presence of sublethal concentrations of CAP, an inhibitor of protein synthesis in plastids. By contrast, treatment with concentrations of the carotenoid biosynthesis inhibitor NFZ that caused a similar visual phenotype without directly affecting plastome gene expression did not result in FSM resistance (Sauret-Gueto et al., 2006). Most interestingly, mutant seedlings and CAP-treated WT plants showed altered levels of the plastome-encoded ClpP1 protein, one of the catalytic subunits of the stromal Clp protease complex, likely resulting in a decreased proteolytic activity of the entire complex as a consequence of impaired subunit stoichiometry (Figure 1.3) (Nishimura and Van Wijk, 2015). This data is consistent with a role of the Clp protease in the regulation of MEP pathway enzyme levels, because mutants with a decreased Clp protease activity showed an increased accumulation of active DXS and DXR enzymes, leading to FSM resistance (Flores-Perez et al., 2008a).

1.4.3 DXS a major regulatory hub of the MEP pathway

The first step of the MEP pathway is catalyzed by DXS, a homodimeric enzyme recently confirmed to have the highest flux control coefficient (*i.e.* to be the main rate-determining step) of the MEP pathway (Wright et al., 2014). Consistent with its prime regulatory role, DXS activity is tightly regulated at several post-translational levels. As mentioned before, DXS enzymatic activity is inhibited by MEP pathway products, IPP and DMAPP (Banerjee et al., 2013; Ghirardo et al., 2014). Such products are also able to repress DXS accumulation at the protein level (Guevara-Garcia et al., 2005; Ghirardo et al., 2014; Rodriguez-Villalon et al., 2009; Han et al., 2013; Pokhilko et al., 2015). The connection between IPP/DMAPP-mediated inhibition and protein stability remains unexplored. However, it has been proposed that inactive forms of DXS might be more prone to proteolytic removal (Pulido et al., 2013; Pokhilko et al., 2015). Recently, a mathematical model showed that the post-translational control of DXS protein abundance and enzyme activity is crucial for the adjustment of the MEP pathway flux to persistent changes in environmental conditions, such as substrate supply or product demand (Pokhilko et al., 2015).

As a strategy to better understand how DXS protein levels and enzymatic activities are regulated in Arabidopsis, our lab aimed to identify and characterize DXS-interacting (DXI) proteins. A yeast two-hybrid assay identified one of these proteins, DXI1, as J20, a plastid-localized J-protein protein previously proposed to contribute to photosynthetic efficiency (Chen et al., 2010). It has been demonstrated that J-proteins, like J20, typically act as adaptors that recognize and deliver protein substrates to Hsp70 (Figure 1.8). The H-domain responsible for the interaction with Hsp70 is well conserved in J20. Upon interaction, ATP hydrolysis is stimulated to transfer the protein substrate to the Hsp70 chaperone and to drive conformational changes (Tsai and Douglas, 1996; Wall et al., 1994). Mutant *j20* plants accumulate higher levels of DXS protein without changes at the transcript levels, but they are sensitive to CLM, indicating that the loss of J20 function leads to reduced DXS activity. It was concluded that DXS accumulated as an inactive enzyme in the mutant, likely because misfolded, damaged, or inactivated forms of the enzyme were not efficiently delivered to the plastidial Hsp70 chaperone system (Pulido et al., 2013).

According to the current model (Figure 1.8), under normal growth conditions J20 would recognize DXS polypeptides that misfold after plastid import or upon ordinary perturbations, transferring them to Hsp70 chaperones for refolding and, hence, enzyme activation. In response to more severe conditions (such as heat shock), DXS misfolding and/or eventual aggregation might overwhelm the capacity of the J20/Hsp70 system to repair them. In this context, J20 might target inactive DXS enzymes for proteolytic removal (Figure 1.8). As discussed above, a role for the Clp protease complex has been proposed for the degradation of DXS and other MEP

pathway enzymes, but whether this protease is directly involved in the specific J20-mediated degradation of DXS in plastids remains an open question.

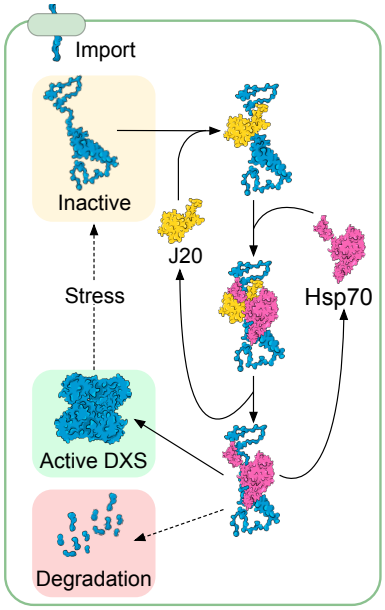

Figure 1.8: J20 delivers DXS to Hsp70 for eventual protein quality control. The contribution of J20 and Hsp70 chaperones to modulate the levels of active DXS enzymes is shown.

On the other hand, unpublished immunoprecipitation data acquired in collaboration with Wilhelm Gruissem (ETH-Zurich, Switzerland) indicated that Arabidopsis DXS-containing complexes were specifically enriched in proteins related to photosynthesis, including components of the protein expression machinery and enzymes of the Calvin cycle (Table 1.1). Although the relevance of these interactions for DXS activity awaits further investigation, our previous conclusion from the characterization of *rif* mutants indicating that the levels and activity of DXS (and other MEP pathway enzymes) depend on the expression of the plastid genome and the supply of metabolic substrates strongly suggests that at least some of the identified DXI proteins might be biologically relevant to regulate DXS activity in Arabidopsis chloroplasts.

Table 1.1: Proteins immunoprecipitated with DXS in Arabidopsis. Light-grown 10-day-old *35S:DXS-GFP* seedlings constituvely expressing a GFP-tagged DXS protein were used for triplicate immunoprecipitation experiments with a GFP-specific antibody. Transgenic *35S:DXR-GFP* seedlings were used as controls to account for unspecific interactions.

Group	Protein	AGI code	Description
Photosynthesis-related	CP22	AT1G44575	Pigment-binding protein associated with PSII
	CSP41A	AT3G63140	Chloroplast Stem-Loop Binding Protein 41 kDaA
	CSP41B	AT1G09340	Chloroplast Stem-Loop Binding Protein 41 kDaB
	FNR1	AT5G66190	Ferredoxina-NAP(+)-Oxidoreductase 1
	THF1	AT2G20890	Photosystem II Reaction Center PSB29 PROTEIN
Calvin cycle	FBA1	AT2G21330	Fructose-Bisphosphate Aldolase 1
	FBA2	AT4G38970	Fructose-Bisphosphate Aldolase 2
	GAPDH-B	AT1G42970	Glyceraldehyde-3-phosphate dehydrogenase B
	PRK	AT1G32060	Phosphoribulokinase
	SBPase	AT3G55800	Sedoheptulose-1,7-bisphosphatase
Plastid Ribosome	RPS9	AT1G74970	Ribosomal protein S9
	RPS13	AT5G14320	Ribosomal protein S13
	RPL9	AT3G44890	Ribosomal protein L9
	RPL24	AT5G54600	Ribosomal protein L24
	RPL19	AT5G65220	Ribosomal protein L29

2. Objectives

DXS is the main control point of the MEP pathway and hence it is not surprising that its activity is tightly regulated at multiple levels beyond gene expression (Cordoba et al., 2009; Pulido et al., 2012; Hemmerlin, 2013; Vranova et al., 2013; Vranova et al., 2012; Rodriguez-Concepcion and Boronat, 2015). The MEP pathway flux, in general, and DXS activity, in particular, are strongly dependent on carbon and energy supply by photosynthesis (which provides substrates, ATP, and reducing power) and feedback control by metabolic intermediates and products (Banerjee et al., 2013; Pokhilko et al., 2015). Work in our lab using *Arabidopsis thaliana* as a model system has shown that the levels of DXS and other MEP pathway enzymes are influenced by plastidial protein synthesis (Sauret-Gueto et al., 2006) and protein quality control systems (Flores-Perez et al., 2008a; Gas et al., 2009; Pulido et al., 2013). Particularly, it has been shown that DXS stability and enzymatic activity can be modulated by interaction with other plastidial DXS-interacting (DXI) proteins. The goal of this thesis work has been to characterize the physiological role of DXS-DXI interactions and the molecular pathways leading from the interactions to the eventual biological effects. Specifically, we set up the two major objectives described below (Figure 2.1).

Objective 1

At the start of this work, a list of DXI proteins identified by co-immunoprecipitation (Co-IP) experiments was available in the laboratory (Table 1.1). They included proteins with roles in photosynthesis, enzymes of the Calvin cycle, and components of the plastid gene expression machinery, which mostly produces photosynthetic components. The **objective 1** of this thesis was to test the biological relevance of the interaction of DXS with these plastidial proteins (Figure 2.1).

Objective 2

Yeast-two hybrid experiments identified DXI1/J20 as the first protein to interact with DXS (Pulido et al., 2013). It was found that it facilitates the recognition of inactive DXS forms to deliver them to eventual reactivation or degradation. Nonetheless, the components involved in these two opposite pathways remained unknown. The

objective 2 of this work was to characterize the J20-dependent molecular pathways resulting in DXS reactivation or degradation (Figure 2.1).

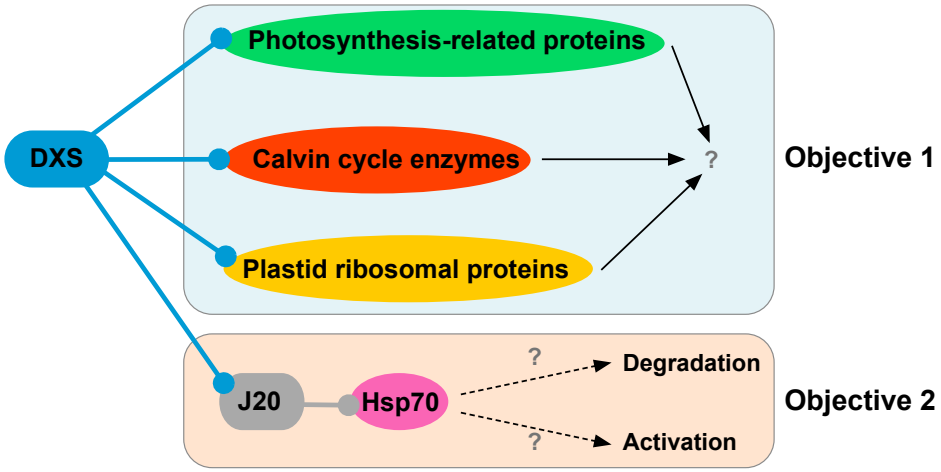

Figure 2.1: Visual representation of the Ph.D. thesis objectives. In objective 1 we will test the biological relevance of the interaction of DXI proteins with DXS. In objective 2 we will characterize the J20-dependent pathways eventually resulting in DXS reactivation or degradation. Protein-protein interactions are shown with roundhead arrows.

3. Results

3.1 Chapter I. Testing the biological relevance of the interaction of DXS with plastidial DXI proteins

3.1.1 Starting point: a list of DXI proteins and their corresponding Arabidopsis *dxi* mutants

As discussed before, we speculated that interaction of DXS with other plastidial (DXI) proteins might be relevant for the control of DXS activity and hence for the metabolic regulation of the MEP pathway flux. To identify such DXI proteins, co-immunoprecipitation (co-IP) experiments had been previously carried out in collaboration with Dr. Wilhelm Gruissem (ETH Zurich, Switzerland) using Arabidopsis *35S:DXS-GFP* lines constitutively overproducing a GFP-tagged DXS protein and a GFP-specific antibody (Ruiz-Sola et al., 2016). Following co-IP and protein identification by mass spectrometry, a list of DXI proteins was created with those showing statistically significant enrichment (Table 1.1).

Among the putative DXI proteins depicted in Table 1.1, we found enzymes of the Calvin cycle, plastid ribosome proteins, and other components of the photosynthetic machinery of chloroplasts. To test whether the identified DXI proteins might be relevant for the metabolic regulation of DXS, we followed a genetic strategy. Briefly, mutants were searched for in the literature and in public Arabidopsis T-DNA collections to be tested for their resistance to CLM as an estimate of potentially altered DXS activity. Notably, among the putative DXI proteins some of them were proteins that form part or the Large and Small subunit of the chloroplast ribosome. We reasoned that specific interactions with certain ribosome subunits are important for DXS regulation. To test out this idea we decided to order mutants affected in other chloroplast subunits to use them as a control (*rpl19a*, *rpl19b*, *rps21*). In total, we ordered 25 T-DNA insertion mutants corresponding to 15 putative DXI proteins (21 alleles) and 3 ribosome subunits (4 alleles) (Table 3.1). We germinated and grew them in MS 0.5X-medium under long-day conditions, and after 10 days they were transferred to substrate. Then, we cut a leaf from the rosette of the adult plant to corroborate by PCR the T-DNA insertion in each line. We could isolate homozygous lines for most of the mutants Figure 3.1. Some of these mutants had been previously isolated and characterized (Table 3.1). Unfortunately, we failed to isolate mutants for the genes *CP22*,

PRK and *RPS13*. Notably, among the obtained homozygous mutants we observed that some of the mutants showed an evident pale phenotype. In particular, mutants corresponding to the genes *SBP*, *RPL24*, *RPS21* and *THF1* accumulated about half the amount of found in WT plants (Table 3.1).

3.1.2 The use of CLM sensitivity assays unveil that only *dxi* mutants defective in SBPase show altered DXS function

Methods to determinate DXS activity are available but they are time consuming and cannot be used for genetic screens. For this reason, we decided to use an inexpensive and high throughput alternative to estimate DXS in vivo activity: the CLM resistance assay (Perello et al., 2014). To analyze if any of the *dxi* mutants have an altered DXS activity, we germinated and grew them for 10 days under LD conditions, with WT plants as a control, in the presence of CLM. We collected the seedlings and then we extracted the photosynthethic pigments to finally determine the chlorophyll levels in treated and untreated plants. The rationale was that any change in DXS activity would be reflected in an altered sensitivity to CLM, as previously shown in our laboratory (Carretero-Paulet et al., 2006; Pulido et al., 2013; Perello et al., 2014). For instance, plants with decreased DXS activity, such as *j20* mutant, showed lower resistance to CLM than WT (Pulido et al., 2013). As a sensitive control line, we also include *j20* mutant in our CLM sensitivity assays. The results are shown in Figure 3.2.

Quantification of CLM sensitivity of 20 homozygous T-DNA insertion lines led to the conclusion that only the two mutant alleles of the *SBP* gene (encoding sedoheptulose-1,7-bisphosphatase, SBPase), *sbp-1* and *sbp-2*, were significantly resistant to the treatment (Figure 3.2). Unlike other enzymes in the Calvin cycle, SBPase is a stromal protein encoded by a single gene in Arabidopsis (just like DXS). To confirm the interaction between DXS and SBPase, we decided to perform a new co-IP assay using tagged proteins transiently expressed in *Nicotiana benthamiana* leaves. To this end, the sequence encoding the full-length Arabidopsis SBPase protein without the stop codon was fused to a C-terminal MYC tag and cloned in a plant expression vector under the control of the 35S promoter (*35S:SBP-MYC* construct). Then, we transformed *Agrobacterium tumefaciens* strains with this construct and the previously available *35S:DXS-GFP* plasmid (Pulido et al., 2013). We transiently expressed both SBPase-MYC and DXS-GFP proteins in agroinfiltrated *N. benthamiana* leaves. After protein extraction, commercial agarose-beads coupled to anti-MYC antibodies were used to immunoprecipitate protein complexes containing SBPase-MYC as described in Materials and methods. Immunoblot analysis of samples before (input) and after co-IP were then carried out with anti-MYC and anti-GFP sera (Figure 3.3). Despite several attempts, however, co-IP samples were found to only contain the SBPase-MYC protein, but not DXS-GFP. An important flaw of these experiments is that

Table 3.1: Mutants used for CLM sensitivity assays. Mutants requested from different Arabidopsis T-DNA collections are shown. In the second column C, R, and P indicate the groups Calvin Cycle, Ribosome and Photosynthesis-related proteins respectively. The last column indicates the relative chlorophyll (CHL) levels (%) of each mutant compared to WT. N.A. not analyzed. Asterisks indicate proteins that were not originally identified as DXI proteins in co-IP experiments.

Protein	Group	Mutant	AGI code	Line	Reference	Found in homozygosis	CHL rel. to WT
Fructose-bisphosphate aldolase 1	C	*fba1*	AT2G21330	SALK_063223	This study	Yes	110.55
Fructose-bisphosphate aldolase 2	C	*fba2*	AT4G38970	SALK_073444	This study	Yes	86.67
GAP dehydrogenase B subunit	C	*gapb*	AT1G42970	SAIL_308_A06	This study	Yes	101.68
Phosphoribulokinase	C	*prk-1*	AT1G32060	GK-117E07	-	No	-
		prk-2		ET5394	-	No	-
Sedoheptulose-1,7-bisphosphatase	C	*sbp-1*	AT3G55800	SALK_130939C	Liu et al., 2012	Yes	55.68
		sbp-2		SALK_090549C	This study	Yes	58.3
Plastid Ribosomal Protein L9	R	*rpl9*	AT3G44890	SALK_052906C	This study	Yes	99.14
Plastid Ribosomal Protein L19a*	R	*rpl19a*	AT5G47190	SALK_023092C	This study	Yes	98.29
Plastid Ribosomal Protein L19b*	R	*rpl19b-1*	AT4G17560	SALK_067948C	This study	Yes	105.73
		rpl19b-2		SALK_059283C	This study	Yes	99.34
Plastid Ribosomal Protein L24	R	*rpl24-1*	AT5G54600	SALK_010822	Romani et al., 2012; Liu et al., 2013	Yes	54.02
	R	*rpl24-2*		SALK_010823	Tiller et al., 2012	Yes	90.24
Plastid Ribosomal Protein L29	R	*rpl29*	AT5G65220	SALK_037831	This study	Yes	94.5
Plastid Ribosomal Protein S9	R	*rps9-1*	AT1G74970	SALK_134633C	This study	Yes	106.17
	R	*rps9-2*		SALK_128849C	This study	Yes	95.46
Plastid Ribosomal Protein S13	R	*rps13*	AT5G14320	SALK_087496	-	No	-
Plastid Ribosomal Protein S21*	R	*rps21*	AT3G27160	SALK_077692C	Morita-Yamamuro et al., 2004	Yes	40.67
Chloroplast Stem-Loop Binding Protein 41 KDa A	P	*csp41a-4*	AT3G63140	C. Koncz collection	Qi et al., 2012	Yes	112.36
Chloroplast Stem-Loop Binding Protein 41 KDa B	P	*csp41b-2*	AT1G09340	SALK_021748C	Qi et al., 2012; Bollenbach et al., 2009	Yes	73.06
Ferredoxin-NADP(+)-Oxidoreductase 1	P	*fnr1-1*	AT5G66190	SALK_085403	Lintala et al., 2007	Yes	103.15
		fnr1-2		SALK_067668	Lintala et al., 2007	Yes	111.54
Photosystem II Reaction Center PSB29 PROTEIN	P	*thf1-1/psb29*	AT2G20890	SALK_094925	Huang et al., 2006; Keren et al., 2005	Yes	31.93
		thf1-2		SALK_113467C	This study	Yes	N.A.
Photosystem II Subunit S	P	*cp22*	AT1G44575	SALK_095156C	-	No	-

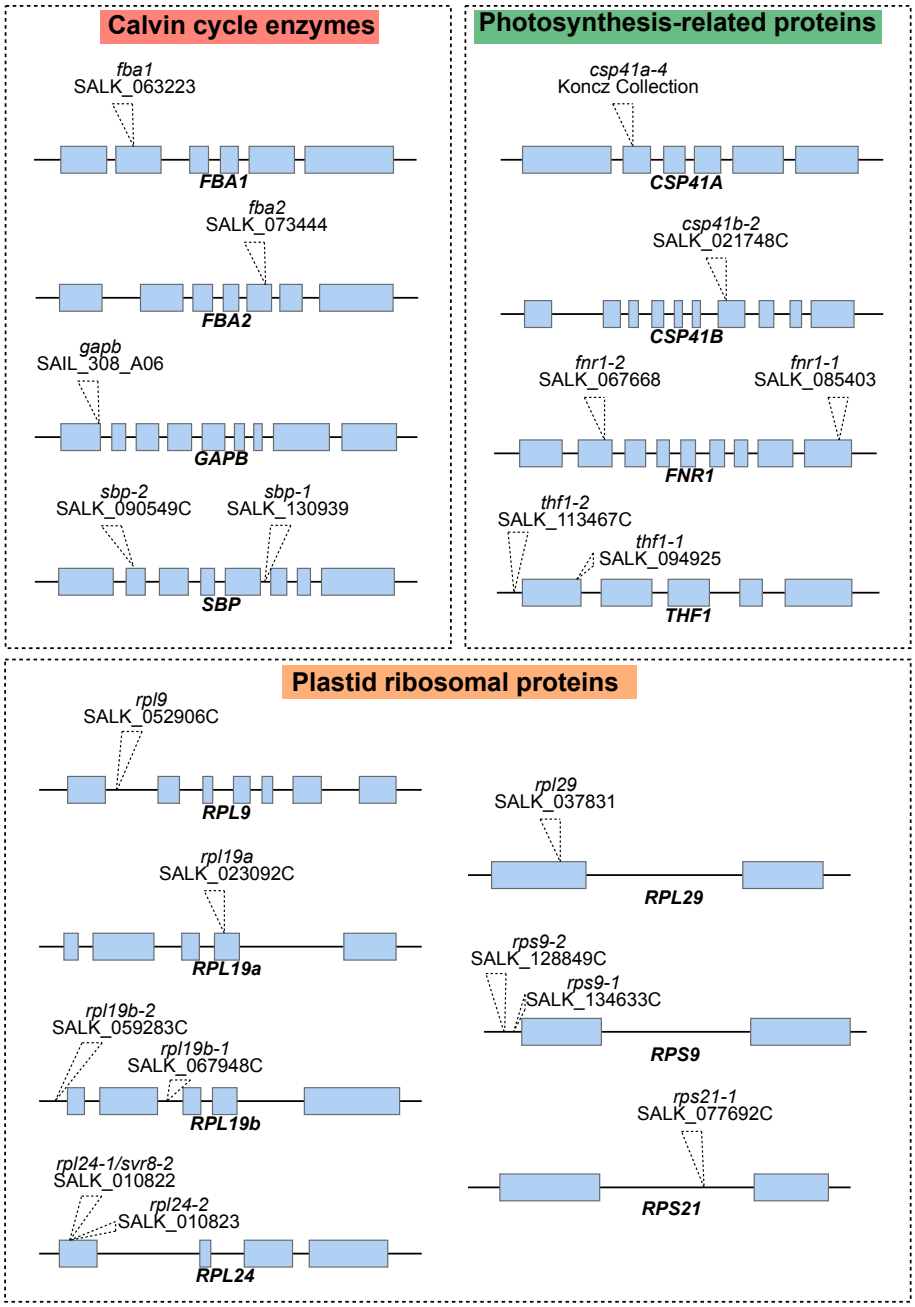

Figure 3.1: T-DNA insertions in the lines from which homozygous mutants defective in DXI and ribosomal proteins were isolated. Blue boxes indicate exons, gray lines introns, and dotted triangles the site of insertion of the T-DNA. Genes are not in scale.

DXS-GFP expression after agroinfiltration of whole *N. benthamiana* leaves was not homogeneously distributed in the tissue. Chloroplast-associated GFP fluorescence signal was evident only in minor sectors of the leaf. In agreement with this observation, detection of the DXS-GFP protein by immunoblot analysis with antibodies against GFP required a high antibody concentration and long exposure times. This fact might explain why no DXS-GFP could be found in co-IP samples with SBPase. Similar experiments using the anti-GFP serum for co-IP and the MYC antibody for immunoblot analysis were also unsuccessful to confirm interaction of DXS with SBPase.

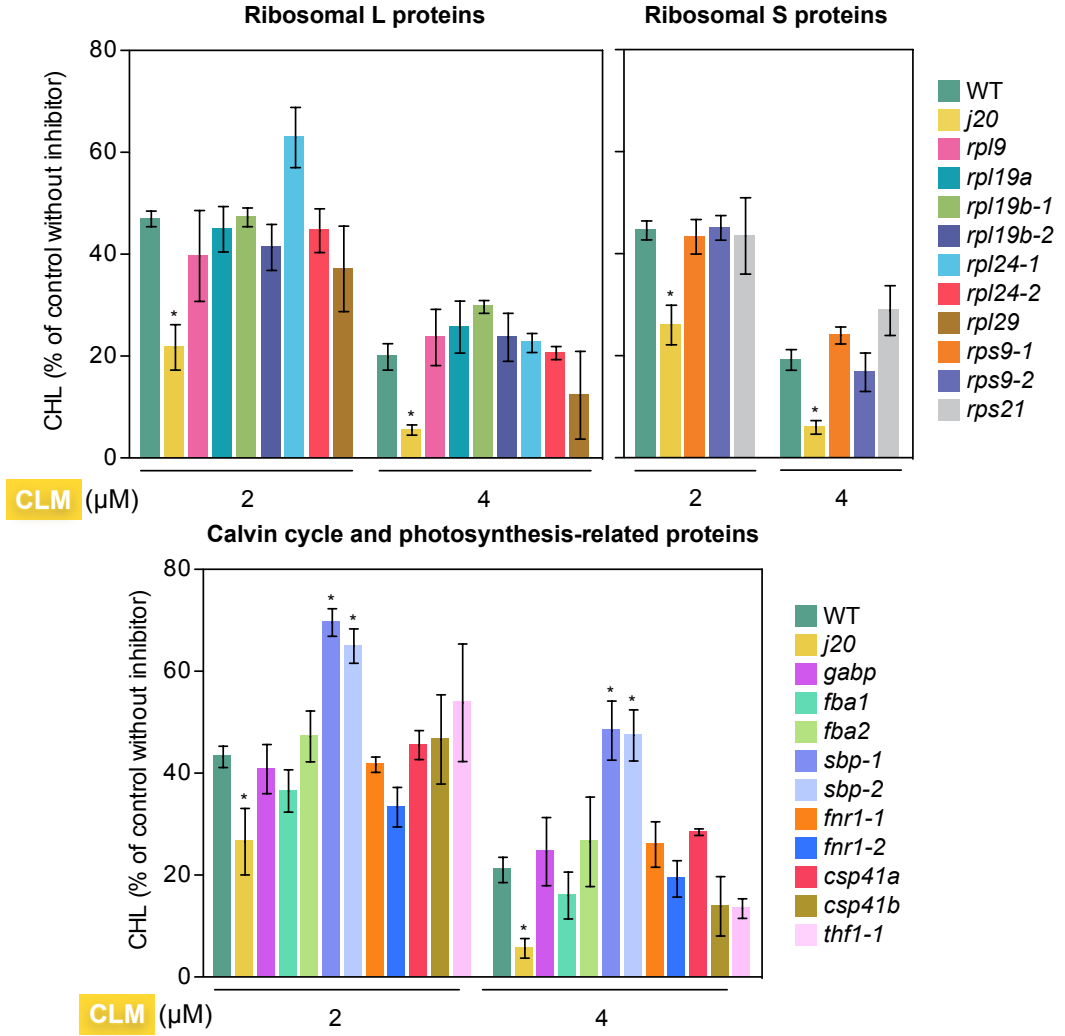

Figure 3.2: CLM sensitivity assays with *dxi* mutants. CLM sensitivity is represented as the loss of chlorophyll (CHL) in CLM-supplemented medium compared to non-supplemented controls (100%) of each line. Data correspond to the mean and SEM values of n≥3 independent experiments, and asterisks mark statistically significant differences (*t* test: p<0.05) relative to WT samples.

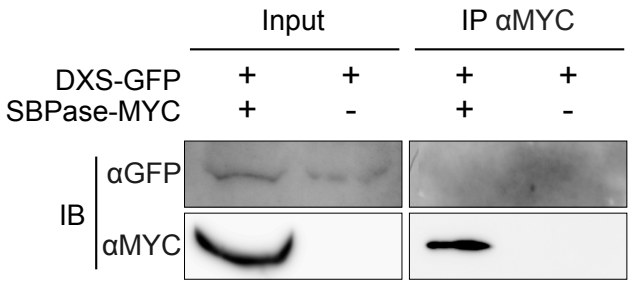

Figure 3.3: Co-IP experiments to confirm DXS-SBPase interaction *in planta*. Protein extracts from *N. benthamiana* plants transiently producing DXS-GFP alone or together with a MYC-tagged SBPase protein were used for co-IP with anti-MYC antibodies and further immunoblot (IB) analysis with anti-GFP or anti-MYC sera.

3.1.3 Inhibitor assays suggest that DXS activity is not increased in plants lacking SBPase

Despite the negative results of co-IP experiments, the fact that DXS function estimated as CLM resistance was altered in SBPase-defective plants prompted us to investigate the functional relationship between these two stromal enzymes. First, we used a more sensitive and direct inhibitor of DXS activity, KCLM (Figure 1.4), to validate our previous conclusions (*i.e.* that *sbp* mutants are more resistant to a pharmacological inhibition of DXS). To this end, we first tested the range of KCLM concentrations leading to decreased chlorophyll levels (Figure 3.4A) and arrested production of true leaves (Figure 3.4B) in WT plants. While germination and growth in the presence of KCLM caused phenotypes of chlorophyll loss and developmental arrest very similar to those obtained with CLM, nM concentrations of KCLM were necessary to produce the same effects caused by μM concentrations of CLM (Figure 3.4).

We next tested whether the conclusions from CLM sensitivity assays were confirmed using KCLM. In particular, we tested the *sbp-1* mutant (from now on, *sbp*) together with WT plants and two additional controls: *j20* mutant plants, with a reduced DXS activity, and a *35S:DXS-GFP* line, found to display higher DXS activity levels and hence reduced sensitivity to CLM (Pulido et al., 2013). As shown in Figure 3.4C, *j20* were indeed sensitive to KCLM, while the DXS overexpressing line and the *sbp* mutant were similarly resistant to the inhibitor. Representative images of the phenotypes of WT and *sbp* plants with or without KCLM in their growth medium are shown in Figure 3.4D.

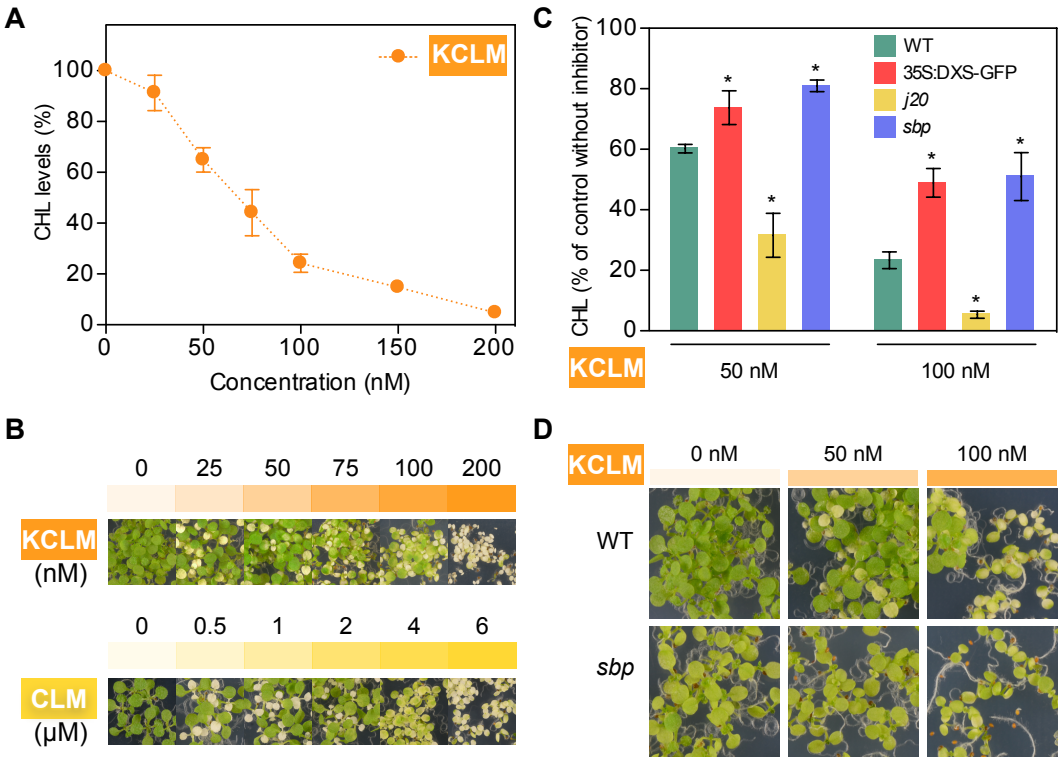

Figure 3.4: KCLM sensitivity assays confirm that plants lacking SBPase are resistant to KCLM. (A) Chlorophyll (CHL) levels of WT plants germinated and grown in medium supplemented with the indicated KCLM concentration relative to those in the absence of inhibitor. (B) Representative phenotype of WT plants grown at the indicated CLM and KCLM concentration. (C) CHL levels of WT, *35S:DXS-GFP*, *j20*, and *sbp* plants at the indicated KCLM concentration. (D) Phenotypic comparison between WT and *sbp* plants grown with or without KCLM. For all the experiments, 10-day-old plants were used.

While an obvious mechanism for the CLM and KCLM resistance phenotype of the *sbp* mutant could be the up-regulation of DXS activity, defects in SBPase activity causes a pale and delayed growth phenotype (Liu et al., 2012), as shown in Figure 3.4C (compare WT and mutant plants grown in the absence of KCLM). This is in sharp contrast with *35S:DXS-GFP* plants, which are green, develop normally, and produce increased levels of MEP-derived isoprenoids such as carotenoids, chlorophylls and tocopherols (Estevez et al., 2001; Carretero-Paulet et al., 2006). HPLC analysis of WT and *sbp* plants confirmed that the mutant only accumulated *ca.* 60% of the photosynthetic pigments found in the WT (Figure 3.5 and Table 3.2). It is possible that defective carbon assimilation and starch biosynthesis in the mutant, which is impaired in the Calvin cycle, prevents normal accumulation of MEP-derived isoprenoids to support normal photosynthesis and growth even when DXS activity is increased. Interestingly, tocopherols (antioxidant isoprenoids) and the carotenoid zeaxanthin (usually absent under normal growth conditions but produced from violaxanthin under high light stress) were not decreased but increased in the mutant. These results suggest that loss of SBPase activity leads to pleiotropic phenotypes impacting isoprenoid metabolism and stress responses at several levels.

Table 3.2: Carotenoid, chlorophyll and tocopherol contents of 10-day-old WT plants and lines with altered SBPase levels (in μg/mg dry weight). The values are the mean with the corresponding SD of n=4 independent samples. N.D. not detected.

Metabolite	**WT**	***35S:SBP-GFP* H**	***35S:SBP-GFP* M**	***35S:SBP-GFP* L**	***sbp***
Violaxanthin	0.44±0.03	0.43±0.03	0.43±0.04	0.48±0.02	0.25±0.02
Neoxanthin	0.23±0.01	0.21±0.00	0.22±0.01	0.24±0.02	0.18±0.01
Lutein	1.48±0.09	1.40±0.04	1.45±0.04	1.52±0.11	1.06±0.02
Zeaxanthin	N.D.	N.D.	N.D.	N.D.	0.10±0.01
β-carotene	0.61±0.03	0.58±0.02	0.59±0.04	0.65±0.04	0.30±0.01
Total carotenoids	2.76±0.14	2.63±0.07	2.70±0.11	2.89±0.18	1.90±0.06
Chlorophyll a	0.71±0.04	0.67±0.01	0.70±0.02	0.74±0.05	0.54±0.04
Chlorophyll b	1.69±0.10	1.60±0.05	1.66±0.04	1.75±0.13	0.96±0.09
Total chlorophylls	2.40±0.14	2.27±0.06	2.36±0.06	2.49±0.19	1.50±0.13
γ-tocohopherol	0.02±0.01	0.03±0.01	0.03±0.01	0.02±0.01	0.04±0.01
α-tocopherol	0.12±0.02	0.11±0.01	0.12±0.01	0.13±0.01	0.21±0.01
Total tocopherols	0.15±0.02	0.13±0.01	0.14±0.01	0.15±0.01	0.25±0.01

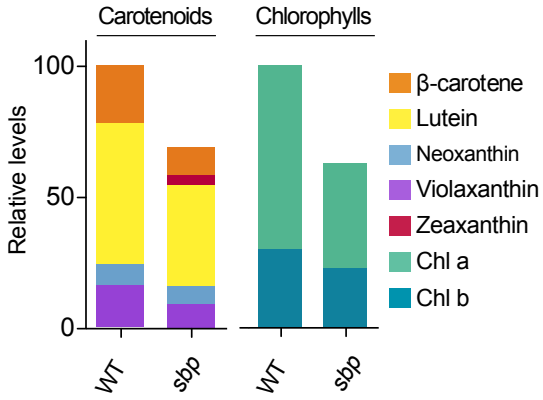

Figure 3.5: Carotenoid and chlorophyll contents of WT and *sbp* plants. The average content from n=4 independent samples of 10-day-old plants germinated and grown in the absence of inhibitors is represented.

Based on the described difficulties to draw robust conclusions on DXS function from the analysis of isoprenoid profiles in *sbp* plants, we decided to perform other experiments in order to test whether DXS protein levels or activity were enhanced in SBPase-defective plants. It has been reported that lines overexpressing DXS show resistance to both CLM and FSM (due to a higher production of DXP, which competes with FSM for the active site of DXR) and those overexpressing DXR are resistant to FSM but not to CLM (Carretero-Paulet et al., 2006; Flores-Perez et al., 2008a; Perello et al., 2014). Similar to that described for CLM and KCLM, germination and growth in the presence of FSM causes a chlorophyll loss that can be quantified to compare resistance of different plant lines to the inhibitor (Perello et al., 2014). As shown in Figure 3.6, similar phenotypes are also caused by NFZ, an inhibitor of carotenoid biosynthesis (Figure 1.4). If DXS activity is specifically increased in SBPase-defective plants, it would be expected that they showed an increased resistance to FSM but not to NFZ compared to WT plants. To investigate whether the *sbp* mutant was resistant to these inhibitors, we used concentrations of FSM and NFZ causing a chlorophyll

loss in WT plants of about 50% compared to no-inhibitor conditions (Figure 3.6A-B). However, these resistance assays showed that the *sbp* mutant was not resistant to FSM or NFZ (Figure 3.6C). Furthermore, immunoblot analysis showed similar DXS protein levels in WT and *sbp* plants (Figure 3.7). We therefore concluded that the resistance of *sbp* plants to CLM and KCLM might not be directly due to increased levels of DXS enzyme or its catalytic activity but result from other alterations in the mutant.

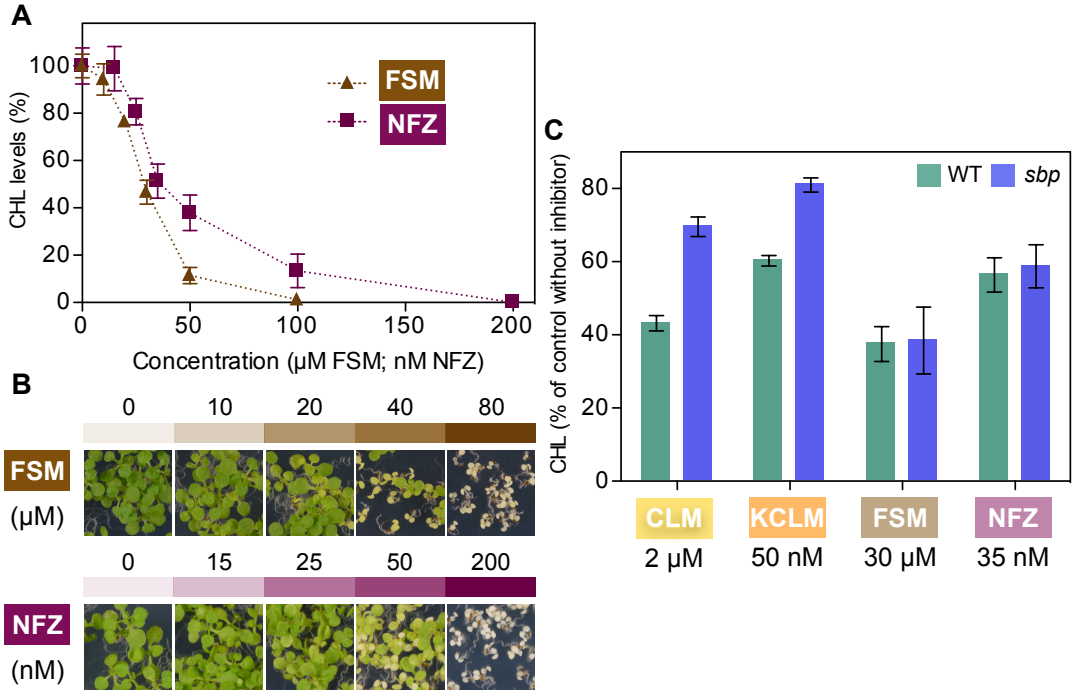

Figure 3.6: *sbp* mutants are not resistant to other isoprenoid biosynthesis inhibitors such as FSM and NFZ. (A) Chlorophyll (CHL) levels of 10-day-old WT plants germinated and grown in medium supplemented with the indicated concentrations of FSM or NFZ. (B) Observed phenotype of WT plants germinated and grown in the presence of the inhibitors. (C) CHL levels of WT and *sbp* plants exposed to the indicated inhibitors. CHL levels are represented relative to each untreated line. Data correspond to the mean and SEM values of n≥3 independent experiments.

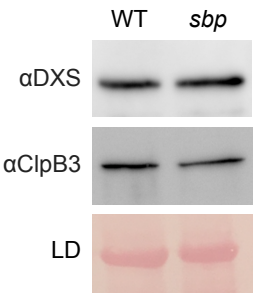

Figure 3.7: WT and *sbp* plants have similar DXS levels. Immunoblot against DXS and ClpB3 from WT and *sbp* 10-day old plants. Ponceau S staining is shown as loading control (LD).

3.1.4 Increased SBPase levels result in sensitivity to KCLM

SBPase functions in the Calvin cycle catalyzing the dephosphorylation of sedoheptulose-1,7-bisphosphate to sedoheptulose-7-phosphate at the branch point where assimilated carbon (GAP) may either go to the regenerative phase (to produce the CO_2 acceptor RuBP) or be exported from the cycle for carbohydrate (and isoprenoid) biosynthesis (Figure 1.6). This particular position makes SBPase one of the major regulators of carbon flow in the Calvin cycle (Raines, 2003).

As the lack of SBPase activity would be expected to result in a lower diversion of GAP to the regenerative phase of the Calvin cycle (Figure 1.6), it is possible that more GAP might be available in the *sbp* mutant to be used for the MEP pathway. Higher levels of GAP might compete with KCLM for binding to DXS, hence causing resistance to this inhibitor but not to FSM or NFZ. If this is the case, it is reasonable to think that an enhanced activity of SBPase diverting GAP away from the MEP pathway would result in enhanced KCLM sensitivity. To test this idea, we generated transgenic Arabidopsis plants overexpressing a full-length SBPase protein fused to GFP. We obtained six independent homozygous lines and selected three of them based on their high (H), medium (M), or low (L) level of SBPase-GFP protein accumulation (Figure 3.8A). These three lines showed a homogeneous stromal localization of the SBPase-GFP protein as previously reported (Liu et al., 2012), in contrast to DXS-GFP, that shows a spotted pattern of plastidial fluorescence (Figure 3.8B) (Pulido et al., 2013). Also in contrast with *35S:DXS-GFP* plants, the *35S:SBP-GFP* lines analyzed by HPLC accumulated WT levels of MEP-derived chlorophylls, carotenoids, and tocopherols (Figure 3.10 and Table 3.2).

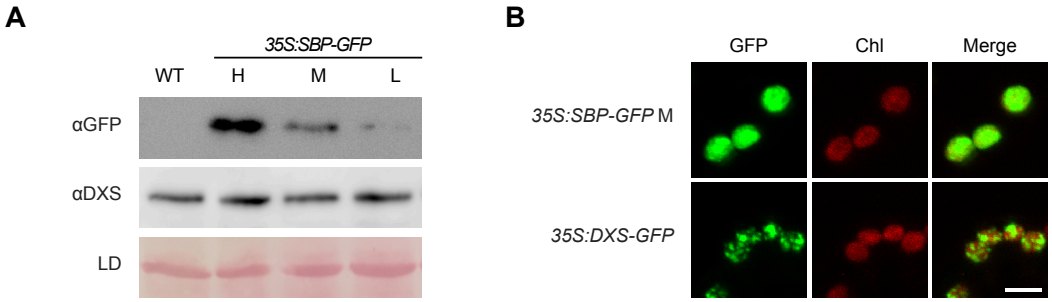

Figure 3.8: Characterization of Arabidopsis plants with different SBPase-GFP levels. (A) Immunoblot analysis of transgenic SBPase-GFP and endogenous DXS proteins in WT plants and *35S:SBP-GFP* lines. Ponceau S staining is shown as a loading control (LD). (B) Confocal analysis of Arabidopsis transgenic plants producing SBPase-GFP or DXS-GFP. Images show GFP fluorescence, chlorophyll autofluorescence (Chl) and a merged image of both channels. White bar indicates 4 μm. 10-day-old plants were used for both analysis.

We next tested the H, M and L lines for KCLM resistance and observed that, as

predicted, they were more sensitive to the inhibitor compared to WT plants (Figure 3.9A). However, there was no correlation between the intensity of the KCLM sensitivity phenotype and the levels of SBPase-GFP protein accumulated in the transgenic lines. Immunoblot analysis indicated that DXS levels remained unchanged among the three transgenic lines compared to WT plants (Figure 3.8A).

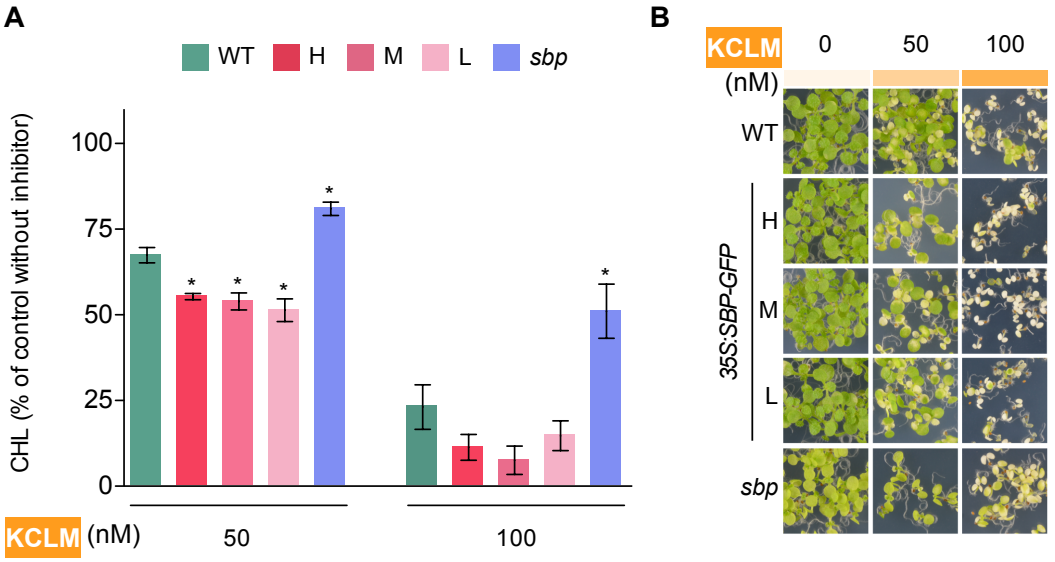

Figure 3.9: Arabidopsis plants with different SBPase-GFP levels are more sensitive to KCLM. (A) KCLM sensitivity assay. Chlorophyll (CHL) levels at the indicated concentrations of KCLM relative to control untreated plants. Mean and SEM of n3 independent experiments are represented. KCLM sensitivity is represented as the loss of chlorophyll in KCLM-supplemented medium compared to non-supplemented controls (100%) of each line. Data correspond to the mean and SEM values of n≥3 independent experiments, and asterisks mark statistically significant differences (*t* test: p<0.05) relative to WT samples. (B) Representative phenotype of WT plants and lines with altered SBPase activity grown at the indicated KCLM concentration.

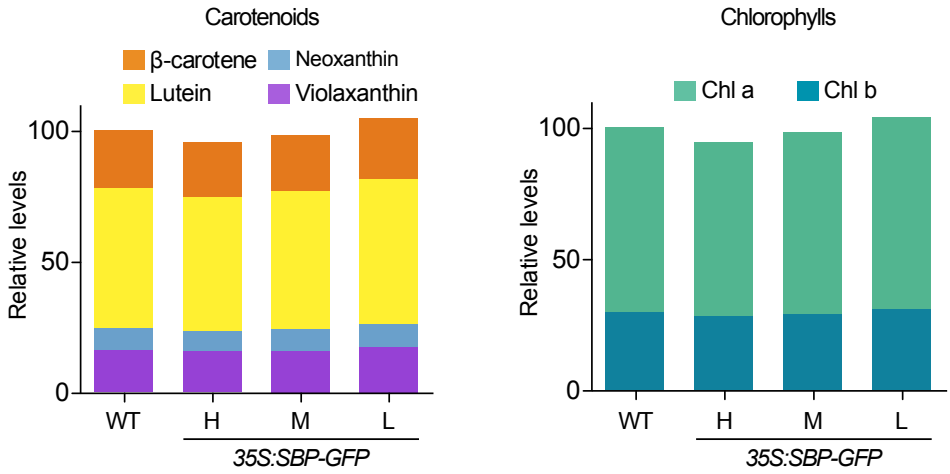

Figure 3.10: Carotenoid and chlorophyll contents of WT plants and lines with higher SBPase levels. The average content from n=4 independent samples of 10-day-old plants germinated and grown in the absence of inhibitors is represented.

Together, the results support our model that the observed phenotypes of KCLM resistance in the case of the *sbp* mutants and KCLM sensitivity in the case of transgenic *35S:SBP-GFP* plants are not due to changes in DXS levels or DXS enzymatic activity. Instead, they likely derive from increased (*sbp*) or decreased (*35S:SBP-GFP*) availability of GAP, respectively, to compete with the inhibitor.

3.2 Chapter II. Protein quality control mechanisms regulating DXS turnover in the plastid

3.2.1 DXS tends to aggregate within the chloroplast

As described in the introduction, it was proposed that DXS polypeptides can become misfolded after plastid import or stress (Pulido et al., 2013). The most common destiny for misfolded proteins is self-aggregation because the mistaken exposure to the solvent of hydrophobic fragments, usually buried inside the protein, lead to a high degree of stickiness (Moreno-Gonzalez and Soto, 2011). In collaboration with Dr. Salvador Ventura, we analyzed if DXS is prone to form aggregates taking advantage of the Aggregascan3D predictor (Zambrano et al., 2015). The active DXS enzyme is a dimer, but misfolded proteins would be expected to remain in a monomer state. The structure of the Arabidopsis DXS monomer was modeled based on the *E. coli* DXS crystal structure to perform a computational analysis. After the bioinformatic analysis, the software revealed the presence of several aggregation-prone clusters in the DXS monomer that were highly attenuated in the dimer (Figure 3.11).

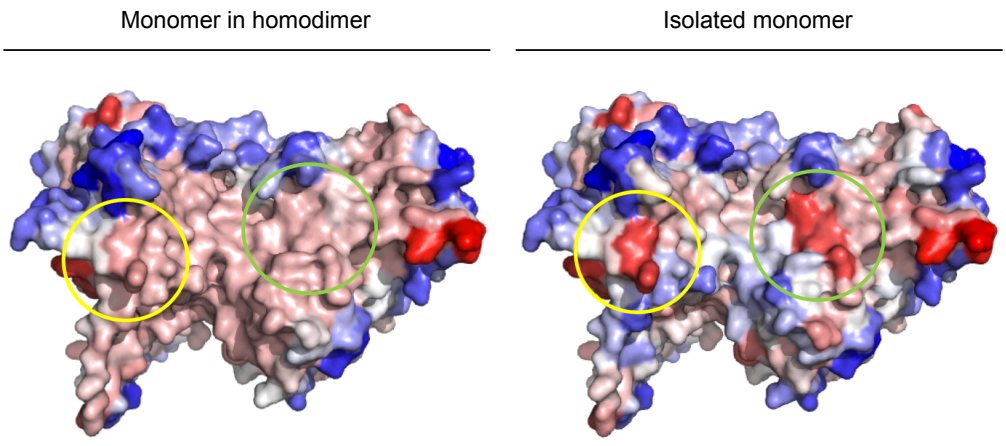

Figure 3.11: Aggregation propensity of Arabidopsis DXS monomer. The protein surface is colored according to Aggregascan3D score in a gradient from red (high-predicted aggregation propensity) to white (negligible impact on protein aggregation) to blue (high-predicted solubility). The model in the left corresponds to the monomeric chain in the dimeric structure of the active DXS enzyme, whereas the model in the right corresponds to the isolated monomer. High aggregation-propensity regions are marked with yellow circles (residues Tyr234 and Leu235) and green circles (residues Phe514, Phe518 and Cys521).

Aggregated proteins become insoluble and many protein aggregates become associated to cell membranes. If DXS aggregates, it would be expected that at least some of the protein (1) could be found in insoluble form and (2) could unspecifically bind to chloroplast membranes. To investigate the subplastidial distribution of DXS, we separated chloroplast structures using flotation centrifugation with sucrose density gradients (Vidi et al., 2007). First, we isolated chloroplasts from transgenic plants producing the plastoglobule marker PGL34-YFP (Vidi et al., 2007) and then we used them for membrane fractionation, protein extraction and immunoblot analysis with antibodies against DXS. In the same fractions, we also analyzed the presence of control proteins known to be localized in plastoglobules (PGL34-YFP), embedded in the thylakoid membrane (PsbA), associated to the stromal side of the thylakoid membrane (AtpB), or found in the stroma (ClpP1). As a MEP pathway control, we also included analyzed the subplastidial distribution of DXR. Both DXS and DXR were found in the soluble (stromal) fraction, as expected (Phillips et al., 2008; Joyard et al., 2009). However, DXS proteins were also detected in fractions corresponding to membrane-containing structures other than plastoglobules (Figure 3.12), whereas most of the DXR protein remained in the soluble (stromal) fraction.

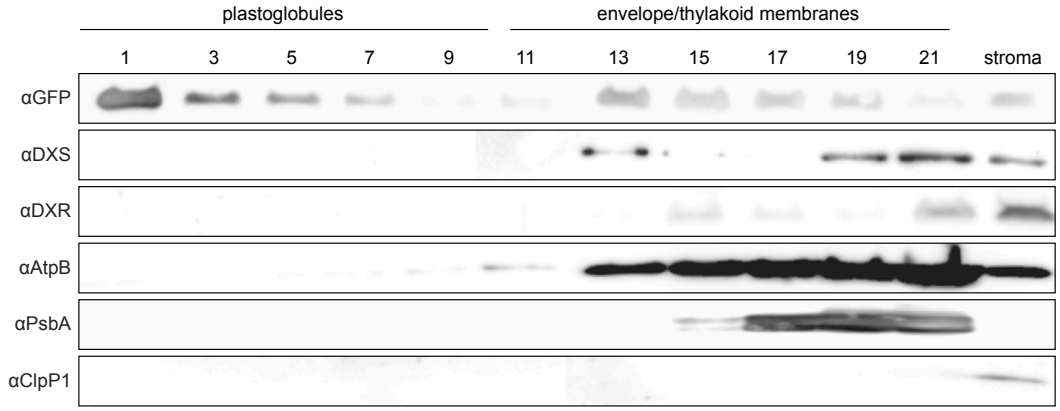

Figure 3.12: Immunoblot analysis of chloroplast subfractions. Chloroplasts isolated from transgenic plants overexpressing PGL34-YFP were used to separate soluble (stromal) and membrane fractions. Chloroplast were loaded in a sucrose density gradient and separated by ultracentrifugation. Proteins contained in 35 μl of sequential fractions collected from the top of the sucrose gradient or the stromal sample were separated by SDS-PAGE and transferred to a membrane for immunoblot analysis with antibodies against GFP (to detect PGL34-YFP) or the indicated endogenous proteins.

We next investigated whether the differential distribution of DXS and DXR in subplastidial fractions could be the result of a stronger aggregation propensity of the DXS protein. To this end, we analyzed the subplastidial localization of full-length versions of the proteins fused to GFP by confocal microscopy at different time points after agroinfiltration of *N. benthamiana* leaves with *35S:DXS-GFP* and *35S:DXR-GFP* constructs. Stromal fluorescence was detected for DXS-GFP and DXR-GFP at all time points analyzed. However, these two fusion proteins were also found to form

fluorescent corpuscles (Figure 3.13). In the case of DXS-GFP, fluorescence was predominantly localized in the stroma at the first days (1-3) after agroinfiltration. Later, on day 5, it showed a spotted distribution. By day 7, fluorescent spots were fainter, and a more general distribution of the DXS-GFP protein inside chloroplasts was observed (Figure 3.13). This dynamic behavior of DXS-GFP distribution is consistent with the aggregation of the protein when its levels in the chloroplast are too high. Speckles within the chloroplast were also observed for DXR-GFP, but in this case, small fluorescent spots were already detected during the first days following agroinfiltration and progressively concentrated in a few large bodies in the chloroplast at later stages. Some fluorescent bodies lacking chlorophyll were also detected outside the chloroplast, especially at late time points (7 days) (Figure 3.13). Other experiments confirmed that, unlike DXS-GFP, the DXR-GFP protein remained soluble but exceeding amounts of the transgenic protein were eventually contained inside intraplastidial vesicles that eventually left the chloroplast, presumably for degradation of its contents (including DXR-GFP) in vacuoles (Perello et al., 2014).

The observation that the fluorescent clumps formed by the DXS-GFP protein are larger in the *j20* mutant (Pulido et al., 2013) is in further agreement with the conclusion that DXS is a MEP pathway enzyme prone to aggregation. To more deeply investigate if DXS becomes more aggregated when J20 is lost, we carried out a protease protection assay, based on the known property of aggregated proteins to be less accessible to proteolytic degradation (*e.g.* by proteinase K). We initially tested whole protein extracts from WT plants, incubating them for 5 minutes with different concentrations of proteinase K (0, 0.1, 0.2, 0.3 and 0.4 μg/mL). Then, the levels of endogenous DXS (and DXR) proteins were analyzed in immunoblots. Using these conditions, we obtained a linear degradation rate of DXS (Figure 3.14A). Interestingly, DXR protein remained stable in such conditions. To degrade DXR at the same rate that DXS we required 20-fold longer incubation times with the same proteinase K concentrations (Figure 3.14A), suggesting that DXR is much more stable (*i.e.* resistant to proteolytic degradation) than DXS. Finally, we proceeded to compare DXS degradation rate between WT and *j20* plants. In this case, DXS polypeptides were less accessible to proteinase K cleavage in the *j20* mutant background (Figure 3.14B).

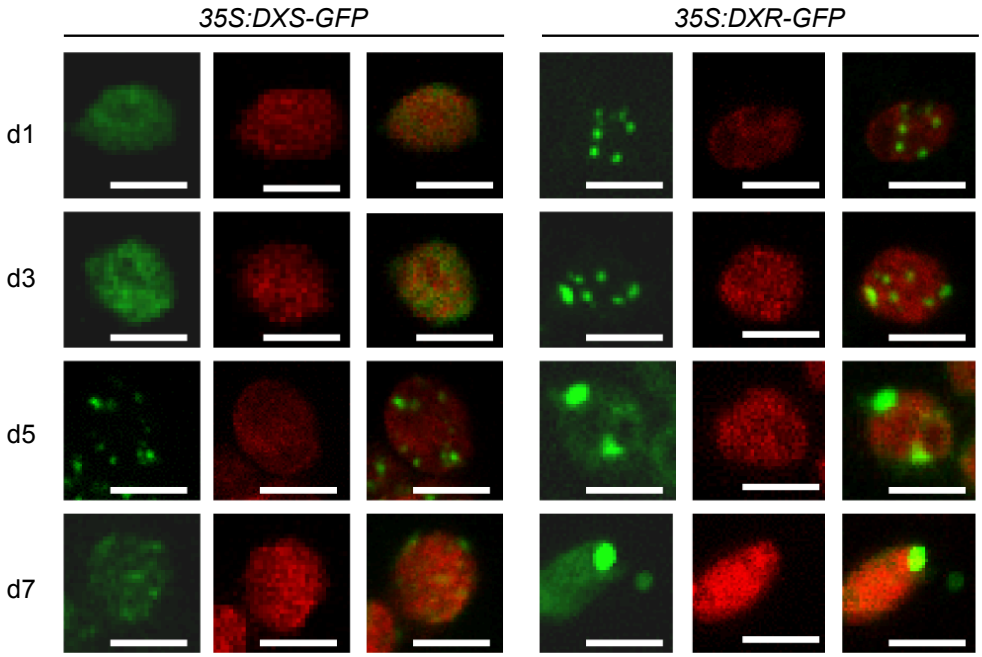

Figure 3.13: Distribution of GFP-tagged isoprenoid enzymes in chloroplasts of agroinfiltrated *N. benthamiana* leaves. Images show representative mesophyll chloroplasts from leaves collected at different days (from from d1 to d7) after agroinfiltration with the indicated constructs. For each construct, GFP fluorescence (left columns), chlorophyll autofluorescence (middle columns) and merged images (right columns) are shown. White bars indicate 5 μm

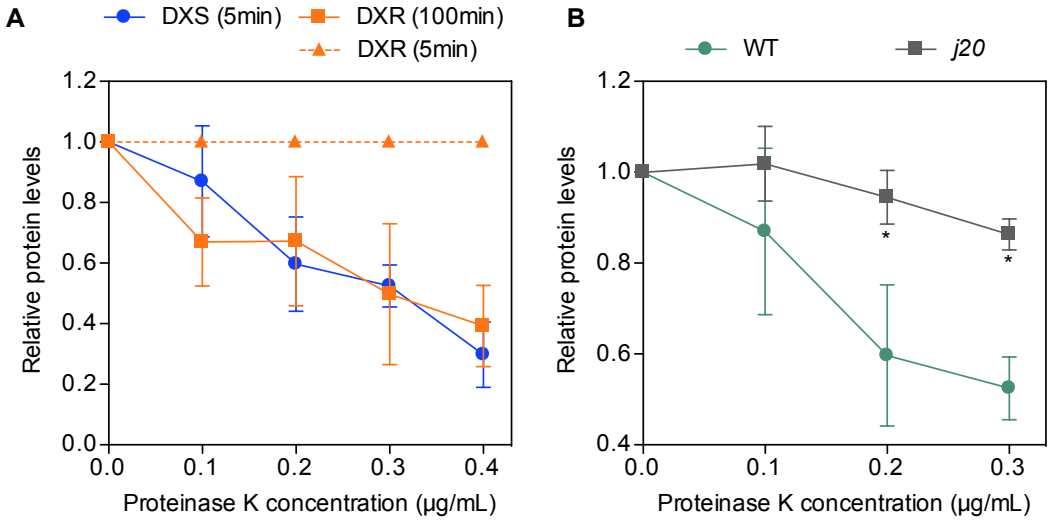

Figure 3.14: Aggregation phenotype of DXS in WT and *j20* plants. (A) Quantification of DXS and DXR protein levels by immunoblot analysis of WT protein extracts incubated with the indicated concentrations of proteinase K for the indicated times. (B) Analysis of DXS protein abundance by immunoblot analysis of protein extracts from WT and *j20* plants incubated with the indicated concentrations of proteinase K for 5 min. Data corresponding to the mean and SE values of n=4 independent experiments. Asterisks mark statistically significant differences (*t* test: $p<0.05$) relative to WT samples.

Our results support the conclusion that DXS enzymes aggregate. They also indicate

that J20 prevents DXS aggregation, likely because it delivers aggregated (and hence inactive) DXS proteins to the Hsp70 chaperone for refolding (and reactivation) or degradation.

3.2.2 DXS appears to be primarily degraded by the stromal Clp protease via ClpC1

The J20 protein was previously found to interact with inactive forms of DXS (Pulido et al., 2013). The experiments shown above suggest that these inactive forms might be misfolded DXS monomers that aggregate and precipitate or associate to plastidial membranes, which might eventually have toxic effects. However, the molecular components involved in the two proposed J20-dependent antagonistic pathways that disaggregate and unfold DXS to either refolding or degradation remained unknown when this thesis work started.

Arabidopsis mutants with a decreased activity of the stromal Clp protease accumulate higher levels of several MEP pathway enzymes, including DXS (Flores-Perez et al., 2008a; Kim et al., 2009; Zybailov et al., 2009; Rudella et al., 2006; Kim et al., 2013; Pulido et al., 2016). More recently, work in our lab analyzed DXS protein levels in mutants for all main groups of plastidial proteases, including the Clp protease but also Lon, Deg, or FtsH. DXS protein levels in the analyzed mutants were like those in WT plants with only three exceptions. Lines defective in Lon1 and Deg7 showed a decreased accumulation of the protein compared to the WT, whereas DXS levels were only increased in Clp protease-defective mutants suh as *clpr1* (Pulido et al., 2016). No changes in DXS transcript levels were detected in the analyzed mutant lines compared to WT plants. From this analysis, it was concluded that the Clp complex is likely the primary protease for DXS removal (Pulido et al., 2016). Specifically, it was suggested that DXS was unfolded prior to delivery to the proteolytic chamber by ClpC1, because plants defective in this Clp complex-bound Hsp100 chaperone accumulated higher levels of DXS proteins and showed slower DXS proteolytic removal when compared to WT plants (Pulido et al., 2016). To confirm whether DXS is degraded by the Clp protease through interaction with ClpC1, we overproduced tagged versions of the Arabidopsis proteins DXS-GFP and ClpC1-MYC in *N. benthamiana* leaves by agroinfiltration. After three days, we performed co-IP assays that confirmed that DXS and ClpC1 could be found together in the same complex (Figure 3.15).

Based on the described results and the available understanding of Hsp100 and Hsp70 chaperones in different systems (Miot et al., 2011), we thought that ClpC1 together with Hsp70 might collaborate to unfold aggregated forms of DXS and deliver them to the Clp protease using J20 as an adaptor. To test our hypothesis, we compared *in vivo* DXS degradation rate in *j20* and WT plants upon treating them with the

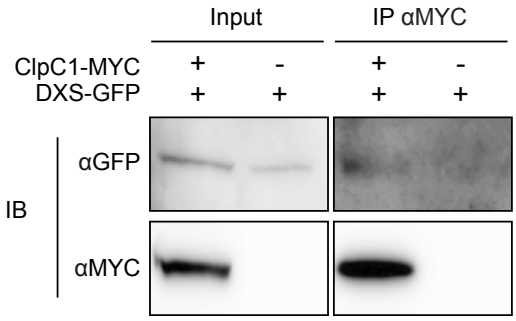

Figure 3.15: ClpC1 interacts with DXS. Protein extracts from *N. benthamiana* leaves transiently producing DXS-GFP alone or together with a MYC-tagged ClpC1 protein were used for co-IP with anti-MYC antibodies (MYC) and further immunoblot (IB) analysis with anti-GFP or anti-MYC sera. Immunoblot analyses of the extracts before immunoprecipitation (input samples) are also shown.

protein synthesis inhibitor cycloheximide (CHX). Consistent with our idea, we observed a reduced degradation rate of DXS enzyme in the *j20* mutant background when compared to WT (Figure 3.16), demonstrating that J20 is necessary to target DXS to degradation.

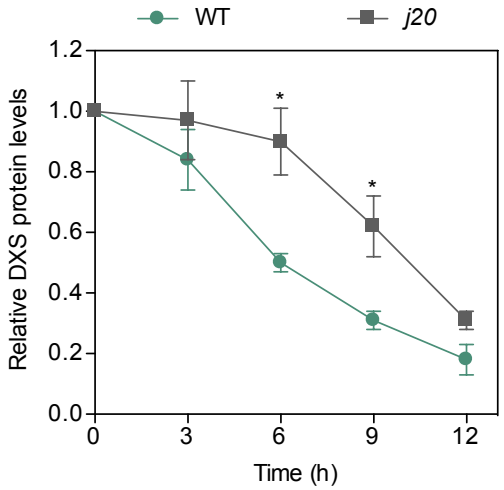

Figure 3.16: J20 is required for normal DXS degradation. WT and *j20* plants were grown for one week on medium lacking the protein synthesis inhibitor CHX and then transferred to a medium supplemented with the inhibitor for the indicated times. DXS protein levels detected by immunoblot analysis are represented relative to those before treatment. Mean, and SEM of n≥3 experiments are shown. Asterisks mark statistically significant differences (*t* test: $p<0.05$) relative to WT samples.

3.2.3 Degradation or activation of DXS might depend on the relative abundance of Hsp100 chaperones

While the Hsp100 chaperone ClpC1 appears to be involved in the J20-Hsp70-dependent degradation of DXS by the Clp protease, work in our laboratory has shown that Hsp70 can be assisted by another type of Hsp100 chaperone, ClpB3, to disaggregate

and solubilize aggregated DXS proteins (Pulido et al., 2016). Unlike ClpC1, ClpB3 lacks the IGF motif (or ClpP-loop) required for interaction with proteolytic subunits of the Clp core (Levchenko et al., 2000; Kim et al., 2001; Doyle et al., 2007) but it harbors a domain that allows its direct interaction with Hsp70 chaperones (Pulido et al., 2016). The results from this thesis and published data (Pulido et al., 2016) are therefore consistent with a model involving the participation of ClpB3 and ClpC1 on different pathways leading in either reactivation or degradation, respectively, of inactive DXS proteins previously recognized by the Hsp70 adaptor J20 (Pulido et al., 2016; Pulido et al., 2013). As shown in Figure 3.17 the levels of ClpB3 chaperones are lower than those of ClpC1 under normal growth conditions (Zybailov et al., 2008; Pulido et al., 2016), but this can change under stress conditions, when the levels of transcripts encoding ClpB3 (but not those encoding ClpC1) are up-regulated (Lee et al., 2007; Myouga et al., 2006; Rasmussen et al., 2013; Zheng et al., 2002). We reasoned that the ratio between plastidial ClpB3 and ClpC1 chaperones and hence the potential capacity of the chloroplast to reactivate damaged or/and aggregated DXS polypeptides increase when plants are challenged with stress.

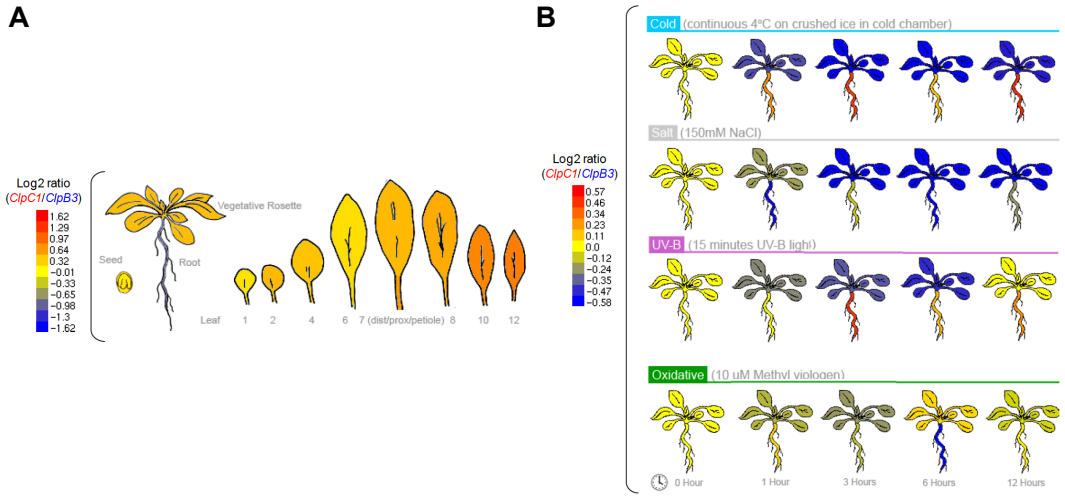

Figure 3.17: Comparison of transcript levels of genes coding ClpC1 and ClpB3. Data were obtained from the Arabidopsis eFP browser at www.bar.utoronto.ca and correspond to the gene expression map of Arabidopsis development (A) and abiotic stress treatments (B).

3.2.4 CLM treatment induces the accumulation of both DXS and ClpB3 proteins

DXS protein abundance is regulated by MEP pathway products, most likely IPP and DMAPP (Guevara-Garcia et al., 2005; Han et al., 2013; Pokhilko et al., 2015). In particular, when IPP and DMAPP levels decrease due to a reduced production or an activated consumption by downstream pathways, the accumulation of DXS enzymes (but not transcripts) increases to up-regulate the MEP pathway flux and restore normal IPP and DMAPP levels. To analyze if J20-Hsp70-dependent pathways involving ClpC1 or/and ClpB3 chaperones were associated to this physiological response, we

germinated and grew WT plants in CLM to reduce DXS activity (and hence IPP and DMAPP production) and studied the impact on DXS, Hsp70, ClpC1 and ClpB3 protein levels. Germination and growth of WT plants in the presence of CLM increased the accumulation of DXS and ClpB3 but not Hsp70 or ClpC chaperones compared to controls grown in the absence of inhibitor (Figure 3.18A). Next, we transferred WT plants germinated and grown on non-supplemented medium to plates containing CLM and collected samples after 5 and 10 h. With this experimental setup, DXS and ClpB3 accumulation was detected as soon as 5 h after reducing the MEP pathway flux by treatment with CLM (Figure 3.18B). Therefore, it is likely that changes in ClpB3 protein levels follow those in DXS enzyme accumulation to prevent its aggregation and hence ensure catalytic activity when the functioning of the MEP pathway is compromised.

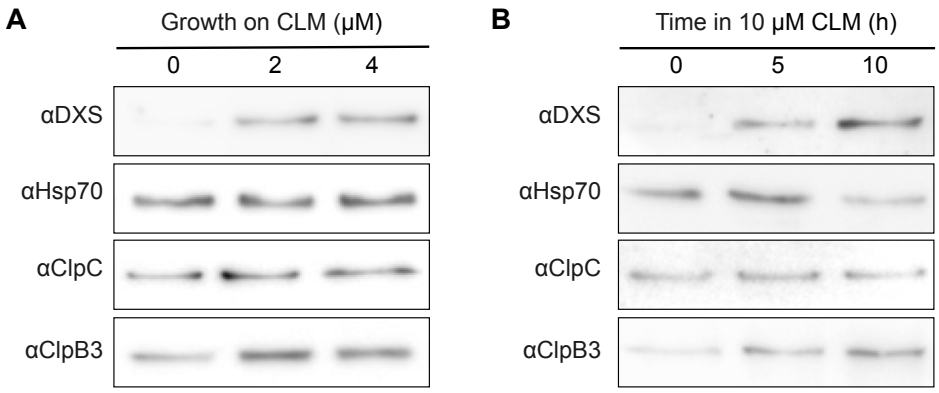

Figure 3.18: Accumulation of ClpB3 but not ClpC chaperones when DXS activity or MEP pathway flux decrease. (A) Representative immunoblot analyses of WT plants germinated and grown for 10 days on media supplemented with the indicated concentrations of CLM. (B) Representative immunoblot analyses of WT plants grown for 7 days on MS medium and then transferred for the indicated times to medium supplemented with 10 μM CLM.

3.3 Chapter III. A Chloroplast Unfolded Protein Response regulates DXS Protein Quality Control

3.3.1 Pharmacological and genetic interference with PGE triggers the accumulation of plastidial ClpB3 chaperones

Inside the organelles, the lifespan and activity of proteins depend on PQC systems to provide correct protein folding and prevent the formation of toxic aggregates. When unfolded or misfolded proteins accumulate and aggregate in mitochondria, the UPR is activated to communicate with the nucleus and induce expression of nuclear genes encoding mitochondria-targeted PQC components (Arnould et al., 2015; Lin and Haynes, 2016; Fiorese and Haynes, 2017). The existence of a cpUPR has been recently proposed (Ramundo and Rochaix, 2014; Colombo et al., 2016). We speculated that such a cpUPR could be behind the increase in ClpB3 levels detected

after stress episodes, when DXS activity needs to be preserved. In particular, when Clp protease activity is compromised (*e.g.* in *clpr1* and *clpc1* mutants), an increase in ClpB3 protein levels occurs, most likely to prevent the formation of protein aggregates (including those of DXS) and promote the refolding and hence reactivation of the proteins that cannot be degraded (Nishimura and Van Wijk, 2015; Pulido et al., 2016). However, the mechanisms controlling the increase in ClpB3 levels are currently unknown.

In mitochondria, UPR can be unleashed through interference with the expression of the organelle genome, *e.g.* by inhibiting protein translation (Arnould et al., 2015). Interestingly, an enhanced accumulation of DXS protein levels (but not transcripts) was observed upon genetic of pharmacological inhibition of PGE (Sauret-Gueto et al., 2006; Flores-Perez et al., 2008a). It was shown that treatment with PGE inhibitors such as CAP interferes with the production of the plastome-encoded ClpP1 subunit of the Clp protease, disrupting the stoichiometry of the whole complex and hence reducing its proteolytic activity (Flores-Perez et al., 2008a). This is a very good system to analyze whether a cpUPR elicits the accumulation of ClpB3 when the Clp protease activity is saturated, as treatment with increasing concentrations of PGE inhibitors would be expected to progressively result in reduced Clp protease activity.

To verify the possible existence of a cpUPR acting in response to alteration in PGE and Clp protease activity (*i.e.* to altered protein homeostasis), we tested different concentrations of a PGE inhibitor in plants for their capacity to up-regulate the accumulation of plastidial chaperones. To this end, we decided to use LIN instead of CAP because LIN specifically blocks translation in the chloroplast without any direct effects on cytoplasmic or mitochondrial protein synthesis whereas CAP inhibits both plastidial and mitochondrial protein synthesis (Mulo et al., 2003). WT plants were germinated and grown for 10 days under LD conditions in the presence of LIN at concentrations causing from no visible symptoms (5 μM) to complete bleaching (100 μM) (Figure 3.19A-B). Then we analyzed the abundance of plastidial chaperones (Hsp70, ClpB3, and ClpC) by immunoblot analysis (Figure 3.19B-C). While chaperones recognized by antibodies against plastidial Hsp70 and ClpC proteins hardly changed in LIN-exposed plants, the levels of ClpB3 did increase even at low concentrations of LIN (Figure 3.19B-C). As the concentration of LIN increased, plants became more bleached and levels of the ClpB3 unfoldase were progressively higher (Figure 3.19B-C). These results suggest that increased ClpB3 activity might be required to alleviate protein aggregation stress as PGE and chloroplast function become more and more compromised.

We next followed a genetic strategy to confirm the accumulation of ClpB3 in chloroplasts with an altered PGE. We used mutants defective in the plastid-targeted exoribonuclease RIF10, implicated in the processing of all major classes of plastid RNAs (Sauret-Gueto et al., 2006), or the chloroplast 50S ribosomal protein L24/SVR8 (Liu et al., 2013). WT plants and T-DNA insertion alleles *rif10-2* and *svr8-2* were grown for

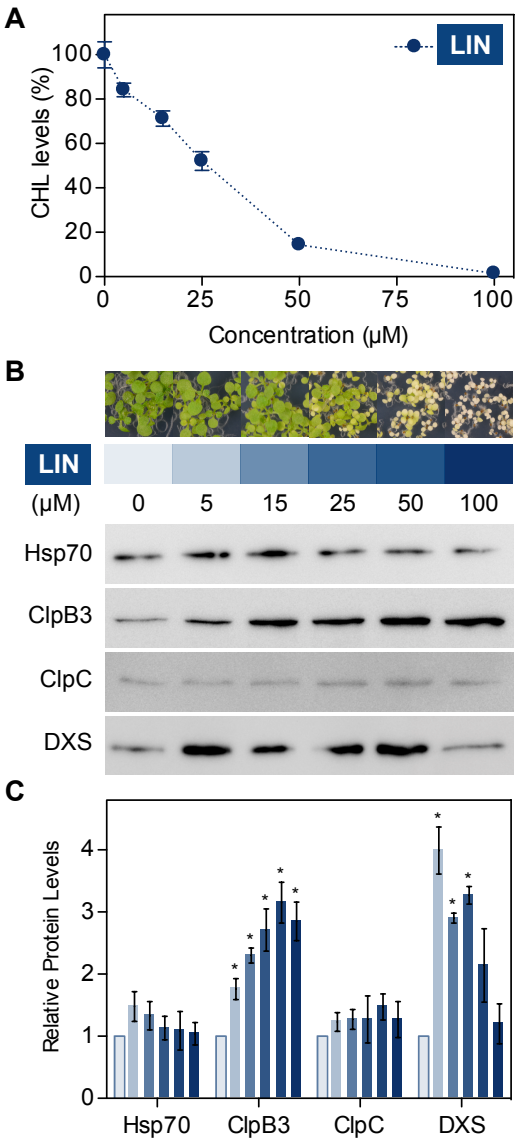

Figure 3.19: LIN treatment boosts accumulation of ClpB3 and DXS proteins. (A) Chlorophyll (CHL) quantification of 10-day-old WT plants germinated and grown in medium supplemented with the indicated LIN concentration. (B) Phenotype of WT plants germinated and grown for 10 days in the presence of the indicated concentrations of inhibitors. The lower panels show representative immunoblots with the indicated antibodies. (C) Quantification of Hsp70, ClpB3, ClpC, and DXS protein levels detected by immunoblot analysis. The mean and SEM values of n≥3 independent experiments are expressed relative to plants grown without LIN. Asterisks mark statistically significant differences (*t* test: p<0.05) relative to untreated control.

10 days under LD and then analyzed for chlorophyll and protein content. While both mutants showed similarly reduced chlorophyll levels, *rif10-2* seedlings displayed green cotyledons and pale true leaves whereas *svr8-2* showed pale cotyledons and leaves (Figure 3.20). WT plants growing on medium supplemented with 15 μM LIN, a concentration that reduced overall chlorophyll levels to those found in the mutants, also showed a general pale phenotype (Figure 3.20). Similar to LIN-treated plants, levels of ClpB3 but not those of Hsp70 and ClpC chaperones, were increased in both *rif10-2* and *svr8-2* mutants compared to untreated WT controls (Figure 3.21). Together, our data confirm that interference with PGE somehow triggers the accumulation of chloroplast-targeted chaperones such as ClpB3.

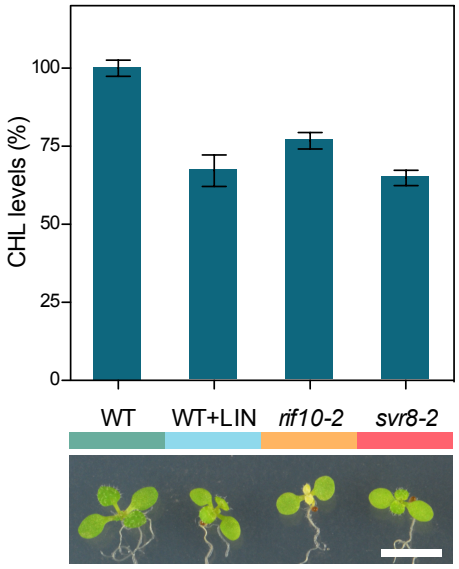

Figure 3.20: Plants affected in PGE show a general pale phenotype. Chlorophyll (CHL) levels and representative pictures of 10-day-old plants affected in PGE. Data corresponds to the mean and SEM values of n≥3 independent experiments and are represented relative to WT plants. WT+LIN corresponds to WT plants germinated and grown in the presence of 15μM LIN. White bar indicates 5 mm.

3.3.2 LIN treatment promotes accumulation of active MEP pathway enzymes and resistance to inhibitors of isoprenoid metabolism

Because ClpB3 helps to refold misfolded and aggregated forms of DXS to recover their solubility and enzymatic activity and to prevent their Clp-mediated degradation (Pulido et al., 2016), it was expected that up-regulation of ClpB3 upon interference with PGE would correlate with higher levels of soluble (*i.e.* enzymatically active) DXS. Indeed, DXS protein levels were increased in PGE-defective mutants and LIN-treated WT plants (Figure 3.19 and 3.21) whereas levels of DXS transcripts remained unchanged (Figure 3.22A). Transgenic *35S:DXS-GFP* lines constitutively expressing a GFP-tagged DXS protein (Pulido et al., 2013) showed enhanced levels of both endogenous DXS and recombinant DXS-GFP proteins when treated with 15

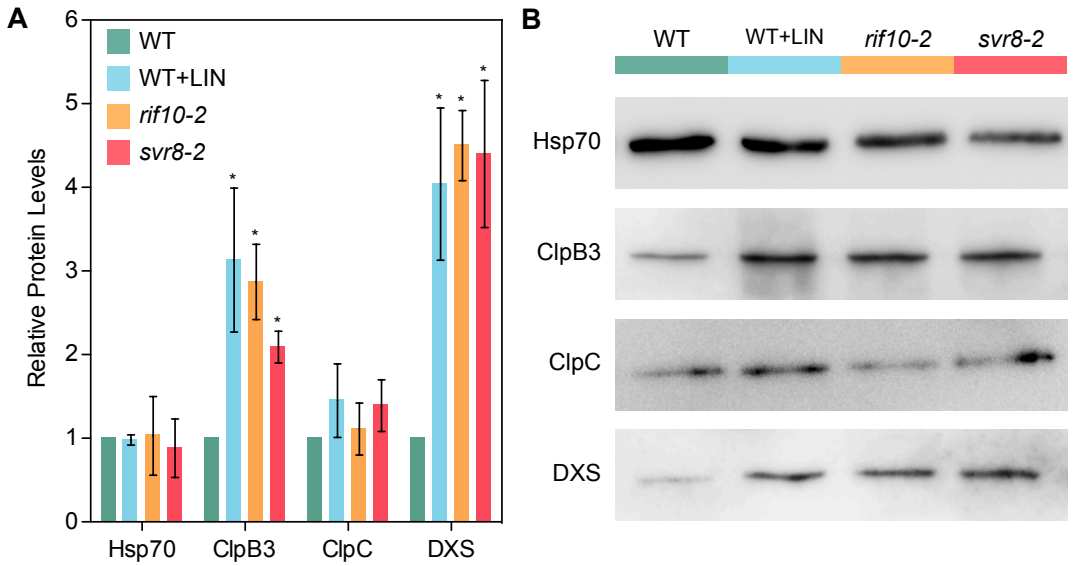

Figure 3.21: Interference with PGE promotes the accumulation of ClpB3 and DXS. (A) Charts represent the average Hsp70, ClpB3, ClpC and DXS protein levels in the plants shown in Figure 3.20. Data corresponds to the mean and SEM values of n≥3 independent experiments and are represented relative to WT plants. Asterisks mark statistically significant differences (*t* test: p<0.05) relative to WT samples. (B) Representative immunoblots analysis with the indicated antibodies are shown.

μM LIN (Figure 3.22B), supporting the conclusion that DXS protein accumulation in plants with PGE defects does not rely on transcriptional DXS changes but most likely derives from decreased degradation. Furthermore, most of the DXS protein accumulated in the soluble fraction in plants with a genetically or pharmacologically impairment of PGE (Figure 3.22C). Like DXS, the next enzyme in the MEP pathway, DXR, was also found to mostly accumulate in the soluble fraction upon interference with PGE (Figure 3.22C). These results suggest that both DXS and DXR enzymes indeed accumulate in an enzymatically active form when PGE (and hence Clp protease activity) is disrupted. In agreement, both *rif10-2* (Sauret-Gueto et al., 2006) and *svr8-2* showed a phenotype of FSM resistance (Figure 3.23). Improved FSM resistance was also observed in WT plants when the growth medium containing 30 μM FSM was additionally supplemented with 15 μM LIN to disrupt PGE (Figure 3.24A).

The FSM resistance phenotype linked to an enhanced accumulation of soluble (*i.e.* active) DXS and DXR enzymes relates to that observed in *clpr1-2* (defective in the ClpR1 subunit of the catalytic domain of the Clp protease) (Figure 3.24A) (Flores-Perez et al., 2008a; Pulido et al., 2016; Perello et al., 2016). However, LIN treatment did not affect FSM resistance in *clpr1-2* seedlings (Figure 3.24A) suggesting that the PGE-dependent mechanism eventually regulating the accumulation of active DXS and DXR levels depends on Clp protease activity. These data support the conclusion that interference with PGE can eventually lead to FSM resistance by triggering the accumulation of soluble and enzymatically functional MEP pathway enzymes (DXS and DXR). At least in the case of DXS, this regulatory mechanism requires the activity of the ClpB3 chaperone to solubilize the misfolded and aggregated forms of

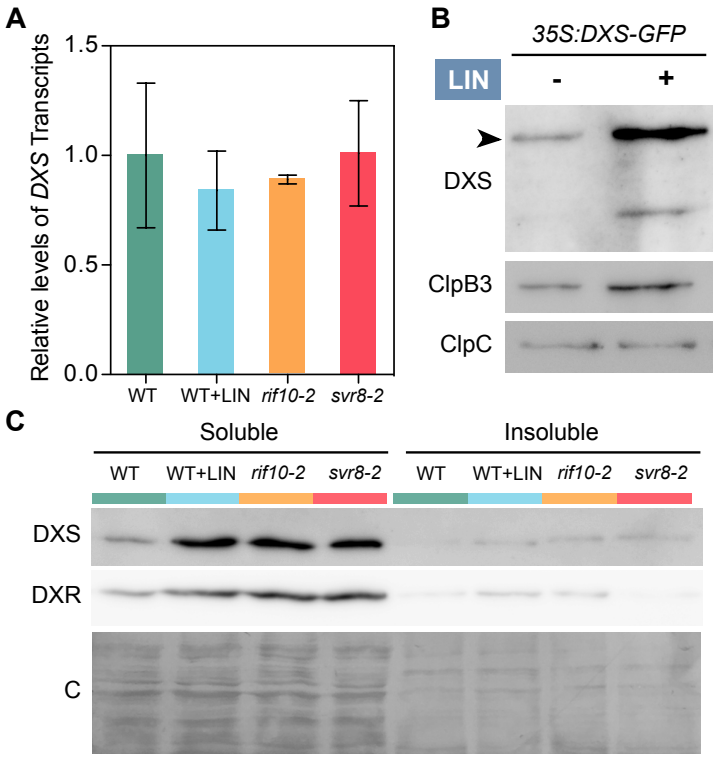

Figure 3.22: Soluble DXS accumulates in PGE-defective plants. (A) *DXS* mRNA levels in the plants shown in in Figure 3.20. Data correspond to the mean and SEM values of n≥3 independent experiments. (B) Immunoblot analysis of DXS, ClpB3 and ClpC from *35S:DXS-GFP* plants grown on media with (+) or without (-) 15 μM LIN. (C) Representative immunoblots of DXS and DXR protein distribution in soluble and insoluble fractions of WT and PGE-defective plants. A Coomassie-Blue (c) staining of the blots is shown for reference.

the enzyme that might otherwise accumulate when their degradation is impaired. Higher ClpB3 levels are expected to also alleviate folding stress of many other protein substrates, therefore impacting other metabolic pathways. In fact, mutants defective in PGE and Clp protease activity (including *clpr1-2*) were identified by screening for mutants able to green in the presence of NFZ (Saini et al., 2011). Indeed, we confirmed that NFZ resistance was gained by partial disruption of PGE in *rif10-2* and *svr8-2* mutants (Figure 3.23) as well as in LIN-treated WT plants (Figure 3.24B).

Interestingly, plants defective in PGE and Clp protease (including *clpr1*) have also been identified as *suppressor of variegation* (*svr*) mutants of the *yellow variegated 2* (*var2*) mutant, defective in one of the subunits of the chloroplast FtsH protease complex (Liu et al., 2010c; Putarjunan et al., 2013; Yu et al., 2008). To analyze if LIN can also suppress variegation, we germinated and grew *var2* plants in medium supplemented with this inhibitor. As expected, after 10 days we observed that LIN suppressed the variegated phenotype or *var2* (Figure 3.25). This result suggests that interference with PGE (or reduced Clp activity) promotes higher chaperone levels to mitigate protein aggregation stress in the *var2* mutant, hence reverting the variegation phenotype.

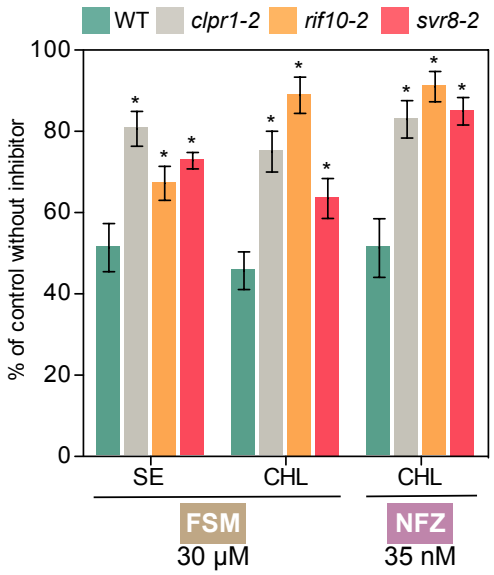

Figure 3.23: Mutants defective in PGE and Clp protease activity are resistant to plastidial isoprenoid inhibitors. Resistance to FSM was estimated by quantifying seedling establishment (SE) and chlorophyll levels (CHL) in plants germinated and grown in the presence of 30 μM FSM relative to those obtained with no inhibitor (100%). Similarly, NFZ resistance was calculated based on chlorophyll levels in media with 35 nM NFZ. Data correspond to the mean and SEM values of n$\geq$3 independent experiments, and asterisks mark statistically significant differences (*t* test: p<0.05) relative to WT samples.

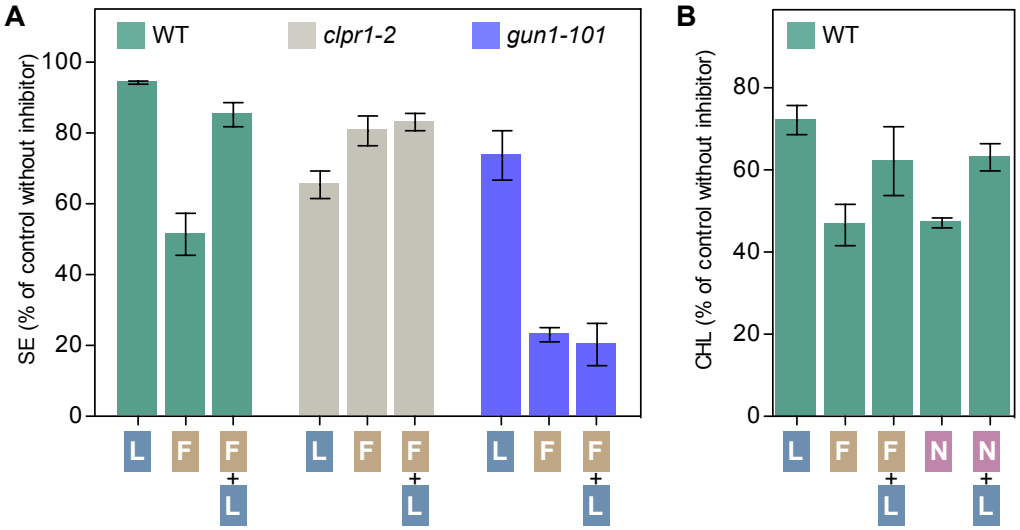

Figure 3.24: Resistance to FSM and NFZ in WT plants is improved by disrupting PGE with LIN. (A) Resistance of WT plants and the indicated mutants was estimated by quantifying SE after germination and growth on media supplemented with 15 μM LIN (L), 30 μM FSM (F), or both (F+L) relative to non-supplemented medium. (B) Resistance of WT plants quantified as chlorophyll levels in media supplemented with 15 μM LIN (L), 30 μM FSM (F), 35 nM NFZ (N) or the indicated combinations relative to non-supplemented medium. Data correspond to the mean and SEM values of n$\geq$3 independent experiments.

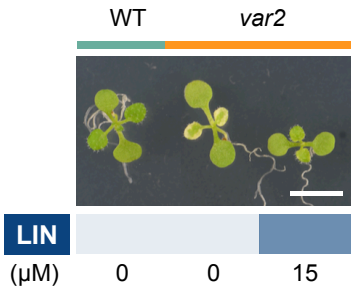

Figure 3.25: LIN treatment suppresses *var2* variegation. Picture shows representative individuals of WT and *var2* plants germinated and grown for 10 days in the presence or absence of LIN (15μM). White bar, 5 mm.

3.3.3 A GUN1-independent pathway up-regulates expression of the nuclear *ClpB3* gene after interfering with PGE

The above-described results suggest that PGE-mediated alteration of protein homeostasis in chloroplasts might lead to an improved capacity to cope with additional stress, in part because it causes the accumulation of chaperones such as ClpB3. If this response is part of a true cpUPR mechanism, it would be expected that PGE defects would rapidly trigger changes in the corresponding nuclear genes. To test this possibility, we grew WT plants on a mesh placed on top of solid medium for 7 days under LD conditions. Then, we transferred the mesh with the seedlings to fresh medium supplemented with 400 μM LIN to ensure a rapid inhibition of PGE. As a PGE-unrelated control, we did a similar experiment using 400 nM NFZ instead of LIN. Samples were collected at different time points after transfer, to extract RNA and protein for quantitative real-time PCR and immunoblot analysis, respectively. As ClpB3 and Hsp70 chaperones can act synergistically to prevent the wasteful accumulation of unfolded, misfolded, and damaged proteins avoiding the formation of toxic aggregates (Mayer and Bukau, 2005; Mishra and Grover, 2016), we included both types of chaperones in the analysis. A strong but transient peak of transcripts encoding ClpB3 and Hsp70-2 (one of the two Hsp70 isoforms imported into Arabidopsis chloroplasts) was detected 2 h after LIN treatment (Figure 3.26A). By contrast, transcripts for Hsp70-1, the other plastidial isoform of the Hsp70 family in Arabidopsis (Su and Li, 2008; Sung et al., 2001) did not show statistically significant changes (*t* test, $p<0.05$) after exposure to LIN (Figure 3.26A). Treatment with NFZ did not induce the expression of any of the genes studied (Figure 3.26A), confirming that the observed cpUPR is caused by direct interference with PGE. At the protein level, both ClpB3 and Hsp70 chaperones tended to progressively accumulate at least up to 9 h, the last time point sampled (Figure 3.26B). However, statistical analysis (*t* test) only detected significant ($p<0.05$) differences between untreated (0h) and LIN-treated samples in the case of ClpB3. As an expected consequence of interfering with PGE and hence down-regulating Clp protease activity, significantly

(t test, $p<0.05$) higher levels of DXS protein were found in LIN-treated plants (Figure 3.26B). Notably, elevation of Hsp70 chaperone supply to the chloroplasts of LIN-treated WT plants seems to exclusively rely on the up regulation of the *Hsp70-2* gene (Figure 3.26B).

Several retrograde signals and pathways have been reported in the literature to regulate nuclear gene expression when normal chloroplast functions are compromised (Kleine and Leister, 2016; Chan et al., 2016; Chi et al., 2013). The plastidial pentatricopeptide repeat protein GUN1 integrates multiple retrograde signals (including those related to PGE) and has been recently proposed to participate in a putative cpUPR signaling pathway (Colombo et al., 2016). However, GUN1-defective mutants showed a WT profile of LIN-induced accumulation of *ClpB3* and *Hsp70-2* transcripts and ClpB3 and DXS proteins (Figure 3.26A-B). These results suggest that GUN1 is not required to produce or/and transduce the PGE-related plastidial signal that eventually regulates nuclear gene expression in LIN-treated seedlings. However, the knock-out *gun1-101* allele (Ruckle et al., 2007) did not show the LIN-promoted increase in FSM resistance observed in WT plants (Figure 3.24A), suggesting that GUN1 is required for the PGE-dependent mechanism eventually regulating the accumulation of active MEP pathway enzymes. Consistent with this possibility, the *gun1-101* mutant shows increased sensitivity to a partial blockage of PGE with LIN, the MEP pathway with FSM, or the carotenoid pathway with NFZ, compared to WT seedlings (Figure 3.27A). A genetic confirmation of this central role of GUN1 came from the analysis of double mutants with *gun1-101* and mutants defective in PGE (*rif10-2* and *svr8-2*). In both cases, double mutants germinated but were unable to develop beyond the cotyledon stage (Figure 3.27B).

3.3.4 The discovered cpUPR does not depent on isoprenoide-related signal metabolites

Among the GUN1-independent retrograde signals, isoprenoid-related metabolites such as the MEP pathway intermediate methylerythritol cyclodiphospahte (MEcPP) and carotenoid derived products such as β-cyclocitral have been found to participate in stress responses (Ramel et al., 2012; Xiao et al., 2012; Avendano-Vazquez et al., 2014). In particular, MEcPP mediates the rapid and transient induction of general stress response genes and triggers the endoplasmic reticulum (ER) UPR in advance of the accumulation of misfolded protein in this cell compartment (Walley et al., 2015; Benn et al., 2016). If any of these isoprenoid metabolites were involved in the cpUPR, it would be expected that their differentially altered levels in WT plants treated with FSM or NFZ resulted in distinct responses to LIN, However plants growing with FSM or NFZ showed similar response to LIN (Figure 3.24B).

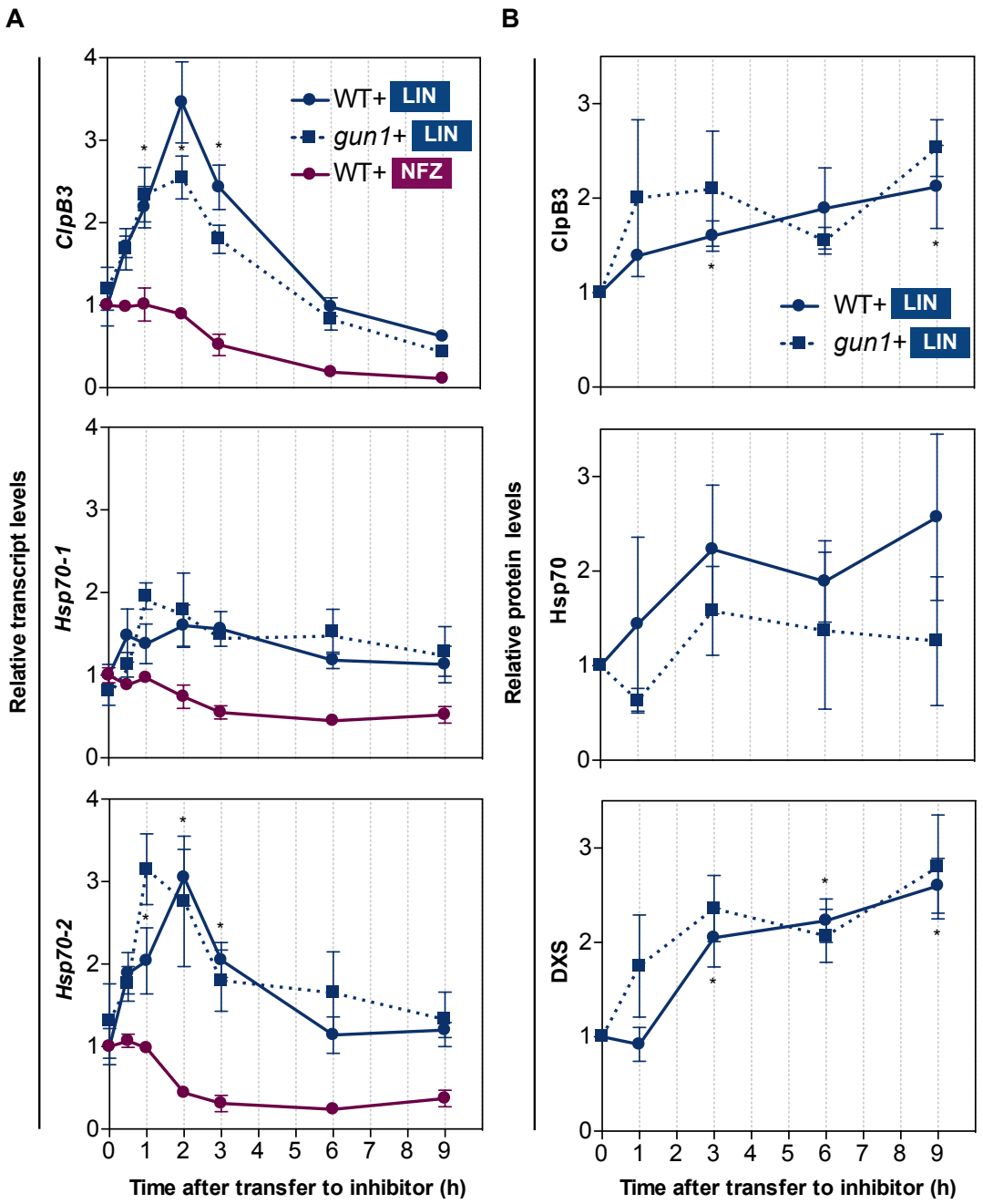

Figure 3.26: Interference with PGE triggers a cpUPR. (A) Quantitative RT-PCR (qPCR) analysis of *ClpB3*, *Hsp70-1* and *Hsp70-2* transcript levels in 7-day-old WT and *gun1-101* plants after transferring to medium with 400 μM LIN or 400 nM NFZ. (B) Levels of ClpB3, Hsp70 and DXS proteins detected by immunoblot analysis in LIN-treated samples. Data correspond to the mean and SEM values of n$\geq$3 independent experiments, and asterisks mark statistically significant differences (*t* test: p<0.05) relative to untreated samples.

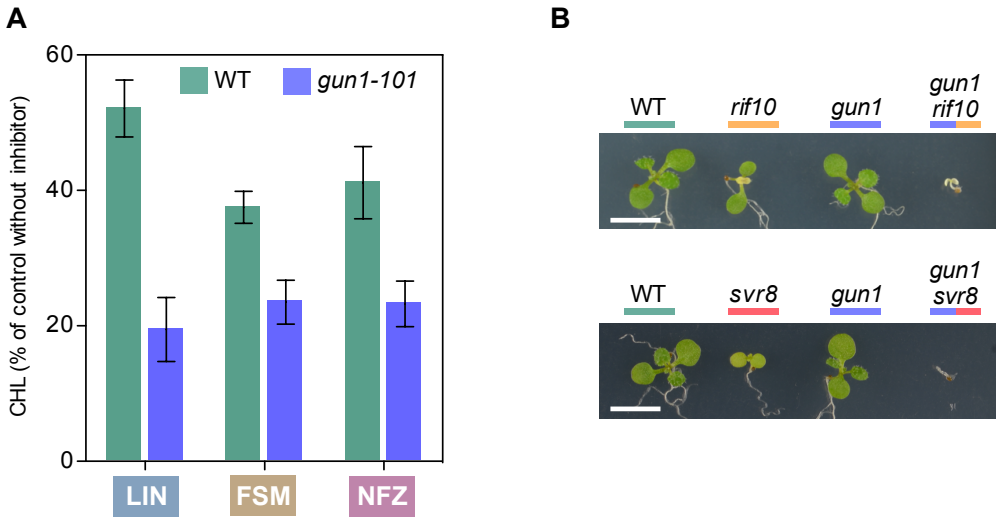

Figure 3.27: GUN1 contributes to chloroplast protein homeostasis and is required for survival of PGE-defective mutants. (A) Resistance of WT and *gun1-101* plants to the indicated inhibitors estimated as CHL level of plants germinated and grown in the presence of 15 μM LIN, 30 μM FSM or 35 nM NFZ relative to no-inhibitor controls. Data correspond to the mean and SEM values of n$\geq$3 independent experiments. (B) Phenotype of 10-day-old WT and mutant lines of the indicated genotypes grown in the same plate. Bar, 5mm.

Arabidopsis mutants accumulating MEcPP also showed a WT response to LIN treatment in terms of gene expression (Figure 3.28) and WT levels of plastidial chaperones (ClpB3 and Hsp70) and MEP pathway enzymes at both transcript and protein levels (Figure 3.29).

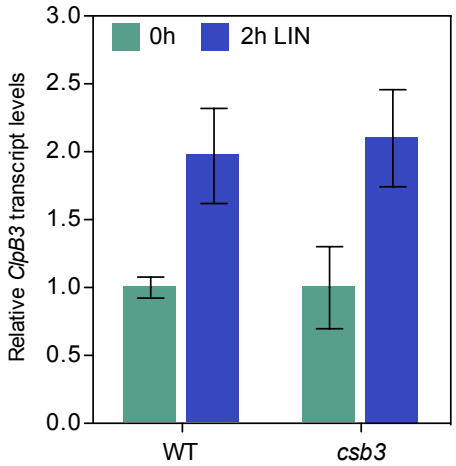

Figure 3.28: Levels of *ClpB3* transcripts in the MEcPP-accumulating mutant *csb3* after LIN treatment. Transcript levels were quantified by qPCR analysis before and after transferring WT and HDS-defective mutant *csb3/clb4-3/hds-3* (Phillips et al., 2008; Flores-Perez et al., 2008b) plants to medium with 400 μM LIN for 2 hours. Data correspond to the mean and SEM values of n=3 experiments.

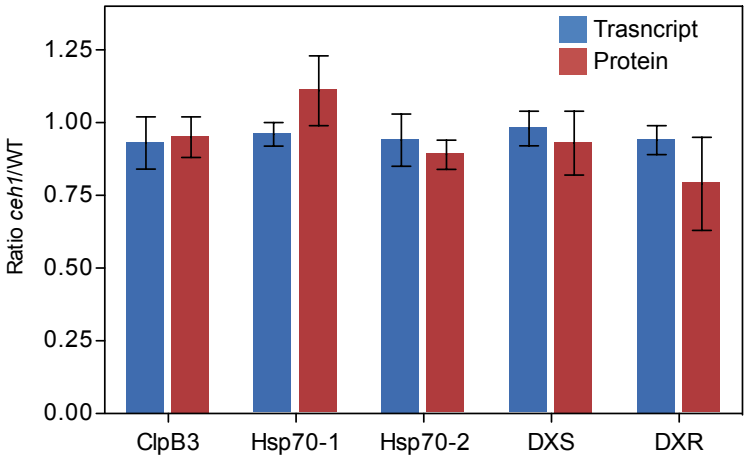

Figure 3.29: Transcript and protein levels of plastidial chaperones and MEP pathway enzymes in the MEcPP-accumulating mutant *ceh1*. Levels are represented as the ratio between mutant and WT plants. Data taken from Walley et al., 2015

4. Discussion

4.1 A functional relationship exists between the MEP pathway and the Calvin cycle

DXS is the most important control point of the MEP pathway to produce essential isoprenoid metabolites for plants (Figure 1.4) and, consistently, it is tightly regulated at multiple levels. During the last years, work in our lab has been centered on studying the post-transcriptional regulation of this enzyme. As a strategy to better understand how DXS protein levels and enzymatic activities are regulated, our lab aimed to identify and characterize DXI proteins. Among them, immunoprecipitation experiments identified the DXI proteins shown in Table 1.1, but the relevance of these interactions for DXS activity remained unexplored.

One of the main goals of the thesis was to analyze if loss-of-function mutants corresponding to the identified DXI proteins displayed an altered DXS phenotype through CLM sensitivity assays (Pulido et al., 2013; Perello et al., 2014). After extensive isolation of homozygous mutants and subsequent CLM sensitivity screenings, we only identified two Arabidopsis mutants with an altered CLM resistance phenotype. Both corresponded to loss-of-funtion alleles of the Calvin cycle enzyme SBPase, *sbp-1* (referred to as *sbp*) and *sbp-2*, and both were resistant to CLM and KCLM (the biologically active inhibitor) when compared to WT controls (Figure 3.2 and 3.4). Transgenic Arabidopsis plants overexpressing a GFP-tagged version of SBPase were sensitive to KCLM, confirming that alterations of SBPase levels directly influence KCLM sensitivity.

SBPase was originally found to be present in complexes containing DXS-GFP identified by co-IP with anti-GFP antibodies in transgenic *35S:DXS-GFP* plants. However, the interaction could not be confirmed after transient expression of tagged proteins followed by co-IP in *N. benthamiana* leaves (Figure 3.3). We had several problems setting up the technique. For instance, DXS-GFP transient expression in *N. benthamiana* was complicated, because GFP fluorescence was only detectable in certain areas even though a whole leave was agroinfiltrated. This low DXS-GFP expression was paralleled by a weak GFP immunoblot signal in the co-IP input (Figure 3.3). It is possible that low levels of DXS-GFP indeed interacted with SBPase-MYC, but GFP signal was too weak to be detectable in the IP lane (Figure 3.3). Due to time limitations,

we were not able to use stable transgenic plants to confirm SBPase as a DXS interactor. In the future, we will try again the co-IP experiments with either *35S:DXS-GFP* or *35S:SBP-GFP* lines using anti-GFP coupled magnetic beads and also testing other alternative antibodies such as the recently available SBPase antibody (Agrisera) and our DXS serum to immunoprecipitate protein complexes. In any case, the fact that we could not detect any direct interaction between DXS and SBPase does not mean that such interaction is not taking place in Arabidopsis chloroplasts. We think that complexes containing DXS and SBPase might be present in the chloroplast for the following reasons: 1) the co-IP followed by MS-based identification of peptides data confirmed the enrichment of SBPase in DXS-containing complexes; 2) another independent co-IP experiment performed in our laboratory, using J20-GFP as bait, also detected SBPase in the complexes whereas this enzyme was not present in controls using DXR-GFP; and 3) there is evidence that the enzymes of the Calvin cycle are organized as a multienzyme complex, an organization that appears to affect metabolic function, providing a mechanism for enhanced efficiency by channeling intermediates and modifying the activity and regulation of the individual enzymes (Winkel, 2004). Although our current data do not allow to conclude whether DXS-SBPase protein-protein interactions are relevant to modulate DXS protein accumulation or activity, they do demonstrate a functional relationship between the MEP pathway and the Calvin cycle.

There are at least three possible mechanisms for CLM resistance (Figure 4.1): (A) enhanced levels of active DXS protein, (B) increased activity of the DXS enzymes, and (C) higher availability of DXS substrates. DXS protein level was not increased in the *sbp* mutant when compared to WT plants (Figure 3.7), arguing against mechanism "A" to explain the CLM resistance phenotype of *sbp* plants. As to mechanism "B". We thought that higher levels of the foldase ClpB3, but not necessary higher levels of DXS protein, could explain the *sbp* CLM-resistance phenotype. However, immunoblot analysis showed similar levels of ClpB3 in WT and mutant plants (Figure 3.3). Also, we could not observe a resistance phenotype in the *sbp* mutant when growing in the presence of FSM (Figure 3.6) despite enhanced DXS activity would be expected to also lead to FSM resistance (Carretero-Paulet et al., 2006; Flores-Perez et al., 2008a; Perello et al., 2014). We therefore concluded that CLM resistance of *sbp* seedlings cannot be explained by a post-transcriptional up-regulation of DXS levels or catalytic activity.

Regarding DXS substrate supply (mechanism "C" above), DXS condenses (hydroxyethyl)thiamin derived from pyruvate with the C_1 aldehyde group of GAP to produce DXP in the first step of the MEP pathway (Figure 1.7). The concentration of pyruvate does not seem to fluctuate in the chloroplast and is believed to be imported from the cytosol (Arrivault et al., 2009). In contrast, GAP is provided directly by the Calvin cycle being an important regulatory hub for MEP pathway flux (Pokhilko et al., 2015). SBPase functions in the regenerative phase of the Calvin cycle,

when triose phosphates (including GAP) are used to produce CO_2 acceptor molecule RuBP. GAP is the net product of the carbon fixation and can be used to build carbohydrates or other cellular constituents like pyruvate and isoprenoids (Figure 1.4 and 1.6) (Malkin and Krishna, 2000). We reasoned that in the *sbp* mutant, lack of SBPase results in an inefficient reincorporation of GAP into the Calvin cycle. Hence, more GAP would be available to be diverted into the MEP pathway. Therefore, GAP would compete with KCLM for binding DXS resulting in increased resistance to the inhibitor without changes in protein levels or activity (Figure 4.1). Decrease GAP availability as DXS substrate in *35S:SBP-GFP* plants would also explain their CLM sensitivity phenotype.

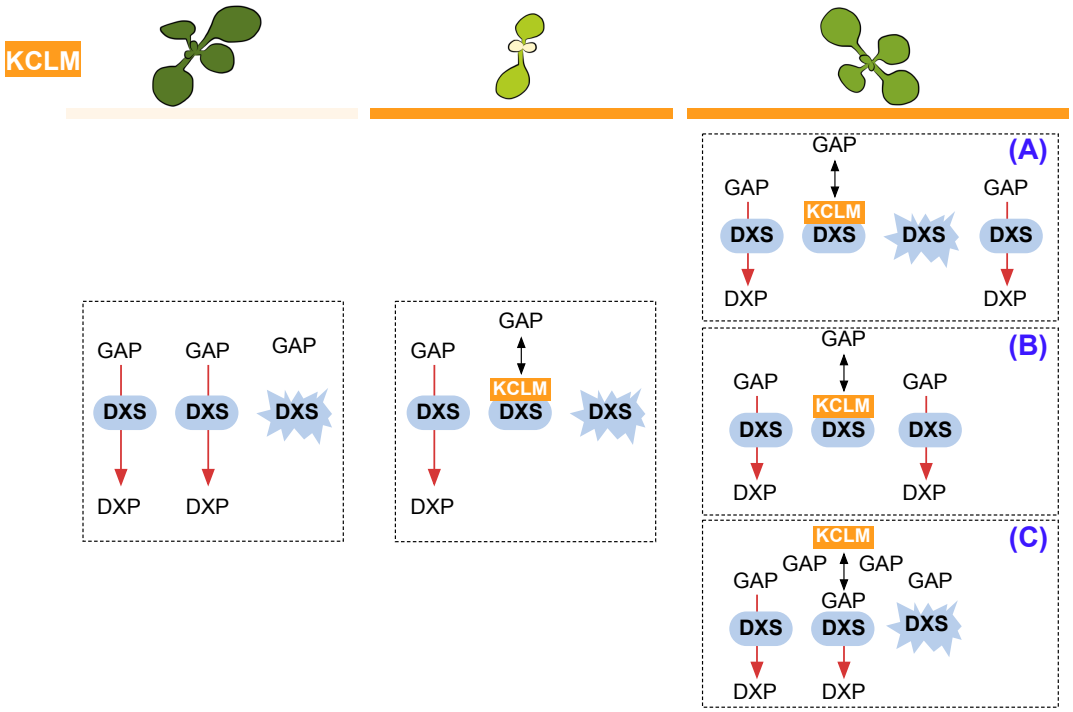

Figure 4.1: Model of the resistance mechanisms to KCLM. The first column represents the situation in Arabidopsis plants growing in the absence of KCLM. Most DXS protein is enzymatically active (round box) and synthesizes DXP from GAP and pyruvate (the latter is not shown). Some DXS protein is misfolded or aggregated (starred box). The second column corresponds to plants grown in the presence of KCLM. The decreased production of DXP leads to a pale phenotype. The third column represents three possible mechanisms for KCLM resistance: (A) increased levels of DXS protein (*e.g.* in DXS-overexpressing lines); (B) improved DXS activity (*e.g.* by proper folding after ClpB3 upregulation); and (C) enhanced availability of GAP (*e.g.* by loss of SBPase activity).

Another interesting possibility explaining the enhanced CLM resistance of SBPase-defective plants arises from the existence of multienzyme complex (or metabolons). SBPase forms part of a metabolon with other Calvin cycle enzymes (Suss et al., 1993). It was suggested that metabolic channeling occurs within this complex (Suss et al., 1993) mantaining high local GAP concentration to use it in the cycle (Winkel, 2004). We reasoned that upon destabilization of the metabolon in the *sbp* mutant, GAP

would not be used efficiently in the Calvin cycle and would divert to the MEP pathway. In this sense, plants with increased SBPase levels, are also expected to have the metabolon stoichiometry affected. However our *35S:DXS-GFP* plants were sensitive to KCLM failing to confirm the metabolon disruption hypothesis.

As shown in Figure 3.2 we did not detect changes in CLM sensitivity in the Calvin cycle mutants *gabp*, *fba1* and *fba2-1*. According to the KEGG data base, the corresponding enzymes are encoded by a gene family in Arabidopsis, suggesting functional redundancy in these lines. On the other hand, SBPase and PRK are enzymes that are unique to the Calvin cycle and both are encoded by a single gene. In fact, it is surprising that plants totally lacking SBPase can even survive. It has been suggested that FBPase might be able to catalyze the conversion of sedoheptulose-1,7-bisphosphate to sedoheptulose-7-phosphate at an extremely low efficiency in *sbp* plants (Liu et al., 2012; Raines et al., 1992). In contrast, we failed to obtain mutants for the gene *PRK*, suggesting that the corresponding enzyme is essential for plant survival.

Despite the putative increased in GAP contribution to the MEP pathway in *sbp* plants, they showed a *ca.* 40% reduction in photosynthetic pigments (carotenoids and chlorophylls) compared to WT plants. This could be explained by pleotropic defects impacting different metabolic pathways. Notably, both tocopherols and zeaxanthin were accumulated in the *sbp* plant. These isoprenoids are normally involved in the protection of plants against excess light and the associated production of ROS (DellaPenna and Pogson, 2006; Havaux, 2014). It is possible that tocopherol biosynthesis is supported by enhanced MEP pathway flux in SBPase-defective plants. Alternatively, it might also be fueled, at least in part, by the phytol groups released from chlorophyll degradation, as shown in many other systems (DellaPenna and Pogson, 2006). We also speculate that low levels of carotenoids cause photooxidation that activates the enzyme violaxanthin deepoxidase, eventually resulting in increased levels of zeaxanthin in the *sbp* mutant (Niyogi, 1999).

A CLM resistance phenotype without changes in DXS protein levels such as that observed in *sbp*, has been previously reported in the mutant *rif18*. This mutant is affected in the gene that codifies for the protein PRL1 that functions as a pleiotropic regulator of sugar and hormone responses (Flores-Perez et al., 2010; Nemeth et al., 1998). Unlike the *sbp* mutant, *rif18* accumulates more chlorophylls and carotenoids than WT plants. This mutant highlighted the importance of sugar availability as the responsible for the accumulation of higher levels of pigments. In fact, WT seedlings grown in the presence of sucrose also show an enhanced accumulation of isoprenoid pigments and show resistance to MEP pathway inhibitors without changes in DXS or DXR protein levels (Flores-Perez et al., 2010). These data and our results suggests that increased resistance to CLM both in *sbp* and *rif18* mutants is possibly due to the high availability of a readily metabolizable carbon source, such as GAP. This increase in GAP availability appears to be an important factor that regulates MEP pathway

flux and influence isoprenoid metabolism as previously suggested (Pokhilko et al., 2015).

4.2 DXS is a protein prone to become aggregated and enzymatically inactive

While all MEP pathway enzymes have been identified in the stroma by proteomic studies (Joyard et al., 2009), *in silico* predictions (Fung et al., 2010; Krushkal et al., 2003) and the experimental data reported in this thesis show that DXS can also associate with membrane structures in the chloroplast (Figure 3.12).

Most DXS is found soluble in the stroma, but this enzyme is prone to become misfolded and to aggregate even under normal conditions. It is, therefore, possible that the DXS proteins detected in insoluble chloroplast fractions correspond to aggregates of inactive protein that unspecifically bind to chloroplast membranes (Figure 3.12). These aggregates were observed as fluorescent speckles in cells expressing the DXS-GFP reporter protein (Figure 3.13) (Pulido et al., 2013). Additionally, the computational analysis revealed the presence of several aggregation-prone clusters in the DXS monomer (Figure 3.11). Also, in this work we demonstrated that DXS aggregation is increased in the absence of J20 because the endogenous DXS enzymes were less accessible to proteinase K cleavage in the *j20* mutant (Figure 3.14).

Unlike DXS, DXR appears to be a very stable protein. It is more resistant than DXS to degradation by unspecific proteases (Figure 3.14A) or by endogenous proteases (like Clp) after a heat shock (Pulido et al., 2013). DXR remains in the soluble (stromal) fraction even under stress conditions that promote general protein aggregation (Perello et al., 2016). An excess of DXR activity might trigger a degradation pathway completely different to that described in this thesis for DXS. It has been observed that vesicles containing DXR-GFP proteins are formed even when there are low levels of this protein. Eventually, the vesicles could be expelled from the chloroplast, perhaps to deliver their stromal content (including DXR-GFP) to degradation by a process likely independent of autophagy. Besides autophagy, other vesicle-mediated pathways have been described for the degradation of chloroplast stroma proteins, including those involving senescence-associated vacuoles (SAVs) and chloroplast vesiculation containing vesicles (CCVs) (Perello et al., 2016).

This thesis confirms that chloroplast protein homeostasis is a complex phenomenon achieved by multiple mechanisms.

4.3 ClpC1 chaperones are required for the degradation of DXS by the Clp protease

In previous work, it was proposed that the J-protein J20 (DXI1) facilitates the recognition inactive forms of DXS to deliver them to the Hsp70 chaperones for eventual activation or degradation (Pulido et al., 2013). In this work, we not only showed that such "inactive" forms likely correspond to misfolded or/and aggregated forms of the enzyme but also identified the components involved in the two proposed J20-dependent antagonistic pathways.

Some insights about a possible degradation of DXS by the Clp protease originated from the analysis of plants defective in ClpR1 and the ClpC1 adaptor. These plants accumulated higher levels of DXS proteins and showed slower proteolytic degradation (Pulido et al., 2016). In this thesis, we demonstrate the importance of J20 to target DXS to degradation (Figure 3.16). Furthermore, we show that Hsp70 and ClpC might collaborate to deliver DXS to the Clp protease using J20 as an adaptor.

Despite the absence of conserved domains for direct interactions between Hsp70 and ClpC-type Hsp100 proteins (Levchenko et al., 2000; Kim et al., 2001; Doyle et al., 2007), such chaperones can be found together in the chloroplast envelope (Su and Li, 2010; Shi and Theg, 2010). It is, therefore, possible that Hsp70 and ClpC interact either directly (using unidentified chaperone binding motifs) or indirectly (via third partners) to participate in PQC in the chloroplast stroma (Sjogren et al., 2014; Flores-Perez et al., 2016; Inoue et al., 2013).

We demonstrated that lack of J20 function causes a reduced degradation rate of the DXS enzyme. However, DXS is still degraded when J20 is not present (Figure 3.16). This result allows us to think in another interesting possibility explaining DXS degradation through a direct J20-independent interaction with ClpC. In a recent work in *Bacillus subtillus* it was described that client proteins are recognized directly by ClpC to deliver them to the ClpP proteolytic complex. It was shown that Arg-phosphorylation by a kinase is required and sufficient for the degradation of substrate proteins. Phosphoarginine works as a tag that is recognized by the ClpC docking site without the need for any additional co-factors (Trentini et al., 2016). It is tempting to speculate that this system is conserved in chloroplasts. Such possibility awaits further investigation.

Independently of the specific mechanism delivering DXS to degradation, we have confirmed DXS as a substrate for the Clp protease. Until now, just some context-dependent *in vivo* Clp targets have been identified. Some examples are a copper-transporting P-type ATPase (PAA2/HMA8) and tetrapyrrole metabolic enzymes (chlorophyllide a oxygenase and glutamyl-tRNA reductase). However, many more Clp protease client proteins remain to be identified (Nishimura et al., 2017).

4.4 Relative abundance of ClpB3 chaperones might determine the fate of DXS

With the evidence provided in this work, we now know about the components and mechanism involved in DXS degradation. Parallel work in our laboratory showed that Hsp70 together with ClpB3 also participates in the recovery of damaged DXS proteins (Pulido et al., 2016).

According to the data presented in thesis and from published data (Pulido et al., 2016), we propose a model for the regulation of DXS enzyme levels and activity by different types of plastidial chaperones (Figure 4.2). According to this model, J20 acts as an adaptor providing substrate specificity (Pulido et al., 2013). J20 delivers inactive (aggregated or/and misfolded) DXS proteins to Hsp70 chaperones that would next act together with Hsp100 proteins to either degrade (via ClpC) or reactivate (via ClpB3) such protein (Figure 4.2). J20 might recognize DXS polypeptides that remain unfolded after plastid import or become misfolded by ordinary perturbations and eventually aggregate, a process that would render the protein more insoluble and enzymatically inactive. Under normal growth conditions, most DXS proteins remain soluble, but some are indeed found associated with the insoluble fraction (Pulido et al., 2016). This might be due to the relatively low levels of ClpB3 in comparison to ClpC1 (Pulido et al., 2016; Sjogren et al., 2014; Zybailov et al., 2008) (Figure 3.17).

How chloroplasts cope with protein aggregation is a relevant question to avoid proteotoxic stress. Results from this thesis, suggest that stress situations (including those causing a decreased DXS activity and a reduction in MEP pathway flux) could rapidly trigger an increase accumulation of ClpB3, but not ClpC chaperones. ClpB3 accumulation likely promotes a reactivation pathway that would keep DXS enzyme in an enzymatically active condition. Furthermore, our data show that ClpB3 levels are more prone to change compared to those of ClpC proteins, suggesting that ClpB3 concentration might be a major factor regulating the fate of inactive DXS polypeptides recognized by J20 and delivered to Hsp70.

Our model proposes an important role for Hsp100 chaperones maintaining proper protein levels in the chloroplast. The lethal seedling phenotype of double mutants with no ClpB3 and Clp protease activity (Zybailov et al., 2009) illustrates the key relevance of these two seemingly opposing pathways for plant life. The main reason for the existence of such sophisticated and expensive pathways for the regulation of DXS levels and activity is likely to be the major role demonstrated for this enzyme in control of the MEP pathway flux (Rodriguez-Concepcion and Boronat, 2015; Hemmerlin, 2013; Wright et al., 2014).

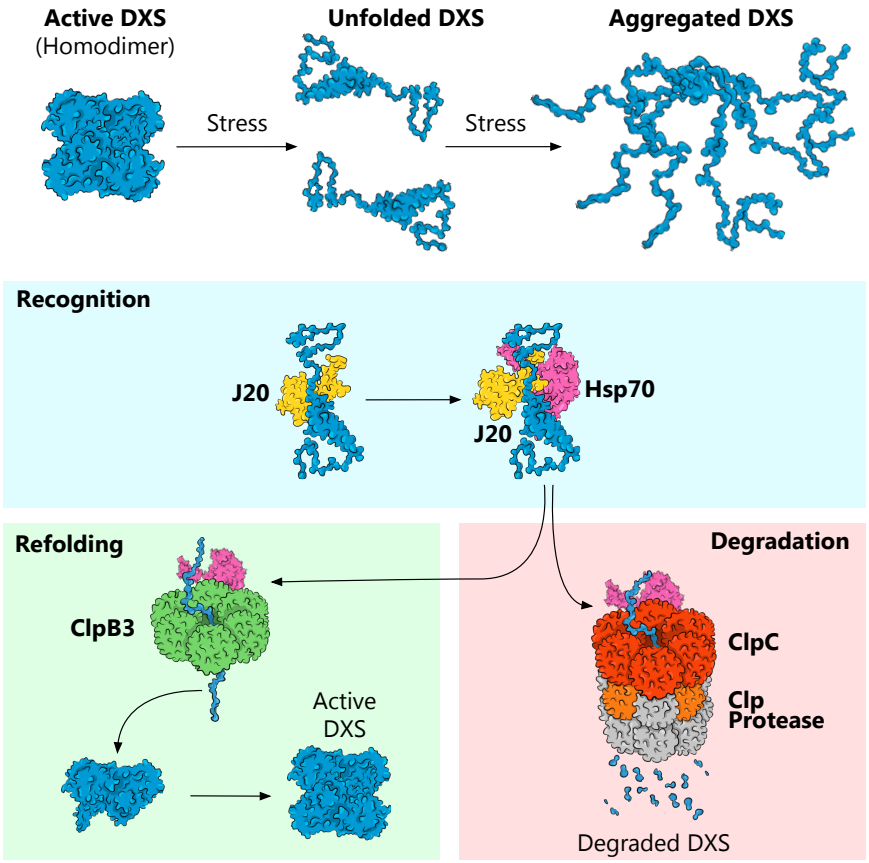

Figure 4.2: Model of the molecular pathways determining the fate of DXS in plastids. Computational and molecular analysis revealed that DXS tends to aggregate. The J-protein J20 facilitates the recognition of damaged (misfolded) or aggregated DXS proteins and their delivery to the Hsp70 chaperone (blue box). Then, the interaction with the Hsp100 chaperone ClpB3 can synergistically contribute to refolding the enzyme back to its active form (green box). Alternatively, Hsp70 can deliver the inactive DXS protein to the Clp protease via ClpC1 for unfolding and degradation (red box).

4.5 A GUN1-independent cpUPR controls ClpB3 levels and hence DXS activity in chloroplasts

In this thesis, we confirmed the existence of a cpUPR in Arabidopsis. Based on our results and published information from other systems, we propose the model presented in Figure 4.3. In brief, stress conditions disrupting chloroplast proteostasis by overwhelming Clp protease activity unleash a specific cpUPR that counteracts protein folding stress by up-regulating nuclear genes encoding PQC components such as ClpB3. Therefore, folding capacity is boosted to restore functional integrity of chloroplast proteins such as DXS, the main rate-determining enzyme of the MEP pathway. We also demonstrate that GUN1 is fundamental for this process. Unexpectedly, however, GUN1 does not participate in the regulation of the nuclear gene

expression response but most likely acts as an integrator of the chloroplast PQC machinery response.

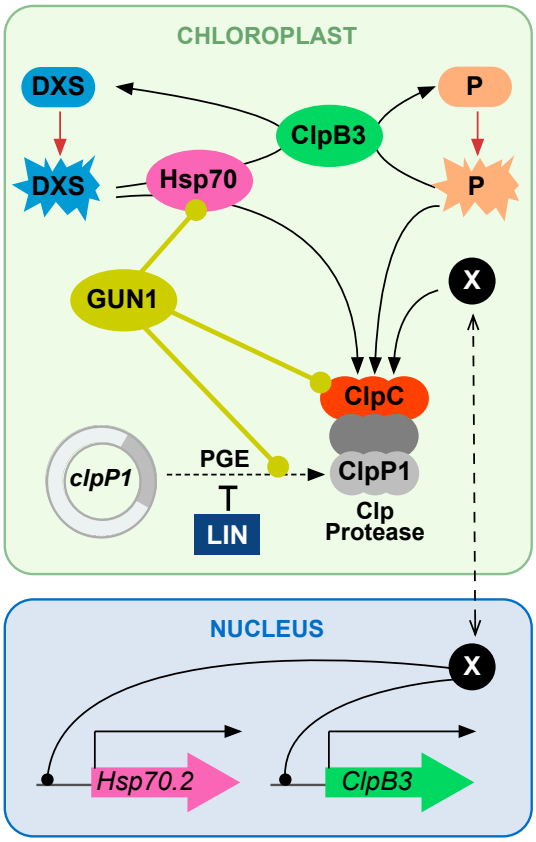

Figure 4.3: Model for the cpUPR mechanism in Arabidopsis. Stress conditions (represented as red arrows) increase the accumulation of misfolded and aggregated forms of DXS and other plastidial proteins (P). This might saturate the capacity of the Clp protease to remove non-functional, proteins eventually causing toxic effects. On the other hand, defects in PGE can be sensed by changes in the level of plastome-encoded ClpP1 protein, which disrupts stoichiometry of the Clp protease complex and hence reduces its proteolytic activity. We speculate that either saturation or down-regulation of Clp protease activity results in the accumulation of a signal X (perhaps a product of the activity of a Clp protease client or the protein itself). Then, X translocates to the nucleus and activates the expression of genes encoding plastidial chaperones such as Hsp70 and ClpB3 to alleviate protein folding stress. Interaction of GUN1 with several protein components of this mechanism appears to contribute to the cpUPR-derived acclimatization response that makes the plant more tolerant to further stress.

The observed cpUPR was triggered by using the PGE inhibitor LIN. The first link between altered PGE, reduced Clp protease activity, and enhanced accumulation of active MEP pathway enzymes (including DXS) was provided by the isolation of FSM-resistant mutants such as *rif1* (Flores-Perez et al., 2008a; Gas et al., 2009) and *rif10* (Sauret-Gueto et al., 2006). Here we reported that a *rif* phenotype is also observed in other PGE mutants such as *svr8-2* (Figure 3.21 and 3.23) and can be induced in WT plants by treatment with sublethal concentrations of LIN (by partially inhibiting PGE) (Figure 3.21 and 3.24), similar to that previously described using

CAP (Sauret-Gueto et al., 2006). Because interference with PGE alters the expression of the plastome-encoded ClpP1 subunit of the catalytic core of the Clp protease complex (Flores-Perez et al., 2008a), it was proposed that the reason behind the accumulation of DXS and DXR proteins (but not transcripts) in *rif* mutants and CAP-treated WT plants was a consequence of reduced Clp proteolytic activity. Consistently, mutants defective in nuclear-encoded subunits of the Clp protease and hence showing a reduced proteolytic activity (such as *clpr1-2*) were also found to display a *rif* phenotype of up-regulated levels of enzymatically active DXS and DXR enzymes (Pulido et al., 2016; Flores-Perez et al., 2008a). The observation that FSM resistance of *clpr1-2* seedlings does not change in the presence of concentrations of LIN that do improve FSM resistance in the WT (Figure 3.24) further supports the conclusion that interference with PGE is signaled via reduced Clp protease activity, eventually decreasing the degradation of DXS and DXR.

The Clp protease not only regulates the accumulation of MEP pathway enzymes but it impacts many other pathways in chloroplasts (Nishimura and Van Wijk, 2015). Interestingly, reduced Clp proteolytic activity in mutants causes accumulation of many plastidial proteins involved in PGE, including components of the RNA processing and editing as well as protein translation machinery (Nishimura and Van Wijk, 2015). Therefore, it is tempting to speculate that inhibition of PGE might trigger a reduction in Clp activity (likely via ClpP1) as a compensatory mechanism to regain balanced levels of PGE-related proteins and maintain overall protein homeostasis in plastids independent of nuclear gene expression. In agreement, the levels of the direct Clp protease client protein DXS (Pulido et al., 2016) were highly increased in WT plants treated with concentrations of LIN that hardly produced visual symptoms (Figure 3.19), suggesting a relatively large decrease in Clp protease activity (*i.e.* in the capacity to degrade DXS) in response to moderate alterations of PGE. Higher concentrations of LIN led to a concomitant increase in the levels of plastidial chaperones such as ClpB3 (Figure 3.19), likely because failure to achieve protein homeostasis unfolds a cpUPR mechanism to release protein folding stress.

In *C. reinhardtii*, reduction of Clp protease activity by depletion of ClpP1 caused up-regulation of both transcript and protein levels for plastidial Hsp70B and ClpB3 chaperones (Ramundo and Rochaix, 2014). HSP70B and ClpB3 are the only plastidial homologues of the Hsp70 (Schroda, 2004) and ClpB-type Hsp100 (Mishra and Grover, 2016) chaperone families in *C. reinhardtii*, respectively. In Arabidopsis plants, we detected transiently increased accumulation of transcripts encoding ClpB3 and Hsp70-2 (but not those encoding Hsp70-1) when WT plants were exposed to LIN treatment. However, our immunoblot analysis only detected a clear increase in protein levels in the case of ClpB3 (Figure 3.26). While Hsp70 chaperones also appeared to accumulate at higher levels after LIN treatment (Figure 3.26B), statistical analysis did not allow to conclude that such differences were significant, mostly due to large differences between replicates. The commercial anti-Hsp70 serum that we

use, raised against both Arabidopsis Hsp70-1 and Hsp70-2 isoforms is presumed to be specific for plastidial Hsp70 proteins. This antibody, however, failed to detect higher Hsp70 levels in Clp protease mutants such as those defective in ClpR1 or ClpC1 (Pulido et al., 2016), whereas proteomic approaches have consistently detected increased levels of these chaperones in *clpr1* (Stanne et al., 2009), *clpc1* (Sjogren et al., 2004), and other Clp-defective Arabidopsis mutants (Nishimura and Van Wijk, 2015). We, therefore, conclude that our immunoblot analysis might not be sensitive enough to detect actual changes in plastidial Hsp70 levels. In any case, it is remarkable that the putative cpUPR-mediated elevation of Hsp70 chaperone supply to the chloroplasts of LIN-treated WT plants might exclusively rely on the up-regulation of the *Hsp70-2* gene (Figure 3.26A). Genes encoding Hsp70-1 and Hsp70-2 are expressed at similar levels in photosynthetic tissues under normal growth conditions (Su and Li, 2008). But in response to heat stress, the *Hsp70-2* gene is activated within minutes (Sung et al., 2001). Arabidopsis mutants defective in Hsp70-2 do not show a visual phenotype, but those impaired in Hsp70-1 show variegation and delayed growth despite they accumulate Hsp70-2 proteins at levels higher than those of the two Hsp70 chaperones combined in the WT (Su and Li, 2008). It is, therefore, possible that Hsp70-1 preferentially plays housekeeping functions while Hsp70-2 might be more specialized in responding to stress.

Unlike LIN, NFZ treatment did not trigger the accumulation of chaperone transcripts (Figure 3.26A). While both inhibitors cause similar bleaching symptoms (Figure 3.6), only LIN has a direct impact on PGE. Blockage of carotenoid biosynthesis with NFZ can eventually alter PGE as it leads to decreased photoprotection and photooxidation, but LIN directly inhibits the translation of plastome-encoded proteins and has a much stronger impact on RNA transcription and processing than NFZ (Tseng et al., 2013). In any case, the secondary effects of NFZ on PGE are not expected to be relevant in green plants at short times like those used to analyze the existence of a cpUPR after transferring WT plants to inhibitor-supplemented media (Figure 3.26). The absence of a cpUPR in NFZ-treated plants was also deduced from the lack of a *rif* phenotype of enhanced FSM resistance when NFZ was added to the growth medium of WT plants (Sauret-Gueto et al., 2006). These results further support the contribution of PGE-triggered changes in Clp protease activity to the cpUPR. NFZ has been widely used to identify retrograde signals and pathways communicating the chloroplasts with the nucleus (Grimm et al., 2014; Kleine and Leister, 2016; Liu et al., 2012; Chan et al., 2016). For example, genomes uncoupled (*gun*) mutants, including *gun1* (Koussevitzky et al., 2007b), were identified based on their ability to de-repress the expression of nuclear genes encoding photosynthetic proteins in a NFZ-supplemented medium. These studies were typically conducted using very high (μM) concentrations of the inhibitor that caused massive photooxidative damage and complete bleaching. By contrast, screening for *happy on norflurazon* (*hon*) mutants able to green in the presence of lower (nM) concentrations of NFZ showed that mutants with altered PGE (*hon23*) or Clp protease activity (such as

hon5, defective in the ClpR4 subunit of the complex) gained resistance to NFZ (Saini et al., 2011), consistent with our results using *rif10-2*, *svr8-2*, and *clpr1-2* mutants (Figure 3.23). It was concluded that perturbance of chloroplast protein homeostasis in *hon* mutants caused a relatively mild stress that led to an activated protection against further stress such as that imposed by NFZ treatment (Saini et al., 2011). This proposed stress acclimatization response (Saini et al., 2011) might well correspond to the cpUPR unveiled here.

Mutants defective in PGE and Clp protease activity were also repeatedly identified in screenings for Arabidopsis mutants with a phenotype of *suppressor of variegation* (*svr*) of the *yellow variegated 2* (*var2*) mutant, defective in one of the subunits of the chloroplast FtsH protease complex (Liu et al., 2013; Putarjunan et al., 2013). In particular, *svr1* (Yu et al., 2008), *svr3* (Liu et al., 2010a), *svr4* (Powikrowska et al., 2014), *svr7* (Liu et al., 2010b), *svr8* (Liu et al., 2013), *svr9* (Zheng et al., 2016), and *svr10/rif1* (Qi et al., 2016) are defective in PGE processes such as RNA editing or protein translation, whereas those impaired in Clp protease activity include *svr2/clpr1* and *clpc1* (Yu et al., 2008). Furthermore, PGE inhibitors such as CAP (Yu et al., 2008) and LIN (Figure 3.25) can suppress *var2* variegation. The existence of a cpUPR in Arabidopsis as demonstrated here could explain why interference with PGE and Clp protease activity generates *rif*, *hon* and *svr* phenotypes, as they can be considered as ultimate consequences of triggering a PQC-based stress protection mechanism in chloroplasts. Thus, higher levels of plastidial chaperones such as ClpB3 in *rif10-2*, *svr8-2*, or *cpr1-2* (Figure 3.21) (Pulido et al., 2016) would contribute to remove protein aggregates and to refold chloroplast proteins that might be damaged and misfolded when mutant plants are stressed by treatment with inhibitors of chloroplast function such as FSM or NFZ, eventually resulting in enhanced resistance to these herbicides (Figure 3.23). Increased chaperone levels might also mitigate the deleterious effects produced by the accumulation of FtsH substrates as misfolded polypeptides and protein aggregates, hence causing a reversion of the variegation phenotype of the *var2* mutant. The relevance of this adaptive mechanism for plant life is illustrated by the lethal seedling phenotype of double mutants impaired in both Clp protease and ClpB3 activities (Flores-Perez et al., 2016).

Arabidopsis ClpB3 levels were previously known to increase in response to heat stress but also when Clp protease activity is reduced (Myouga et al., 2006; Nishimura and Van Wijk, 2015; Pulido et al., 2016). However, the mechanism connecting chloroplast protein folding stress and activation of ClpB3 supply remained unknown. Our results show that ClpB3 accumulation results from a cpUPR mechanism, *i.e.* from the activation of *ClpB3* gene expression in the nucleus by unknown retrograde factors (Figure 4.3). The observation that *gun1-101* plants showed a WT induction of *ClpB3* gene expression and protein accumulation in response to LIN treatment (Figure 3.26) suggests that this central integrator of retrograde pathways is not required to trigger cpUPR signaling. However, the inability of *gun1-101* plants to unfold

the subsequent acclimation response (Figure 3.24) and to efficiently cope with stress caused by inhibition of chloroplast function (Figure 3.24) (Saini et al., 2011) as well as the seedling lethal phenotype of double mutants defective in GUN1 and PGE (Figure 3.27) strongly suggest that the GUN1 protein is a pivotal component of the overall cpUPR response at the protein level. This is consistent with the observation that GUN1 interacts with many proteins involved in PGE and PQC processes (Figure 4.3) (Tadini et al., 2016) and with the conclusion that GUN1 is a coordinator of chloroplast PGE, protein import, and protein homeostasis (Colombo et al., 2016). It has been proposed that GUN1 might act as a platform to bring different protein together to promote or/and prevent particular interactions (Colombo et al., 2016).

We also demonstrated that isoprenoid-related metabolites involved in signaling the ER UPR were not involved in the cpUPR (Figure 3.28 and 3.28). While much work is still ahead to unveil the molecular factors connecting chloroplast protein folding stress and activation of target cpUPR-regulated genes, work in *Caenorhabditis elegans* and mammals supports our view that Clp protease activity might be an active player in the process (Arnould et al., 2015). In *C. elegans*, the small peptides that result from degradation of protein clients by the mitochondrial Clp protease are exported to trigger nuclear translocation of ATFS-1, a bZIP transcription factor that orchestrates expression of mitochondrial UPR-related genes (Haynes et al., 2007; Haynes et al., 2010). ATFS-1 is normally imported in mitochondria and degraded by the Lon protease, which is also found in plant chloroplasts (Rigas et al., 2014). Under protein folding stress conditions, mitochondrial import of ATFS-1 decreases, resulting in more protein in the cytosol that can be translocated to the nucleus (Nargund et al., 2012). Some plastidial retrograde signaling pathways also rely on transcription factors that can relocate from the chloroplast to the nucleus (Sun et al., 2011; Isemer et al., 2012). As indicated in our model (Figure 4.3), a similar Clp-based system might therefore operate in mitochondria and plastids to control the subcellular localization of transcription factors so they unfold UPR when protein aggregation and folding stress overwhelm the capacity of the Clp protease (*e.g.* under particular stress conditions, in LIN-treated WT plants, or in mutants with a reduced PGE or Clp protease activity). In any case, it is likely that multiple pathways might work together to sense chloroplast stress and transduce the signal to the nucleus to ultimately activate target PQC genes.

5. Conclusions

1. A functional relationship exists between the MEP pathway and the Calvin cycle. Arabidopsis lines with altered levels of the Calvin cycle enzyme SBPase show concomitant changes in their sensitivity to inhibitors of the first and main rate-determining enzyme of the MEP pathway, DXS.
2. DXS protein levels and its enzymatic activity appear not be altered in SBPase-defective mutants.
3. Availability of GAP for the MEP pathway is expected to increase in the *sbp* mutant and to decrease in SBPase-overproducing plants. GAP might compete with DXS inhibitors for binding to the enzyme, hence explaining the altered resistance phenotypes of these plants.
4. DXS protein homeostasis is controlled by specific molecular mechanisms that are different from those regulating the turnover of other MEP pathway enzymes such as DXR.
5. DXS is prone to aggregation within the chloroplast.
6. J20 recognizes misfolded and aggregated forms of DXS and delivers them to the Hsp100/ClpC1 chaperone for subsequent degradation by the stromal Clp protease or to the Hsp100/ClpB3 disaggregase for refolding and reactivation.
7. Reduced MEP pathway flux, protein folding stress, or defective expression of the plastome (eventually causing insufficient Clp protease activity) promote accumulation of ClpB3.
8. A chloroplast Unfolded Protein Response (cpUPR) can be elicited by interference with plastome gene expression or/and Clp protease activity to increase ClpB3 protein levels through up-regulation of *ClpB3* gene expression.
9. Increased levels of ClpB3 and other chaperones by cpUPR results in acclimation to stress caused by different types of inhibitors.
10. GUN1 has a central role in the cpUPR beyond gene expression, likely acting as an integrator of different pathways controlling chloroplast protein homeostasis.

6. Materials and methods

6.1 Plant Material and Growth Conditions

Arabidopsis thaliana (Col-0) lines used in this work are described in Table 6.1. Seeds were surface-sterilized as following. 1 ml of a solution containing 70 % ethanol with 0.05% TritonX-100 was added to an Eppendorf tube containing the seeds. The solution was vortexed for 2 minutes, then discarded. Next, 1 ml of 100% ethanol was added. After 2 minutes of continuous agitation, ethanol was removed and the seeds were dried under a hood. Once the seeds were dry, they were sow in petri plates on solid 0.5X Murashige and Skoog medium without sucrose and vitamins (0.5X MS-). Seeds were stratified for 3 days at 4°C, then plates were incubated in a growth chamber at 22°C under long day conditions (8 h in darkness and 16 h under fluorescent white light at a PPFD of 60 $molm^{-2}s^{-1}$.

For transient expression and Co-IP experiments *Nicotiana benthamiana* RDR6i plants were used. This plants were grown under standard greenhouse conditions (14 h light at 27°C and 10 h dark at 24°C).

6.1.1 Gain- or loss-of-function lines used in this study

Table 6.1: Loss-of-function lines

Protein	AGI code	Allele	Line	Reference
ClpR1	AT1G49970	*clpr1-2*	SALK_088407	Koussevitzky et al., 2007a
HDS	AT5G60600	*csb3/clb4-3*	EMS	Gil et al., 2005
CSP41a	AT3G63140	*csp41a-4*	C. Koncz collection	Qi et al., 2012
CSP41b	AT1G09340	*csp41b-2*	SALK_021748C	Qi et al., 2012; Bollenbach et al., 2009
FNR1	AT5G66190	*fnr1-1/ΔFNR1*	SALK_085403	Lintala et al., 2007
		fnr1-2/ΔFNR1b	SALK_067668	Lintala et al., 2007
FBA1	AT2G21330	*fba1*	SALK_063223	This study
FBA2	AT4G38970	*fba2*	SALK_073444	This study
GAPDH-B	AT1G42970	*gapb1*	SAIL_308_A06	This study
GUN1	AT2G31400	*gun1-101*	SAIL_33_D01	Ruckle et al., 2007
J20	AT4G13830	*j20-1*	SAIL_1179_E04	Pulido et al., 2013
RIF10	AT3G03710	*rif10-2*	SALK_037353	Sauret-Gueto et al., 2006
Rpl9	AT3G44890	*rpl9*	SALK_052906C	This study
Rpl19a	AT5G47190	*rpl19a*	SALK_023092C	This study
Rpl19b	AT4G17560	*rpl19b-1*	SALK_067948C	This study
		rpl19b-2	SALK_059283C	This study
Rpl24	AT5G54600	*rpl24-1/prpl24-1/svr8-2*	SALK_010822	Romani et al., 2012; Liu et al., 2013
		rpl24-2/rpl24	SALK_010823	Tiller et al., 2012
Rpl29	AT5G65220	*rpl29-1*	SALK_037831	This study
Rps21	AT3G27160	*rps21-1/ghs1-3*	SALk_077692C	Morita-Yamamuro et al., 2004
Rps9	AT1G74970	*rps9-1*	SALK_134633C	This study
		rps9-2	SALK_128849C	This study
SBPase	AT3G55800	*sbp-1*	SALK_130939C	Liu et al., 2012
		sbp-2	SALK_090549C	This study
THF1	AT2G20890	*thf1-1/psb29*	SALK_094925	Huang et al., 2006; Keren et al., 2005
		thf1-2	SALK_113467C	This study
VAR2	AT2G30950	*var2-8*	EMS	Takechi et al., 2000

Table 6.2: Gain-of-function lines

Transgenic line	Other names	Ecotype	Resistance	Reference
35S:DXS-GFP	*35S:DXS-GFP* #32	Col-0	Basta	Pulido et al., 2013
35S:DXR-GFP	*35S:DXR-GFP* #11	Col-0	Basta	Perello et al., 2016
35S:SBP-GFP High	*35S:SBP-GFP* #1031	Col-0	Km	This study
35S:SBP-GFP Medium	*35S:SBP-GFP* #1211	Col-0	Km	This study
35S:SBP-GFP Low	*35S:SBP-GFP* #811	Col-0	Km	This study

6.1.2 Double mutants generation

For the generation of double mutants, single homozygous mutants were crossed, and the F2 progeny was screened for the characteristic pale phenotype associated to the *rif10-2* or *svr8-2* mutations in homozygosis. Then, pale individuals were PCR-genotyped to identify the T-DNA insertion of the *gun1-101* allele as described (Ruckle et al., 2007). Individuals confirmed to be homozygous for *rif10-2* or *svr8-2* and heterozygous for *gun1-101* were allowed to self-cross. Double mutants, segregated as tiny albino plants in the F3 generation, were confirmed by PCR analysis of the T-DNA insertions in both genes.

6.2 Inhibitor treatments

For long-term inhibitor treatments Arabidopsis seedlings were germinated on 0.5X MS- medium supplemented with indicated concentrations of CLM (Sigma), KCLM (Echelon Biosciences), FSM (Life technologies), NFZ (Zorial) or LIN (Sigma). FSM resistance phenotype was measure by Seedling establishment (SE) represented as the percentage of plants that could develop the first pair of true leaves after 14 days (Perello et al., 2014). Additionally, FSM resistance was also estimated quantifying chlorophyll levels after 7 days of treatment. Resistance to NFZ or LIN was estimated by quantifying chlorophyll levels after 10 days of treatment (Perello et al., 2014). For CHX (Sigma), LIN and NFZ seedling transfer experiments, seeds were germinated on top of a sterile disc of Mesh (SefarNitex 03-100/44) on 0.5X MS- medium. At day 7, the disc with the seedlings was transferred to fresh medium supplemented with 100 μM CHX, 400 μM LIN or 400 nM NFZ. Samples were collected at indicated time points for qPCR and/or immunoblot analysis.

6.3 Generation of the DNA constructs

For the generation of the constructs *35S:ClpC1-MYC*, *35S:SBPase-MYC* and *35S:SBPase-GFP*. The protein coding sequence (without the stop codon) of each gene was PCR amplified (6.4). PCR products were cloned into the *pDONOR207* vector (Invitrogen), and subcloned into the Gateway vector *pGWB417* (for the *35S:ClpC1-MYC* and *35S:SBPase-MYC* constructs) and *pGWB405* (for the *35S:SBPase-GFP*). The rest of the constructs used in this thesis were previously generated (Pulido et al., 2013; Perello et al., 2016). The Table 6.3 shows the constructs used in this work.

Table 6.3: DNA constructs

Construct	Vector name	Bacterial selection	Marker for plant	Reference
35S:ClpC1-MYC	*pGWB417*	Spc	Km	This work
35S:SBP-GFP High	*pGWB405*	Spc	Km	This study
35S:SBP-MYC Medium	*pGWB417*	Spc	Km	This study
35S:DXS-GFP Low	*pB7FWG2*	Spc	Basta	Pulido et al., 2013
35S:DXR-GFP Low	*pB7FWG2*	Spc	Basta	Perello et al., 2016

Table 6.4: Primers used for generating DNA constructs

Primer	Gene	Sequence
SBPASE-BP-ATG-Fw	*SBP*	5′-GGGGACAAGTTTGTACAAAAAAGCAGGC TATGGAGACCAGCATCGCGTGCTACTCAC-3′
SBPASE-BP-Rv-nstp		5′-GGGGACCACTTTGTACAAGAAAGCTGGGTCA GCGGTAACTCCAATGGGAACATTC-3′
ClpC1-BP-FW	*ClpC1*	5′-GGGGACAAGTTTGTACAAAAAAGCAGG CTATGGCTATGGCCACAAGGGTGTTG-3′
ClpC1-nstp-Rv-BP		5′-GGGGACCACTTTGTACAAGAAAGCTGGGTC AGCAACAGGGAGAGAATCTTCCTGC-3′

Materials and Kits used for the generation of DNA constructs

Amplification of cDNA was carried out using the Phusion High-Fidelity PCR Master Mix (New England BioLabs).

Table 6.5: Phusion PCR mix

Component	50 μl total reaction
10 μM Forward primer	2.5
10 μM Reverse primer	2.5
DMSO	1.5
2X Phusion Master Mix	25
Template (cDNA)	1
Nuclease-free water	to 50

Table 6.6: Phusion thermocycling conditions

Step	Temperature	Time
Initial denaturation	98°C	30 seconds
25-35 cycles	98°C	5-10 seconds
	45°-72°C	10-30 seconds
	72°C	10-30 seconds/kb
Final extension	72°C	5 minutes
Hold	4°C	Forever

For purifying the amplified DNA from agarose gel, the Wizard SV Gel and PCR Clean-UP System (Promega) was used. PCR products were cloned using the Gatway BP Clonase II Enzyme Mix (Invitrogen). Finally, the LR clonase II enzyme Mix (Invitrogen) was used to obtained the destination vectors with our genes of interest. During the cloning process, the High Pure Plasmid Isolation Kit (Roche) was used to purify plasmids from DHα5 transformed strains.

6.4 Genotyping of the loss-of-function mutants

Genomic DNA from Arabidopsis leafs was extracted according to the protocol develop by Edwards et al., 1991. Samples for PCR analysis (leaf tissue) were collected using the lid of an Eppendorf tube to pinch out a disc of material into the tube containing 3mm crystal beads. Then, 50 μl of extraction buffer (200mM Tris HCL pH 7.5, 250 mM NaCl, 25 nM EDTA, 0.5% SDS) was added to the tube. Next, the samples were macerated (at room temperature) using a Tyssue Lyser II (QIAGEN). The rest of extraction buffer (350 μl) was added to the macerated tissue and vortexed for 5 seconds. The extracts were centrifuged at 13,000 rpm for 1 minute and 300 μl of the supernatant was transferred to a fresh Eppendorf tube. The supernatant was mixed with 300 μl of isopropanol and left at room temperature for 2 minutes. Following centrifugation at 13,000 rpm for 5 minutes, the remaining liquid was discarded and the pellet was dried at 42°C and then dissolved in 50 μl of miliQ water.

Table 6.7: Primers used for genotyping T-DNA *dxi* mutants

Gene	AGI code	Allele	Line	Primer	Sequence
CP22	AT1G44575	*cp22*	SALK_095156C	CP22-LP	TGACCAGACACAATTCATTTACATC
				CP22-RP	ATAAACATAAAGCCGATCCGG
CSP41a	AT3G63140	*csp41a-4*	C. Koncz T-DNA	CSP41a-4-genotipado-F	ATG GCG GCT TTA TCA TCC TCC TC
				CSP41A-4-genotipado-R	CCA GAG CCG ATC ATG TAC TGC G
CSP41b	AT1G09340	*csp41b-2*	SALK_021748C	CSP41b-LP	TCAAGTCTTTCAGCAGAAGGC
				CSP41b-RP	GCAATGATCCAAAAAGCTCAG
FNR1	AT5G66190	*fnr1-1/ΔFNR1*	SALK_085403	fnr-1-LP-R	ATG TTC TTT GAG GAG CAC GAG
				fnr1-1-RP-F	TTG CAA AAA TCA GGA AAT TGC
	AT5G66190	*fnr1-2/ΔFNR1b*	SALK_067668	fnr1-2-LP-F	AGC GAG ACC ATA ATG TCA TCG
				fnr1-2-RP-R	ACA TTG TCT TCA CCA CCG AAG
FBA1	AT2G21330	*fba1-1*	SALK_063223	fba1-1-LP-R	TTG TTG GGA ATT GTC GAT TTC
				fba1-1-RP-F	CTT GTT GGT AGT AAG CAG CGG
FBA2	AT4G38970	*fba2-1*	SALK_073444	FBA2-LP S073444	CCAAGAGAGTGGTCTGAGCTG
				FBA2-RP S073444	TTGTCCCTGGTATCAAAGTCG
	AT4G38970	*fba2-2*	SALK_000898	FBA2-LP S000898	TCCATCCAACAAGATCTCTGG
				FBA2-RP S000898	TGTTCTGTTTTGCCCTGTTTC
GAPB	AT1G42970	*gapb1*	SAIL_308_A06	gapb-1-genotipado-F	AGC TCA AAT CAG AAG ATA CTC C
				gapb-1-genotipado-R	GAG AGT CTT TAC GAC CAT GC
PRK	AT1G32060	*prk-1*	GK-117E07	pkr-1-RP-F	TTG TCA TCG AAG GTC TTC ACC
				pkr-1-LP-R	TGG AAA AA CCA GTA CCG TTG
		prk-2	ET5394	pkr-1-Rv	CCA GTA CCG TTG TTG CTA CCC
Rpl9	AT3G44890	*rpl19*	SALK_052906C	RPL9-LP	TCAGATTCGACTGGTTCTTGC
				RPL9-RP	AGTCCCTCGAAATACAAAGGC
Rpl19a	AT5G47190	*rpl19a*	SALK_023092C	RPL19a-LP	AAGGAGAAGGAGAAGCCACTG
				RPL19a-RP	TCAGCCAATAGTACTGGAAAGTTC
Rpl19b	AT4G17560	*rpl19b-1*	SALK_067948C	RPL19b-LP S067948	CTTGAGGTGGCTTAGTGCTTG
				RPL19b-RP S067948	GGTTTAGCTTCGACCACTTCC
Rpl19b	AT4G17560	*rpl19b-2*	SALK_059283C	RPL19b -LP S059283	ACTAACCCCCATGACATCTCC
				RPL19b-RP S059283	GGTTTAGCTTCGACCACTTCC
Rpl24	AT5G54600	*rpl24-1/prpl24-1/svr8-2*	SALK_010822	PRPL24-LP	GCAAGAACAAGACATGGGTTC
				PRPL24-RP	AACTGCAAACGGATCATTACG
	AT5G54600	*rpl24-2/rpl24*	SALK_010823	Prpl24-RP Tiller	CGG AGG GAT AAT TCC TTG GAC
Rpl29	AT5G65220	*rpl29*	SALK_037831	RPL29-LP	CATTCCTCAGGTGAATTCTGC
				RPL29-RP	CGACGAAAGTCGCTAGATTTG
Rpl13	AT5G14320	*rps13*	SALK_087496	RPS13-LP	CAA GAA ACT GCT CGA GAA TGG
				RPS13-RP	AAC GAA GTG AAC GAC CAT CTC
Rps21	AT3G27160	*rps21-1/ghs1-2*	SALK_066068C	RPS21-RP	TGC TTG TGC AGT GAT TGA TTC
		rps21-2/ghs1-3	SALk_077692C	RPS21 SALK_066068 -LP	GAACACTTGTTCAGTTGTTCCG
				RPS21 SALK_077692-LP	ACG AAA ATC AAC GAA GCA AAG
Rps9	AT1G74970	*rps9-1*	SALK_134633C	RPS9-LP	ACC GAT CGT GAC TCT ATG TGG
		rps9-2	SALK_128849C	RPS9-RP	TAC CGT GGC GGT GAT AGA TAG
SBPase	AT3G55800	*sbp-1*	SALK_130939C	SBPASE-LP S130939	TCCAATGGGAACATTCTTGAG
				SBPASE-RP S130939	CTGAGCTTCAAGACATGGGAG
	AT3G55800	*sbp-2*	SALK_090549C	SBPASE-LP S090549	GGAATCTTATGACATTCCAAAAATG
				SBPASE-RP S090549	TCAATCCCTTGTCAGGAGTTG

For the PCRs, GoTaq Green Master Mix (Promega) was used. We used the primers SAIL_LB3 (TAGCATCTGAATTTCATAACCAATCTCGATACAC), LBb1 (GCGTGGAC CGCTTGCTGCAACT), LBb1.3 (ATTTTGCCGATTTCGGAAC), LBa1 (TGGTTCACGTAGTGGGCCATCG) and others available in Table 6.7. The premixed ready-to-use solution contains Taq DNA polymerase, dNTPs, $MgCl_2$ and reaction buffers at optimal concentrations for efficient amplification of DNA.

Table 6.8: GreenTaq PCR mix

Component	**10 μl total reaction**
GoTaq Green Master Mix (2X)	5
10 μM Forward primer	0.5
10 μM Reverse primer	0.5
DNA template	1
Nuclease-free water	to 10

Table 6.9: GoTaq Green thermocycling conditions

Step	Temperature	Time
Initial denaturation	95°C	2 minutes
25-35 cycles	95°C	30 seconds
	55°-58°C	30 seconds
	72°C	1 minute/kb
Final extension	72°C	5 minutes
Hold	4°C	Forever

6.5 Generation of transgenic Arabidopsis plants

The full-length coding sequence of Arabidopsis *SBPase* was cloned in frame with a C-terminal enhanced GFP tag under control of the 35S promoter using entry vector *pDONR207* using BP and LR clonase II kits (Invitrogen Technologies). GV3101 *A. tumefaciens* cultures containing the *35S:SBPase-GFP* constructs were grown overnight at 28°C in YEB medium containing rifampicin, gentamycin, and spectinomycin, centrifuged, and resuspended in infiltration medium (0.5X MS, 5% sucrose, Silwet L-77 (0.01% [v/v]). Then, Arabidopsis plants were transformed by the floral dip method (Clough and Bent, 1998). Homozygous lines containing a single T-DNA insertion were selected based on the segregation of the resistance marker (Km) (Harrison et al., 2006) (Table 6.3).

6.6 Protease protection assays

For protease protection (accessibility) assays, protein extracts from 10-day-old plants containing 30 μg of total protein (See 6.9 for protein concentration determination) were incubated for 5 minutes at 37°C with increasing concentrations of Proteinase K

(Invitrogen) (See Figure 3.14A). After stopping the reaction with SDS-PAGE loading buffer, extracts were used for immunoblotting analysis (See section 6.9).

6.7 Transient expression in *N. benthamiana*

*A. tumefacien*s GV3101 strains were transformed with the vector of interest. Were streaked on plates with the appropriate antibiotics and grown at 28°C for 2-3 days. A single colony (previous PCR colony corroboration) was inoculated in 5 ml YEB media, the culture was grown overnight at 28°C with a 300 rpm rotation rate. The next day, 500 μl of the grown culture was added to 20 ml of YEB media. Culture was incubated overnight at 28°C. OD_{600} values were obtained of each liquid culture with a spectrophotometer. The culture was centrifuged 10 minutes 4,000 rpm 4°C. Then, bacteria was resuspended in the infiltration buffer (10 mM MES pH5.5.-6, 10 mM $MgSO_4$, Acetosyringone 100 μM).

Leafs from 4-week-old *N. benthamiana* plants were entirely infiltrated with the desired combination of *A. tumefaciens* strains in the infiltration buffer. After agroinfiltration, the plants were left on the bench or the greenhouse for the indicated times. Leafs were used to perform co-IP assays or confocal microscopy analysis.

6.8 Co-immunoprecipitation assays

After three days, total protein of agroinfiltrated *N. benthamiana* leaf was extracted at 4°C. 1.6 g of agroinfiltrated leaf tissue was grinded in a prechilled mortar. The grinded tissue was transferred to a 50 mL falcon tube and 7.5 ml of Co-IP extraction buffer (25 mM Tris-HCl pH 7.5, 150 mM NaCl, 5% glycerol, 0.05% Nonidet P-40, 2.5 mM EDTA, 1mM PMSF, 1X plant protease inhibitor) was added, forming a consistent slurry. The slurry was centrifuged at 13,500 rpm in a refrigerated microcentrifuge for 2 minutes. Then, the supernatant was transferred to a 2 ml Eppendorf tube and centrifuged for an additional 10 minutes. Then, the supernatant was transferred to a 1.5 ml Eppendorf tube. In this step, the input was recollected.

A preclearing step was performed to the extracts using 60 μl of agarose conjugated IgG beads (Sigma) to eliminate nonspecific binding. The extract with the beads were incubated end-over-end in a rotating microtube mixer at 4°C for 30 minutes. Then, the sample was centrifuged 1 minute at full speed. 1.4 ml of the supernatant was transferred to a new tube for the specific immunoprecipitation. 60 μl of slurry anti-MYC (Covance) with the coupled antibody agarose beads was added. Extracts and the slurry were incubated end-over-end for 4 h at 4°C. Then the sample was centrifuged for 5 seconds to then discard the supernatant. 1 ml of Co-IP extraction

buffer was added to the slurry. This last step was repeated four more times. After the last wash, the sample is centrifuged and any remaining liquid was removed with a 1 ml syringe. The beads were resuspended in 1X SDS-PAGE loading buffer for subsequent analysis. More details about the co-IP are found in Lee et al., 2010 and Moffett, 2011

6.9 Protein analysis

Total protein extracts were obtained from *ca.* 10 mg of Arabidopsis lyophilized powder. The powder was resuspended in 200-600 μl of ice-cold TKMES homogenization buffer (100 mM Tricine-potassium hydroxide pH 7.5, 10 mM KCl, 1 mM MgCl2, 1 mM EDTA, and 10% [w/v] Sucrose) supplemented with 0.2% (v/v) Triton X-100, 1mM DTT, 100 μg/ml PMSF, 3 μg/ml E64, and 1X Sigma plant protease inhibitor. The resuspended sample was centrifuged at 12,000 rpm for 10 minutes at 4°C and the supernatant recovered for a second step of centrifugation Supernatant recovered for a second step of centrifugation.

For the separation of soluble and insoluble (with protein aggregates) fractions, native protein extracts were obtained in a buffer containing 100 mM Tris-HCl pH 7.9, 10 mM $MgCl_2$, 1% (v/v) glycerol, and 1X plant protease inhbibitor (Sigma). After centrifugation for 10 minutes at 10,000 x g, the supernatant was collected as the soluble fraction. The pellet was washed with fresh buffer and centrifuged again. The obtained pellet fraction was then resuspended in denaturing TKMES buffer and centrifuged again to collect the supernatant as the insoluble fraction.

In all cases protein concentration was determined using the kit Coomasie Plus-The Better Bradford Assay Kit (Thermo Scientific). Measurements were performed in a total volume of 200 μl of Bradford with 2 μl of protein extract in a 96 well plate using the SpectraMax M3 multi-mode microplate reader (Molecular Devices).

After SDS-PAGE, the proteins were electrotransferred to hybond-P polyvinylidene difluoride membranes (Amersham) using a Trans blot Turbo transfer system (Bio-Rad). After the protein transference was completed, membranes were incubated overnight at 4°C with the corresponding primary antibody. Incubation with the horseradish peroxidase-conjugated secondary antibody (1:10,000) was performed for 30 minutes at room temperature. Detection of protein bands was performed using the ECL Plus reagent (Amersham). Chemiluminescent signals were visualized using a LAS-4000 (Fujifilm) image analyzer and quantified with ImageJ.

Finally, total protein in membranes were stained with Coomasie blue (Coomassie 0,6% (w/v), ethanol 40% (v/v), acetic acid 10% (v/v) and 50% water (v/v)) or Ponceu S.

Table 6.10: Antibodies used

Antibody	Dilution	Origin	Protein concentration	Supplier
DXS	1:500	Rabbit	30 μg	Abintek
DXR	1:7,000	Rabbit	5 μg	
cpHsp70	1:7,000	Rabbit	5 μg	Agrisera
ClpC	1:1,500	Rabbit	5 μg	Agrisera
ClpB3	1:2,000	Rabbit	30 μg	Agrisera
MYC	1:1,000	Mouse		Calbiochem
GFP	1:1,000	Rabbit		Life Technologies
ClpP1	1:1,000	Rabbit	30 μg	Agrisera
AtpB	1:5,000	Rabbit	5 μg	
PsbA	1:2,000	Rabbit	5 μg	

The intensities of immunoblot signals obtained were quantified using Image J, The corresponding RubisCO band from the stained membranes were used as loading control and as normalizer for quantification.

6.10 Gene expression analysis

Total RNA was extracted for seedlings using the Maxwell 16 LEV Plant RNA Kit (Promega). RNA was quantified using a NanoDrop (Thermo Scientific) and its integrity was analyzed by agarose gel electrophoresis. The cDNA synthesis was performed as follows according the recommendations of the Transcriptor First Strand cDNA synthesis Kit (Roche). RT-qPCR was done in a total reaction volume of 20 μL using LightCycler 480 SYBR Green I Master (Roche) on a LightCycler 480 Real-Time PCR System (Roche).The normalized expression of target genes was calculated using *UBC* as the endogenous reference gene. Information about primers used for qPCR is described in Table 6.14.

Table 6.11: cDNA synthesis

Reagent	Volume (μl)	Thermocycling conditions
Template RNA (1 μg)	Up to 11	5 minutes 55°C
Oligo dT	1	
Nuclease-free water	Up to 13	
Buffer (1X)	4	30 minutes 4°C
dNTPs (1 mM)	2	5 minutes 65°C
RNase Inhibitor (4U/ μl)	0.5	
RTase (10U)	0.5	
Final volume	20	

Table 6.12: qPCR mix reaction

Reagent	Volume (μl
SYBR Green I Master Mix	10
Primer Fw (300 nM)	0.6
Primer Rv (300 nM)	0.6
Template cDNA (50 ng)	1
Nuclease-free water	7.8
Final volume	20

Table 6.13: qPCR program

Step	Temperature	Time	Cycles
Taq activation	95°C	10 minutes	45
Primer Fw (300 nM)	95°C	10 seconds	
Primer Rv (300 nM)	60°C	30 seconds	

Table 6.14: qPCR primers

Gene	AGI Locus	Primers used for qPCR (Fw/Rv)	Reference
ClpB3	At5G15450	5′ TGAATGCTGCAAGGTCAATC 3′ 5′ TCCTGTCTGCAATTCGCTTC 3′	Myouga et al., 2006
Hsp70-1	At4G24280	5′ CTCGTGAGGAAGGTGACTGG 3′ 5′ AACACCACCTAGGGTCTCCA 3′	This study
Hsp70-2	At5G49910	5′ GCTGACTCCGTCGTTTACCA 3′ 5′ CCTGGTTGGGGTTGGTTGTA 3′	This study
DXS	At4G15560	5′ TCGCAAAGGGTATGACAAAG 3′ 5′ CCAGTCCCGCTTATCATTCC 3′	Pulido et al., 2013
UBC	At5G25760	5′ TCAAATGGACCGCTCTTATC 3′ 5′ CACAGACTGAAGCGTCCAAG 3′	Llorente et al., 2016

6.11 Confocal microscopy analysis

Subcellular localization of GFP fluorescence and chlorophyll fluorescence was determined with an Olympus FV 1000 confocal laser-scanning microscope (Olympus) using an argon laser for excitation (at 488 nm) and 500-510 nm filter for detection of GFP fluorescence and 610-700 nm filter for detection of chlorophyll fluorescence.

6.12 Metabolite analysis

6.12.1 Chlorophyll quantification by spectrophotometry

Seedlings were recollected (between 25-100 mg of fresh weight) in 2 ml microcentrifuge tube with crystal beads (3mm). Samples were grinded in a Tissue Lyser II (Qiagen) to a fine powder. 1 ml of acetone 80% were added to the tube. Samples were mixed for 1 h in darkness at 4 °C. Samples were centrifuged at 12,000 rpm at 4°C for 3 minutes. The supernatant was transfer to a fresh tube. Absorbance spectra were measured using a SpectraMax M3 multi-mode microplate reader (Molecular Devices).

The concentration of chlorophylls *a* and *b*, as well as the major carotenoids, comprising xanthophyll and carotene, was calculated as follows (Lichtenthaler, 1987):

$$Chlorophyll\ a\ \ (C_a) = 12.25\ A_{663} - 2.79\ A_{647}$$

$$Chlorophyll\ b\ \ (C_b) = 21.50\ A_{647} - 5.10\ A_{663}$$

$$Total\ chlorophyll = 7.15\ A_{663} + 18.71\ A_{647}$$

$$Total\ carotenoids = \frac{(1000\ A_{470} - 1.82\ C_a - 85.02\ C_b)}{198}$$

Results obtained equated to μg of chlorophyll or carotenoids per ml (mg fresh weight material).

6.12.2 Analysis of metabolites by HPLC

Carotenoids and chlorophylls were extracted from 4 mg of lyophilized Arabidopsis seedlings using 1 ml cold extraction solvent as previously described (Saladie et al., 2014), and were analyzed by HPLC in an Agilent 1200 series HPLC system (Agilent Technologies), as previously described (Fraser et al., 2000). Cantanxanthin, a carotenoid not present in plants, was used as an internal standard in HPLC experiments. Individual peaks in chromatograms were quantified by integrating the area under the curve using the software provided by the supplier and normalized to the cantaxanthin value.

6.13 Chloroplast subfractioning

Chloroplasts were isolated from 10 day-old-seedlings as described (Flores-Perez et al., 2008a) and further fractionation was performed as indicated (Vidi et al., 2006; Wang et al., 2015). Briefly, chloroplasts were hypertonically lysed in 0.6 M sucrose supplemented with 0.5% (w/v) protease inhibitor cocktail (Sigma). Stromal fraction was collected after centrifugation at 100,000 xg. The membrane pellet was resuspended in the same buffer and centrifuged again to prevent stromal contamination. A Potter Elvehjem homogenizer was used to resuspend the chloroplast membranes in 1 ml TED buffer (50 mM Tricine pH 7.5, 2 mM EDTA, 2 mM dithiothreitol). Subsequent separation was performed in sucrose density gradients as described (Vidi et al., 2006; Wang et al., 2015).

6.14 Prediction of aggregation propensity

The Aggrescan3D algorithm (Zambrano et al., 2015) was used to analyze protein aggregation propensity. Predictions were performed in static mode using a distance of aggregation analysis of 10 Å. The Arabidopsis DXS structure was modelled using Swiss-Model (Bordoli and Schwede, 2012) on top of the 2.40 Å resolution *E. coli* DXS structure with PDB code 2O1S. Residues 72 to 707 of the Arabidopsis DXS

monomer, sharing a sequence identity of 41.08% with the *E. coli* protein, were structurally aligned and modelled. The interface of the generated homodimer was evaluated with PDBePISA (http://www.ebi.ac.uk/pdbe/pisa/) rendering an area of 8892 Å and a predicted dissociation ΔG for the dimer of 51.2 kcal/mol (close to those of the template E. coli crystal structure, which exhibits an interface of 7970 Å and a dissociation ΔG of 59.1 kcal/mol).

6.15 Statistical analyses

Student's *t* test were calculated using the software GraphPad Prism.

7. Bibliography

Alberts, Bruce, John Wilson, and Tim Hunt (2008). *Molecular biology of the cell*. New York: Garland Science. ISBN: 9780815341055 0815341059 0815341067 9780815341062 0815341105 9780815341109 0815341113 9780815341116.

Allison, L. A., L. D. Simon, and P. Maliga (1996). "Deletion of rpoB reveals a second distinct transcription system in plastids of higher plants". In: *EMBO J* 15.11, pp. 2802–9. ISSN: 0261-4189 (Print) 0261-4189 (Linking). URL: https://www.ncbi.nlm.nih.gov/pubmed/8654377.

Arnould, T., S. Michel, and P. Renard (2015). "Mitochondria Retrograde Signaling and the UPR mt: Where Are We in Mammals?" In: *Int J Mol Sci* 16.8, pp. 18224–51. ISSN: 1422-0067 (Electronic) 1422-0067 (Linking). DOI: 10.3390/ijms160818224. URL: http://www.ncbi.nlm.nih.gov/pubmed/26258774.

Arrivault, S., M. Guenther, A. Ivakov, R. Feil, D. Vosloh, J. T. van Dongen, R. Sulpice, and M. Stitt (2009). "Use of reverse-phase liquid chromatography, linked to tandem mass spectrometry, to profile the Calvin cycle and other metabolic intermediates in Arabidopsis rosettes at different carbon dioxide concentrations". In: *Plant J* 59.5, pp. 826–39. ISSN: 1365-313X (Electronic) 0960-7412 (Linking). DOI: 10.1111/j.1365-313X.2009.03902.x. URL: https://www.ncbi.nlm.nih.gov/pubmed/19453453.

Avendano-Vazquez, A. O., E. Cordoba, E. Llamas, C. San Roman, N. Nisar, S. De la Torre, M. Ramos-Vega, M. D. Gutierrez-Nava, C. I. Cazzonelli, B. J. Pogson, and P. Leon (2014). "An Uncharacterized Apocarotenoid-Derived Signal Generated in zeta-Carotene Desaturase Mutants Regulates Leaf Development and the Expression of Chloroplast and Nuclear Genes in Arabidopsis". In: *Plant Cell* 26.6, pp. 2524–2537. ISSN: 1532-298X (Electronic) 1040-4651 (Linking). DOI: 10.1105/tpc.114.123349. URL: https://www.ncbi.nlm.nih.gov/pubmed/24907342.

Banerjee, A., Y. Wu, R. Banerjee, Y. Li, H. Yan, and T. D. Sharkey (2013). "Feedback inhibition of deoxy-D-xylulose-5-phosphate synthase regulates the methylerythritol 4-phosphate pathway". In: *J Biol Chem* 288.23, pp. 16926–36. ISSN: 1083-351X (Electronic) 0021-9258 (Linking). DOI: 10.1074/jbc.M113.464636. URL: https://www.ncbi.nlm.nih.gov/pubmed/23612965.

Barkan, A. (2011). "Expression of plastid genes: organelle-specific elaborations on a prokaryotic scaffold". In: *Plant Physiol* 155.4, pp. 1520–32. ISSN: 1532-2548 (Electronic) 0032-0889 (Linking). DOI: 10.1104/pp.110.171231. URL: https://www.ncbi.nlm.nih.gov/pubmed/21346173.

Benn, G., M. Bjornson, H. Ke, A. De Souza, E. I. Balmond, J. T. Shaw, and K. Dehesh (2016). "Plastidial metabolite MEcPP induces a transcriptionally centered stress-response hub via the transcription factor CAMTA3". In: *Proc Natl Acad Sci U S A* 113.31, pp. 8855–60. ISSN: 1091-6490 (Electronic) 0027-8424 (Linking). DOI: 10.1073/pnas.1602582113. URL: https://www.ncbi.nlm.nih.gov/pubmed/27432993.

Bollenbach, T. J., R. E. Sharwood, R. Gutierrez, S. Lerbs-Mache, and D. B. Stern (2009). "The RNA-binding proteins CSP41a and CSP41b may regulate transcription and translation of chloroplast-encoded RNAs in Arabidopsis". In: *Plant Mol Biol* 69.5, pp. 541–52. ISSN: 0167-4412 (Print) 0167-4412 (Linking). DOI: 10.1007/s11103-008-9436-z. URL: https://www.ncbi.nlm.nih.gov/pubmed/19067181.

Bordoli, L. and T. Schwede (2012). "Automated protein structure modeling with SWISS-MODEL Workspace and the Protein Model Portal". In: *Methods Mol Biol* 857, pp. 107–36. ISSN: 1940-6029 (Electronic) 1064-3745 (Linking). DOI: 10.1007/978-1-61779-588-6_5. URL: https://www.ncbi.nlm.nih.gov/pubmed/22323219.

Boston, R. S., P. V. Viitanen, and E. Vierling (1996). "Molecular chaperones and protein folding in plants". In: *Plant Mol Biol* 32.1-2, pp. 191–222. ISSN: 0167-4412 (Print) 0167-4412 (Linking). URL: https://www.ncbi.nlm.nih.gov/pubmed/8980480.

Bowsher, C. G. and A. K. Tobin (2001). "Compartmentation of metabolism within mitochondria and plastids". In: *J Exp Bot* 52.356, pp. 513–27. ISSN: 0022-0957 (Print) 0022-0957 (Linking). URL: https://www.ncbi.nlm.nih.gov/pubmed/11373301.

Brehelin, C., F. Kessler, and K. J. van Wijk (2007). "Plastoglobules: versatile lipoprotein particles in plastids". In: *Trends Plant Sci* 12.6, pp. 260–6. ISSN: 1360-1385 (Print) 1360-1385 (Linking). DOI: 10.1016/j.tplants.2007.04.003. URL: https://www.ncbi.nlm.nih.gov/pubmed/17499005.

Carretero-Paulet, L., I. Ahumada, N. Cunillera, M. Rodriguez-Concepcion, A. Ferrer, A. Boronat, and N. Campos (2002). "Expression and molecular analysis of the Arabidopsis DXR gene encoding 1-deoxy-D-xylulose 5-phosphate reductoisomerase, the first committed enzyme of the 2-C-methyl-D-erythritol 4-phosphate pathway". In: *Plant Physiol* 129.4, pp. 1581–91. ISSN: 0032-0889 (Print) 0032-0889 (Linking). DOI: 10.1104/pp.003798. URL: https://www.ncbi.nlm.nih.gov/pubmed/12177470.

Carretero-Paulet, L., A. Cairo, P. Botella-Pavia, O. Besumbes, N. Campos, A. Boronat, and M. Rodriguez-Concepcion (2006). "Enhanced flux through the methylerythritol 4-phosphate pathway in Arabidopsis plants overexpressing deoxyxylulose 5-phosphate reductoisomerase". In: *Plant Mol Biol* 62.4-5, pp. 683–95. ISSN: 0167-4412 (Print) 0167-4412 (Linking). DOI: 10.1007/s11103-006-9051-9. URL: https://www.ncbi.nlm.nih.gov/pubmed/16941216.

Cavalier-Smith, T. (2004). "Only six kingdoms of life". In: *Proc Biol Sci* 271.1545, pp. 1251–62. ISSN: 0962-8452 (Print) 0962-8452 (Linking). DOI: 10.1098/rspb.2004.2705. URL: https://www.ncbi.nlm.nih.gov/pubmed/15306349.

Cazzonelli, C. I. and B. J. Pogson (2010). "Source to sink: regulation of carotenoid biosynthesis in plants". In: *Trends Plant Sci* 15.5, pp. 266–74. ISSN: 1878-4372 (Electronic) 1360-1385 (Linking). DOI: 10.1016/j.tplants.2010.02.003. URL: https://www.ncbi.nlm.nih.gov/pubmed/20303820.

Chan, K. X., S. Y. Phua, P. Crisp, R. McQuinn, and B. J. Pogson (2016). "Learning the Languages of the Chloroplast: Retrograde Signaling and Beyond". In: *Annu Rev Plant Biol* 67, pp. 25–53. ISSN: 1545-2123 (Electronic) 1543-5008 (Linking). DOI: 10.1146/annurev-arplant-043015-111854. URL: https://www.ncbi.nlm.nih.gov/pubmed/26735063.

Chen, K. M., M. Holmstrom, W. Raksajit, M. Suorsa, M. Piippo, and E. M. Aro (2010). "Small chloroplast-targeted DnaJ proteins are involved in optimization of photosynthetic reactions in Arabidopsis thaliana". In: *BMC Plant Biol* 10, p. 43. ISSN: 1471-2229 (Electronic) 1471-2229 (Linking). DOI: 10.1186/1471-2229-10-43. URL: https://www.ncbi.nlm.nih.gov/pubmed/20205940.

Chi, W., X. Sun, and L. Zhang (2013). "Intracellular signaling from plastid to nucleus". In: *Annu Rev Plant Biol* 64, pp. 559–82. ISSN: 1545-2123 (Electronic) 1543-5008 (Linking). DOI: 10.1146/annurev-arplant-050312-120147. URL: https://www.ncbi.nlm.nih.gov/pubmed/23394498.

Chowdhury, T., P. Chien, S. Ebrahim, R. T. Sauer, and T. A. Baker (2010). "Versatile modes of peptide recognition by the ClpX N domain mediate alternative adaptor-binding specificities in different bacterial species". In: *Protein Sci* 19.2, pp. 242–54. ISSN: 1469-896X (Electronic) 0961-8368 (Linking). DOI: 10.1002/pro.306. URL: https://www.ncbi.nlm.nih.gov/pubmed/20014030.

Clarke, A. K. (2012). "The chloroplast ATP-dependent Clp protease in vascular plants - new dimensions and future challenges". In: *Physiol Plant* 145.1, pp. 235–44. ISSN: 1399-3054 (Electronic) 0031-9317 (Linking). DOI: 10.1111/j.1399-3054.2011.01541.x. URL: https://www.ncbi.nlm.nih.gov/pubmed/22085372.

Clarke, Adrian K., Tara M. MacDonald, and Lars L. E. Sjögren (2005). "The ATP-dependent Clp protease in chloroplasts of higher plants". In: *Physiologia Plantarum* 123.4, pp. 406–412. ISSN: 1399-3054. DOI: 10.1111/j.1399-3054.2005.00452.x. URL: http://dx.doi.org/10.1111/j.1399-3054.2005.00452.x.

Clough, S. J. and A. F. Bent (1998). "Floral dip: a simplified method for Agrobacterium-mediated transformation of Arabidopsis thaliana". In: *Plant J* 16.6, pp. 735–43. ISSN: 0960-7412 (Print) 0960-7412 (Linking). URL: https://www.ncbi.nlm.nih.gov/pubmed/10069079.

Colombo, M., L. Tadini, C. Peracchio, R. Ferrari, and P. Pesaresi (2016). "GUN1, a Jack-Of-All-Trades in Chloroplast Protein Homeostasis and Signaling". In: *Front Plant Sci* 7, p. 1427. ISSN: 1664-462X (Linking). DOI: 10.3389/fpls.2016.01427. URL: https://www.ncbi.nlm.nih.gov/pubmed/27713755.

Cordoba, E., M. Salmi, and P. Leon (2009). "Unravelling the regulatory mechanisms that modulate the MEP pathway in higher plants". In: *J Exp Bot* 60.10, pp. 2933–43. ISSN: 1460-2431 (Electronic) 0022-0957 (Linking). DOI: 10.1093/jxb/erp190. URL: https://www.ncbi.nlm.nih.gov/pubmed/19584121.

Covington, M. F., J. N. Maloof, M. Straume, S. A. Kay, and S. L. Harmer (2008). "Global transcriptome analysis reveals circadian regulation of key pathways in plant growth and development". In: *Genome Biol* 9.8, R130. ISSN: 1474-760X (Electronic) 1474-7596 (Linking). DOI: 10.1186/gb-2008-9-8-r130. URL: https://www.ncbi.nlm.nih.gov/pubmed/18710561.

Dale, S., M. Arro, B. Becerra, N. G. Morrice, A. Boronat, D. G. Hardie, and A. Ferrer (1995). "Bacterial expression of the catalytic domain of 3-hydroxy-3-methylglutaryl-CoA reductase (isoform HMGR1) from Arabidopsis thaliana, and its inactivation by phosphorylation at Ser577 by Brassica oleracea 3-hydroxy-3-methylglutaryl-CoA reductase kinase". In: *Eur J Biochem* 233.2, pp. 506–13. ISSN: 0014-2956 (Print) 0014-2956 (Linking). URL: https://www.ncbi.nlm.nih.gov/pubmed/7588795.

DellaPenna, D. and B. J. Pogson (2006). "Vitamin synthesis in plants: tocopherols and carotenoids". In: *Annu Rev Plant Biol* 57, pp. 711–38. ISSN: 1543-5008 (Print) 1543-5008 (Linking). DOI: 10.1146/annurev.arplant.56.032604.144301. URL: https://www.ncbi.nlm.nih.gov/pubmed/16669779.

Diemand, A. V. and A. N. Lupas (2006). "Modeling AAA+ ring complexes from monomeric structures". In: *J Struct Biol* 156.1, pp. 230–43. ISSN: 1047-8477 (Print) 1047-8477 (Linking). DOI: 10.1016/j.jsb.2006.04.011. URL: https://www.ncbi.nlm.nih.gov/pubmed/16765605.

Dougan, D. A., A. Mogk, K. Zeth, K. Turgay, and B. Bukau (2002). "AAA+ proteins and substrate recognition, it all depends on their partner in crime". In: *FEBS Lett* 529.1, pp. 6–10. ISSN: 0014-5793 (Print) 0014-5793 (Linking). URL: https://www.ncbi.nlm.nih.gov/pubmed/12354604.

Doyle, S. M., J. R. Hoskins, and S. Wickner (2007). "Collaboration between the ClpB AAA+ remodeling protein and the DnaK chaperone system". In: *Proc Natl Acad Sci U S A* 104.27, pp. 11138–44. ISSN: 0027-8424 (Print) 0027-8424 (Linking). DOI: 10.1073/pnas.0703980104. URL: https://www.ncbi.nlm.nih.gov/pubmed/17545305.

Edwards, K., C. Johnstone, and C. Thompson (1991). "A simple and rapid method for the preparation of plant genomic DNA for PCR analysis". In: *Nucleic Acids Res* 19.6, p. 1349. ISSN: 0305-1048 (Print) 0305-1048 (Linking). URL: https://www.ncbi.nlm.nih.gov/pubmed/2030957.

Erbse, A., D. A. Dougan, and B. Bukau (2003). "A folding machine for many but a master of none". In: *Nat Struct Biol* 10.2, pp. 84–6. ISSN: 1072-8368 (Print) 1072-8368 (Linking). DOI: 10.1038/nsb0203-84. URL: https://www.ncbi.nlm.nih.gov/pubmed/12555083.

Estevez, J. M., A. Cantero, C. Romero, H. Kawaide, L. F. Jimenez, T. Kuzuyama, H. Seto, Y. Kamiya, and P. Leon (2000). "Analysis of the expression of CLA1, a gene that encodes the 1-deoxyxylulose 5-phosphate synthase of the 2-C-methyl-D-erythritol-4-phosphate pathway in Arabidopsis". In: *Plant Physiol* 124.1, pp. 95–104. ISSN: 0032-0889 (Print) 0032-0889 (Linking). URL: https://www.ncbi.nlm.nih.gov/pubmed/10982425.

Estevez, J. M., A. Cantero, A. Reindl, S. Reichler, and P. Leon (2001). "1-Deoxy-D-xylulose-5-phosphate synthase, a limiting enzyme for plastidic isoprenoid biosynthesis in plants". In: *J Biol Chem* 276.25, pp. 22901–9. ISSN: 0021-9258 (Print) 0021-9258 (Linking). DOI: 10.1074/jbc.M100854200. URL: https://www.ncbi.nlm.nih.gov/pubmed/11264287.

Ferhatoglu, Yurdagul and Michael Barrett (2006). "Studies of clomazone mode of action". In: *Pesticide biochemistry and physiology* 85.1, pp. 7–14. ISSN: 0048-3575.

Fiorese, C. J. and C. M. Haynes (2017). "Integrating the UPRmt into the mitochondrial maintenance network". In: *Crit Rev Biochem Mol Biol*, pp. 1–10. ISSN: 1549-7798 (Electronic) 1040-9238 (Linking). DOI: 10.1080/10409238.2017.1291577. URL: https://www.ncbi.nlm.nih.gov/pubmed/28276702.

Flores-Perez, U. and P. Jarvis (2013). "Molecular chaperone involvement in chloroplast protein import". In: *Biochim Biophys Acta* 1833.2, pp. 332–40. ISSN: 0006-3002 (Print) 0006-3002 (Linking). DOI: 10.1016/j.bbamcr.2012.03.019. URL: https://www.ncbi.nlm.nih.gov/pubmed/22521451.

Flores-Perez, U., S. Sauret-Gueto, E. Gas, P. Jarvis, and M. Rodriguez-Concepcion (2008a). "A mutant impaired in the production of plastome-encoded proteins uncovers a mechanism for the homeostasis of isoprenoid biosynthetic enzymes in Arabidopsis plastids". In: *Plant Cell* 20.5, pp. 1303–15. ISSN: 1040-4651 (Print) 1040-4651 (Linking). DOI: 10.1105/tpc.108.058768. URL: http://www.ncbi.nlm.nih.gov/pubmed/18469163.

Flores-Perez, U., J. Perez-Gil, A. Rodriguez-Villalon, M. J. Gil, P. Vera, and M. Rodriguez Concepcion (2008b). "Contribution of hydroxymethylbutenyl diphosphate synthase to carotenoid biosynthesis in bacteria and plants". In: *Biochem Biophys Res Commun* 371.3, pp. 510–4. ISSN: 1090-2104 (Electronic) 0006-291X (Linking). DOI: 10.1016/j.bbrc.2008.04.115. URL: https://www.ncbi.nlm.nih.gov/pubmed/18452711.

Flores-Perez, U., J. Perez-Gil, M. Closa, L. P. Wright, P. Botella-Pavia, M. A. Phillips, A. Ferrer, J. Gershenzon, and M. Rodriguez-Concepcion (2010). "Pleiotropic regulatory locus 1 (PRL1) integrates the regulation of sugar responses with isoprenoid metabolism in Arabidopsis". In: *Mol Plant* 3.1, pp. 101–12. ISSN: 1674-2052 (Print) 1674-2052 (Linking). DOI: 10.1093/mp/ssp100. URL: https://www.ncbi.nlm.nih.gov/pubmed/20008452.

Flores-Perez, U., J. Bedard, N. Tanabe, P. Lymperopoulos, A. K. Clarke, and P. Jarvis (2016). "Functional Analysis of the Hsp93/ClpC Chaperone at the Chloroplast Envelope". In: *Plant Physiol* 170.1, pp. 147–62. ISSN: 1532-2548 (Electronic) 0032-0889 (Linking). DOI: 10.1104/pp.15.01538. URL: https://www.ncbi.nlm.nih.gov/pubmed/26586836.

Fraser, P. D., M. E. Pinto, D. E. Holloway, and P. M. Bramley (2000). "Technical advance: application of high-performance liquid chromatography with photodiode array detection to the metabolic profiling of plant isoprenoids". In: *Plant J* 24.4, pp. 551–8. ISSN: 0960-7412 (Print) 0960-7412 (Linking). URL: https://www.ncbi.nlm.nih.gov/pubmed/11115136.

Fung, P. K., J. Krushkal, and P. J. Weathers (2010). "Computational analysis of the evolution of 1-deoxy-D-xylulose-5-phosphate Reductoisomerase, an important enzyme in plant terpene biosynthesis". In: *Chem Biodivers* 7.5, pp. 1098–110. ISSN: 1612-1880 (Electronic) 1612-1872 (Linking). DOI: 10.1002/cbdv.200900313. URL: https://www.ncbi.nlm.nih.gov/pubmed/20491066.

Furumoto, T., T. Yamaguchi, Y. Ohshima-Ichie, M. Nakamura, Y. Tsuchida-Iwata, M. Shimamura, J. Ohnishi, S. Hata, U. Gowik, P. Westhoff, A. Brautigam, A. P. Weber, and K. Izui (2011). "A plastidial sodium-dependent pyruvate transporter". In: *Nature* 476.7361, pp. 472–5. ISSN: 1476-4687 (Electronic) 0028-0836 (Linking). DOI: 10.1038/nature10250. URL: https://www.ncbi.nlm.nih.gov/pubmed/21866161.

Gas, E., U. Flores-Perez, S. Sauret-Gueto, and M. Rodriguez-Concepcion (2009). "Hunting for plant nitric oxide synthase provides new evidence of a central role for plastids in nitric oxide metabolism". In: *Plant Cell* 21.1, pp. 18–23. ISSN: 1040-4651 (Print) 1040-4651 (Linking). DOI: 10.1105/tpc.108.065243. URL: https://www.ncbi.nlm.nih.gov/pubmed/19168714.

Ghassemian, M., J. Lutes, J. M. Tepperman, H. S. Chang, T. Zhu, X. Wang, P. H. Quail, and B. M. Lange (2006). "Integrative analysis of transcript and metabolite profiling data sets to evaluate the regulation of biochemical pathways during photomorphogenesis". In: *Arch Biochem Biophys* 448.1-2, pp. 45–59. ISSN: 0003-9861 (Print) 0003-9861 (Linking). DOI: 10.1016/j.abb.2005.11.020. URL: https://www.ncbi.nlm.nih.gov/pubmed/16460663.

Ghirardo, A., L. P. Wright, Z. Bi, M. Rosenkranz, P. Pulido, M. Rodriguez-Concepcion, U. Niinemets, N. Bruggemann, J. Gershenzon, and J. P. Schnitzler (2014). "Metabolic flux analysis of plastidic isoprenoid biosynthesis in poplar leaves emitting and

nonemitting isoprene". In: *Plant Physiol* 165.1, pp. 37–51. ISSN: 1532-2548 (Electronic) 0032-0889 (Linking). DOI: 10.1104/pp.114.236018. URL: https://www.ncbi.nlm.nih.gov/pubmed/24590857.

Gil, M. J., A. Coego, B. Mauch-Mani, L. Jorda, and P. Vera (2005). "The Arabidopsis csb3 mutant reveals a regulatory link between salicylic acid-mediated disease resistance and the methyl-erythritol 4-phosphate pathway". In: *Plant J* 44.1, pp. 155–66. ISSN: 0960-7412 (Print) 0960-7412 (Linking). DOI: 10.1111/j.1365-313X.2005.02517.x. URL: https://www.ncbi.nlm.nih.gov/pubmed/16167903.

Glover, J. R. and S. Lindquist (1998). "Hsp104, Hsp70, and Hsp40: a novel chaperone system that rescues previously aggregated proteins". In: *Cell* 94.1, pp. 73–82. ISSN: 0092-8674 (Print) 0092-8674 (Linking). URL: https://www.ncbi.nlm.nih.gov/pubmed/9674429.

Goloubinoff, P., A. Mogk, A. P. Zvi, T. Tomoyasu, and B. Bukau (1999). "Sequential mechanism of solubilization and refolding of stable protein aggregates by a bichaperone network". In: *Proc Natl Acad Sci U S A* 96.24, pp. 13732–7. ISSN: 0027-8424 (Print) 0027-8424 (Linking). URL: https://www.ncbi.nlm.nih.gov/pubmed/10570141.

Grimm, B., K. Dehesh, L. Zhang, and D. Leister (2014). "Intracellular communication". In: *Mol Plant* 7.7, pp. 1071–4. ISSN: 1752-9867 (Electronic) 1674-2052 (Linking). DOI: 10.1093/mp/ssu073. URL: http://www.ncbi.nlm.nih.gov/pubmed/24994836.

Guevara-Garcia, A., C. San Roman, A. Arroyo, M. E. Cortes, M. de la Luz Gutierrez-Nava, and P. Leon (2005). "Characterization of the Arabidopsis clb6 mutant illustrates the importance of posttranscriptional regulation of the methyl-D-erythritol 4-phosphate pathway". In: *Plant Cell* 17.2, pp. 628–43. ISSN: 1040-4651 (Print) 1040-4651 (Linking). DOI: 10.1105/tpc.104.028860. URL: https://www.ncbi.nlm.nih.gov/pubmed/15659625.

Han, M., S. C. Heppel, T. Su, J. Bogs, Y. Zu, Z. An, and T. Rausch (2013). "Enzyme inhibitor studies reveal complex control of methyl-D-erythritol 4-phosphate (MEP) pathway enzyme expression in Catharanthus roseus". In: *PLoS One* 8.5, e62467. ISSN: 1932-6203 (Electronic) 1932-6203 (Linking). DOI: 10.1371/journal.pone.0062467. URL: https://www.ncbi.nlm.nih.gov/pubmed/23650515.

Hanson, P. I. and S. W. Whiteheart (2005). "AAA+ proteins: have engine, will work". In: *Nat Rev Mol Cell Biol* 6.7, pp. 519–29. ISSN: 1471-0072 (Print) 1471-0072 (Linking). DOI: 10.1038/nrm1684. URL: https://www.ncbi.nlm.nih.gov/pubmed/16072036.

Harrison, S. J., E. K. Mott, K. Parsley, S. Aspinall, J. C. Gray, and A. Cottage (2006). "A rapid and robust method of identifying transformed Arabidopsis thaliana seedlings following floral dip transformation". In: *Plant Methods* 2, p. 19. ISSN: 1746-4811 (Electronic) 1746-4811 (Linking). DOI: 10.1186/1746-4811-2-19. URL: https://www.ncbi.nlm.nih.gov/pubmed/17087829.

Haslberger, T., J. Weibezahn, R. Zahn, S. Lee, F. T. Tsai, B. Bukau, and A. Mogk (2007). "M domains couple the ClpB threading motor with the DnaK chaperone activity". In: *Mol Cell* 25.2, pp. 247–60. ISSN: 1097-2765 (Print) 1097-2765 (Linking). DOI: 10.1016/j.molcel.2006.11.008. URL: https://www.ncbi.nlm.nih.gov/pubmed/17244532.

Havaux, M. (2014). "Carotenoid oxidation products as stress signals in plants". In: *Plant J* 79.4, pp. 597–606. ISSN: 1365-313X (Electronic) 0960-7412 (Linking). DOI: 10.1111/tpj.12386. URL: https://www.ncbi.nlm.nih.gov/pubmed/24267746.

Haynes, C. M., K. Petrova, C. Benedetti, Y. Yang, and D. Ron (2007). "ClpP mediates activation of a mitochondrial unfolded protein response in C. elegans". In: *Dev Cell* 13.4, pp. 467–80. ISSN: 1534-5807 (Print) 1534-5807 (Linking). DOI: 10.1016/j.devcel.2007.07.016. URL: https://www.ncbi.nlm.nih.gov/pubmed/17925224.

Haynes, C. M., Y. Yang, S. P. Blais, T. A. Neubert, and D. Ron (2010). "The matrix peptide exporter HAF-1 signals a mitochondrial UPR by activating the transcription factor ZC376.7 in C. elegans". In: *Mol Cell* 37.4, pp. 529–40. ISSN: 1097-4164 (Electronic) 1097-2765 (Linking). DOI: 10.1016/j.molcel.2010.01.015. URL: https://www.ncbi.nlm.nih.gov/pubmed/20188671.

Hedtke, B., J. Legen, A. Weihe, R. G. Herrmann, and T. Borner (2002). "Six active phage-type RNA polymerase genes in Nicotiana tabacum". In: *Plant J* 30.6, pp. 625–37. ISSN: 0960-7412 (Print) 0960-7412 (Linking). URL: https://www.ncbi.nlm.nih.gov/pubmed/12061895.

Hemmerlin, A. (2013). "Post-translational events and modifications regulating plant enzymes involved in isoprenoid precursor biosynthesis". In: *Plant Sci* 203-204, pp. 41–54. ISSN: 1873-2259 (Electronic) 0168-9452 (Linking). DOI: 10.1016/j.plantsci.2012.12.008. URL: https://www.ncbi.nlm.nih.gov/pubmed/23415327.

Hsieh, M. H. and H. M. Goodman (2005). "The Arabidopsis IspH homolog is involved in the plastid nonmevalonate pathway of isoprenoid biosynthesis". In: *Plant Physiol* 138.2, pp. 641–53. ISSN: 0032-0889 (Print) 0032-0889 (Linking). DOI: 10.1104/pp.104.058735. URL: https://www.ncbi.nlm.nih.gov/pubmed/15863698.

Hsieh, M. H., C. Y. Chang, S. J. Hsu, and J. J. Chen (2008). "Chloroplast localization of methylerythritol 4-phosphate pathway enzymes and regulation of mitochondrial genes in ispD and ispE albino mutants in Arabidopsis". In: *Plant Mol Biol* 66.6, pp. 663–73. ISSN: 0167-4412 (Print) 0167-4412 (Linking). DOI: 10.1007/s11103-008-9297-5. URL: https://www.ncbi.nlm.nih.gov/pubmed/18236010.

Huang, J., J. P. Taylor, J. G. Chen, J. F. Uhrig, D. J. Schnell, T. Nakagawa, K. L. Korth, and A. M. Jones (2006). "The plastid protein THYLAKOID FORMATION1 and the plasma membrane G-protein GPA1 interact in a novel sugar-signaling mechanism in Arabidopsis". In: *Plant Cell* 18.5, pp. 1226–38. ISSN: 1040-4651 (Print) 1040-4651

(Linking). DOI: 10.1105/tpc.105.037259. URL: https://www.ncbi.nlm.nih.gov/pubmed/16582010.

Inoue, H., M. Li, and D. J. Schnell (2013). "An essential role for chloroplast heat shock protein 90 (Hsp90C) in protein import into chloroplasts". In: *Proc Natl Acad Sci U S A* 110.8, pp. 3173–8. ISSN: 1091-6490 (Electronic) 0027-8424 (Linking). DOI: 10.1073/pnas.1219229110. URL: https://www.ncbi.nlm.nih.gov/pubmed/23382192.

Isemer, R., M. Mulisch, A. Schafer, S. Kirchner, H. U. Koop, and K. Krupinska (2012). "Recombinant Whirly1 translocates from transplastomic chloroplasts to the nucleus". In: *FEBS Lett* 586.1, pp. 85–8. ISSN: 1873-3468 (Electronic) 0014-5793 (Linking). DOI: 10.1016/j.febslet.2011.11.029. URL: https://www.ncbi.nlm.nih.gov/pubmed/22154598.

Joyard, J., M. Ferro, C. Masselon, D. Seigneurin-Berny, D. Salvi, J. Garin, and N. Rolland (2009). "Chloroplast proteomics and the compartmentation of plastidial isoprenoid biosynthetic pathways". In: *Mol Plant* 2.6, pp. 1154–80. ISSN: 1674-2052 (Print) 1674-2052 (Linking). DOI: 10.1093/mp/ssp088. URL: https://www.ncbi.nlm.nih.gov/pubmed/19969518.

Jung, S. (2004). "Effect of chlorophyll reduction in Arabidopsis thaliana by methyl jasmonate or norflurazon on antioxidant systems". In: *Plant Physiol Biochem* 42.3, pp. 225–31. ISSN: 0981-9428 (Print) 0981-9428 (Linking). DOI: 10.1016/j.plaphy.2004.01.001. URL: https://www.ncbi.nlm.nih.gov/pubmed/15051046.

Kampinga, H. H. and E. A. Craig (2010a). "The HSP70 chaperone machinery: J proteins as drivers of functional specificity". In: *Nat Rev Mol Cell Biol* 11.8, pp. 579–92. ISSN: 1471-0080 (Electronic) 1471-0072 (Linking). DOI: 10.1038/nrm2941. URL: https://www.ncbi.nlm.nih.gov/pubmed/20651708.

Kampinga, H. H. and E. A. Craig (2010b). "The HSP70 chaperone machinery: J proteins as drivers of functional specificity". In: *Nat Rev Mol Cell Biol* 11.8, pp. 579–92. ISSN: 1471-0080 (Electronic) 1471-0072 (Linking). DOI: 10.1038/nrm2941. URL: https://www.ncbi.nlm.nih.gov/pubmed/20651708.

Kasahara, H., A. Hanada, T. Kuzuyama, M. Takagi, Y. Kamiya, and S. Yamaguchi (2002). "Contribution of the mevalonate and methylerythritol phosphate pathways to the biosynthesis of gibberellins in Arabidopsis". In: *J Biol Chem* 277.47, pp. 45188–94. ISSN: 0021-9258 (Print) 0021-9258 (Linking). DOI: 10.1074/jbc.M208659200. URL: https://www.ncbi.nlm.nih.gov/pubmed/12228237.

Kato, Y. and W. Sakamoto (2010). "New insights into the types and function of proteases in plastids". In: *Int Rev Cell Mol Biol* 280, pp. 185–218. ISSN: 1937-6448 (Print) 1937-6448 (Linking). DOI: 10.1016/S1937-6448(10)80004-8. URL: https://www.ncbi.nlm.nih.gov/pubmed/20797683.

Keren, N., H. Ohkawa, E. A. Welsh, M. Liberton, and H. B. Pakrasi (2005). "Psb29, a conserved 22-kD protein, functions in the biogenesis of Photosystem II complexes in Synechocystis and Arabidopsis". In: *Plant Cell* 17.10, pp. 2768–81. ISSN:

1040-4651 (Print) 1040-4651 (Linking). DOI: 10.1105/tpc.105.035048. URL: https://www.ncbi.nlm.nih.gov/pubmed/16155179.

Kim, J., A. Rudella, V. Ramirez Rodriguez, B. Zybailov, P. D. Olinares, and K. J. van Wijk (2009). "Subunits of the plastid ClpPR protease complex have differential contributions to embryogenesis, plastid biogenesis, and plant development in Arabidopsis". In: *Plant Cell* 21.6, pp. 1669–92. ISSN: 1040-4651 (Print) 1040-4651 (Linking). DOI: 10.1105/tpc.108.063784. URL: https://www.ncbi.nlm.nih.gov/pubmed/19525416.

Kim, J., P. D. Olinares, S. H. Oh, S. Ghisaura, A. Poliakov, L. Ponnala, and K. J. van Wijk (2013). "Modified Clp protease complex in the ClpP3 null mutant and consequences for chloroplast development and function in Arabidopsis". In: *Plant Physiol* 162.1, pp. 157–79. ISSN: 1532-2548 (Electronic) 0032-0889 (Linking). DOI: 10.1104/pp.113.215699. URL: https://www.ncbi.nlm.nih.gov/pubmed/23548781.

Kim, J., M. S. Kimber, K. Nishimura, G. Friso, L. Schultz, L. Ponnala, and K. J. van Wijk (2015). "Structures, Functions, and Interactions of ClpT1 and ClpT2 in the Clp Protease System of Arabidopsis Chloroplasts". In: *Plant Cell* 27.5, pp. 1477–96. ISSN: 1532-298X (Electronic) 1040-4651 (Linking). DOI: 10.1105/tpc.15.00106. URL: https://www.ncbi.nlm.nih.gov/pubmed/25921872.

Kim, Y. I., I. Levchenko, K. Fraczkowska, R. V. Woodruff, R. T. Sauer, and T. A. Baker (2001). "Molecular determinants of complex formation between Clp/Hsp100 ATPases and the ClpP peptidase". In: *Nat Struct Biol* 8.3, pp. 230–3. ISSN: 1072-8368 (Print) 1072-8368 (Linking). DOI: 10.1038/84967. URL: https://www.ncbi.nlm.nih.gov/pubmed/11224567.

Kleine, T. and D. Leister (2016). "Retrograde signaling: Organelles go networking". In: *Biochim Biophys Acta* 1857.8, pp. 1313–25. ISSN: 0006-3002 (Print) 0006-3002 (Linking). DOI: 10.1016/j.bbabio.2016.03.017. URL: https://www.ncbi.nlm.nih.gov/pubmed/26997501.

Kotak, S., J. Larkindale, U. Lee, P. von Koskull-Doring, E. Vierling, and K. D. Scharf (2007). "Complexity of the heat stress response in plants". In: *Curr Opin Plant Biol* 10.3, pp. 310–6. ISSN: 1369-5266 (Print) 1369-5266 (Linking). DOI: 10.1016/j.pbi.2007.04.011. URL: https://www.ncbi.nlm.nih.gov/pubmed/17482504.

Koussevitzky, S., T. M. Stanne, C. A. Peto, T. Giap, L. L. Sjogren, Y. Zhao, A. K. Clarke, and J. Chory (2007a). "An Arabidopsis thaliana virescent mutant reveals a role for ClpR1 in plastid development". In: *Plant Mol Biol* 63.1, pp. 85–96. ISSN: 0167-4412 (Print) 0167-4412 (Linking). DOI: 10.1007/s11103-006-9074-2. URL: https://www.ncbi.nlm.nih.gov/pubmed/17009084.

Koussevitzky, S., A. Nott, T. C. Mockler, F. Hong, G. Sachetto-Martins, M. Surpin, J. Lim, R. Mittler, and J. Chory (2007b). "Signals from chloroplasts converge to regulate nuclear gene expression". In: *Science* 316.5825, pp. 715–9. ISSN: 1095-9203

(Electronic) 0036-8075 (Linking). DOI: 10.1126/science.1140516. URL: http://www.ncbi.nlm.nih.gov/pubmed/17395793.

Kovacheva, S., J. Bedard, R. Patel, P. Dudley, D. Twell, G. Rios, C. Koncz, and P. Jarvis (2005). "In vivo studies on the roles of Tic110, Tic40 and Hsp93 during chloroplast protein import". In: *Plant J* 41.3, pp. 412–28. ISSN: 0960-7412 (Print) 0960-7412 (Linking). DOI: 10.1111/j.1365-313X.2004.02307.x. URL: https://www.ncbi.nlm.nih.gov/pubmed/15659100.

Kovacheva, S., J. Bedard, A. Wardle, R. Patel, and P. Jarvis (2007). "Further in vivo studies on the role of the molecular chaperone, Hsp93, in plastid protein import". In: *Plant J* 50.2, pp. 364–79. ISSN: 0960-7412 (Print) 0960-7412 (Linking). DOI: 10.1111/j.1365-313X.2007.03060.x. URL: https://www.ncbi.nlm.nih.gov/pubmed/17376159.

Kress, W., Z. Maglica, and E. Weber-Ban (2009). "Clp chaperone-proteases: structure and function". In: *Res Microbiol* 160.9, pp. 618–28. ISSN: 1769-7123 (Electronic) 0923-2508 (Linking). DOI: 10.1016/j.resmic.2009.08.006. URL: https://www.ncbi.nlm.nih.gov/pubmed/19732826.

Krushkal, J., M. Pistilli, K. M. Ferrell, F. F. Souret, and P. J. Weathers (2003). "Computational analysis of the evolution of the structure and function of 1-deoxy-D-xylulose-5-phosphate synthase, a key regulator of the mevalonate-independent pathway in plants". In: *Gene* 313, pp. 127–38. ISSN: 0378-1119 (Print) 0378-1119 (Linking). URL: https://www.ncbi.nlm.nih.gov/pubmed/12957384.

Kuzuyama, T., T. Shimizu, S. Takahashi, and H. Seto (1998). "Fosmidomycin, a specific inhibitor of 1-deoxy-D-xylulose 5-phosphate reductoisomerase in the nonmevalonate pathway for terpenoid biosynthesis." In: *Tetrahedron letters* 39.43, pp. 79 13–7916.

Laule, O., A. Furholz, H. S. Chang, T. Zhu, X. Wang, P. B. Heifetz, W. Gruissem, and M. Lange (2003). "Crosstalk between cytosolic and plastidial pathways of isoprenoid biosynthesis in Arabidopsis thaliana". In: *Proc Natl Acad Sci U S A* 100.11, pp. 6866–71. ISSN: 0027-8424 (Print) 0027-8424 (Linking). DOI: 10.1073/pnas.1031755100. URL: https://www.ncbi.nlm.nih.gov/pubmed/12748386.

Lee, J. H., H. J. Yoon, W. Terzaghi, C. Martinez, M. Dai, J. Li, M. O. Byun, and X. W. Deng (2010). "DWA1 and DWA2, two Arabidopsis DWD protein components of CUL4-based E3 ligases, act together as negative regulators in ABA signal transduction". In: *Plant Cell* 22.6, pp. 1716–32. ISSN: 1532-298X (Electronic) 1040-4651 (Linking). DOI: 10.1105/tpc.109.073783. URL: https://www.ncbi.nlm.nih.gov/pubmed/20525848.

Lee, U., I. Rioflorido, S. W. Hong, J. Larkindale, E. R. Waters, and E. Vierling (2007). "The Arabidopsis ClpB/Hsp100 family of proteins: chaperones for stress and chloroplast development". In: *Plant J* 49.1, pp. 115–27. ISSN: 0960-7412 (Print) 0960-7412 (Linking). DOI: 10.1111/j.1365-313X.2006.02940.x. URL: https://www.ncbi.nlm.nih.gov/pubmed/17144892.

Levchenko, I., M. Seidel, R. T. Sauer, and T. A. Baker (2000). "A specificity-enhancing factor for the ClpXP degradation machine". In: *Science* 289.5488, pp. 2354–6. ISSN: 0036-8075 (Print) 0036-8075 (Linking). URL: https://www.ncbi.nlm.nih.gov/pubmed/11009422.

Lichtenthaler, H. K. (1987). "Chlorophylls and Carotenoids: Pigments of Photosynthetic Biomembranes". In: *Methods in Enzymology* 148, pp. 350–382. DOI: http://dx.doi.org/10.1016/0076-6879(87)48036-1.

Lin, Y. F. and C. M. Haynes (2016). "Metabolism and the UPR(mt)". In: *Mol Cell* 61.5, pp. 677–82. ISSN: 1097-4164 (Electronic) 1097-2765 (Linking). DOI: 10.1016/j.molcel.2016.02.004. URL: https://www.ncbi.nlm.nih.gov/pubmed/26942672.

Lintala, M., Y. Allahverdiyeva, H. Kidron, M. Piippo, N. Battchikova, M. Suorsa, E. Rintamaki, T. A. Salminen, E. M. Aro, and P. Mulo (2007). "Structural and functional characterization of ferredoxin-NADP+-oxidoreductase using knock-out mutants of Arabidopsis". In: *Plant J* 49.6, pp. 1041–52. ISSN: 0960-7412 (Print) 0960-7412 (Linking). DOI: 10.1111/j.1365-313X.2006.03014.x. URL: https://www.ncbi.nlm.nih.gov/pubmed/17335513.

Liu, X., S. R. Rodermel, and F. Yu (2010a). "A var2 leaf variegation suppressor locus, SUPPRESSOR OF VARIEGATION3, encodes a putative chloroplast translation elongation factor that is important for chloroplast development in the cold". In: *BMC Plant Biol* 10, p. 287. ISSN: 1471-2229 (Electronic) 1471-2229 (Linking). DOI: 10.1186/1471-2229-10-287. URL: https://www.ncbi.nlm.nih.gov/pubmed/21187014.

Liu, X., F. Yu, and S. Rodermel (2010b). "An Arabidopsis pentatricopeptide repeat protein, SUPPRESSOR OF VARIEGATION7, is required for FtsH-mediated chloroplast biogenesis". In: *Plant Physiol* 154.4, pp. 1588–601. ISSN: 1532-2548 (Electronic) 0032-0889 (Linking). DOI: 10.1104/pp.110.164111. URL: https://www.ncbi.nlm.nih.gov/pubmed/20935174.

Liu, X., F. Yu, and S. Rodermel (2010c). "Arabidopsis chloroplast FtsH, var2 and suppressors of var2 leaf variegation: a review". In: *J Integr Plant Biol* 52.8, pp. 750–61. ISSN: 1744-7909 (Electronic) 1672-9072 (Linking). DOI: 10.1111/j.1744-7909.2010.00980.x. URL: https://www.ncbi.nlm.nih.gov/pubmed/20666930.

Liu, X., M. Zheng, R. Wang, R. Wang, L. An, S. R. Rodermel, and F. Yu (2013). "Genetic interactions reveal that specific defects of chloroplast translation are associated with the suppression of var2-mediated leaf variegation". In: *J Integr Plant Biol* 55.10, pp. 979–93. ISSN: 1744-7909 (Electronic) 1672-9072 (Linking). DOI: 10.1111/jipb.12078. URL: http://www.ncbi.nlm.nih.gov/pubmed/23721655.

Liu, X. L., H. D. Yu, Y. Guan, J. K. Li, and F. Q. Guo (2012). "Carbonylation and loss-of-function analyses of SBPase reveal its metabolic interface role in oxidative stress, carbon assimilation, and multiple aspects of growth and development in

Arabidopsis". In: *Mol Plant* 5.5, pp. 1082–99. ISSN: 1752-9867 (Electronic) 1674-2052 (Linking). DOI: 10.1093/mp/sss012. URL: https://www.ncbi.nlm.nih.gov/pubmed/22402261.

Llorente, B., L. D'Andrea, M. A. Ruiz-Sola, E. Botterweg, P. Pulido, J. Andilla, P. Loza-Alvarez, and M. Rodriguez-Concepcion (2016). "Tomato fruit carotenoid biosynthesis is adjusted to actual ripening progression by a light-dependent mechanism". In: *Plant J* 85.1, pp. 107–19. ISSN: 1365-313X (Electronic) 0960-7412 (Linking). DOI: 10.1111/tpj.13094. URL: https://www.ncbi.nlm.nih.gov/pubmed/26648446.

Lopez-Juez, E. and K. A. Pyke (2005). "Plastids unleashed: their development and their integration in plant development". In: *Int J Dev Biol* 49.5-6, pp. 557–77. ISSN: 0214-6282 (Print) 0214-6282 (Linking). DOI: 10.1387/ijdb.051997el. URL: https://www.ncbi.nlm.nih.gov/pubmed/16096965.

Lu, S. and L. Li (2008). "Carotenoid metabolism: biosynthesis, regulation, and beyond". In: *J Integr Plant Biol* 50.7, pp. 778–85. ISSN: 1744-7909 (Electronic) 1672-9072 (Linking). DOI: 10.1111/j.1744-7909.2008.00708.x. URL: https://www.ncbi.nlm.nih.gov/pubmed/18713388.

Lupas, A. N. and J. Martin (2002). "AAA proteins". In: *Curr Opin Struct Biol* 12.6, pp. 746–53. ISSN: 0959-440X (Print) 0959-440X (Linking). URL: https://www.ncbi.nlm.nih.gov/pubmed/12504679.

Malkin, R. and N. Krishna (2000). "Photosynthesis". In: *Biochemistry & Molecular Biology of Plants*. Ed. by B. Buchanan, W. Gruissem, and Jones R. American Society of Plant Physiologists. Chap. 12.

Matsue, Y., H. Mizuno, T. Tomita, T. Asami, M. Nishiyama, and T. Kuzuyama (2010). "The herbicide ketoclomazone inhibits 1-deoxy-D-xylulose 5-phosphate synthase in the 2-C-methyl-D-erythritol 4-phosphate pathway and shows antibacterial activity against Haemophilus influenzae". In: *J Antibiot (Tokyo)* 63.10, pp. 583–8. ISSN: 0021-8820 (Print) 0021-8820 (Linking). DOI: 10.1038/ja.2010.100. URL: https://www.ncbi.nlm.nih.gov/pubmed/20808315.

Mayer, M. P. and B. Bukau (2005). "Hsp70 chaperones: cellular functions and molecular mechanism". In: *Cell Mol Life Sci* 62.6, pp. 670–84. ISSN: 1420-682X (Print) 1420-682X (Linking). DOI: 10.1007/s00018-004-4464-6. URL: https://www.ncbi.nlm.nih.gov/pubmed/15770419.

Miot, M., M. Reidy, S. M. Doyle, J. R. Hoskins, D. M. Johnston, O. Genest, M. C. Vitery, D. C. Masison, and S. Wickner (2011). "Species-specific collaboration of heat shock proteins (Hsp) 70 and 100 in thermotolerance and protein disaggregation". In: *Proc Natl Acad Sci U S A* 108.17, pp. 6915–20. ISSN: 1091-6490 (Electronic) 0027-8424 (Linking). DOI: 10.1073/pnas.1102828108. URL: https://www.ncbi.nlm.nih.gov/pubmed/21474779.

Mishra, R. C. and A. Grover (2016). "ClpB/Hsp100 proteins and heat stress tolerance in plants". In: *Crit Rev Biotechnol* 36.5, pp. 862–74. ISSN: 1549-7801 (Electronic)

0738-8551 (Linking). DOI: 10.3109/07388551.2015.1051942. URL: https://www.ncbi.nlm.nih.gov/pubmed/26121931.

Moffett, P. (2011). "Fragment complementation and co-immunoprecipitation assays for understanding R protein structure and function". In: *Methods Mol Biol* 712, pp. 9–20. ISSN: 1064-3745. DOI: 10.1007/978-1-61737-998-7_2.

Moreno, J. C., N. Tiller, M. Diez, D. Karcher, M. Tillich, M. A. Schottler, and R. Bock (2017). "Generation and characterization of a collection of knock-down lines for the chloroplast Clp protease complex in tobacco". In: *J Exp Bot*. ISSN: 1460-2431 (Electronic) 0022-0957 (Linking). DOI: 10.1093/jxb/erx066. URL: https://www.ncbi.nlm.nih.gov/pubmed/28369470.

Moreno-Gonzalez, I. and C. Soto (2011). "Misfolded protein aggregates: mechanisms, structures and potential for disease transmission". In: *Semin Cell Dev Biol* 22.5, pp. 482–7. ISSN: 1096-3634 (Electronic) 1084-9521 (Linking). DOI: 10.1016/j.semcdb.2011.04.002. URL: https://www.ncbi.nlm.nih.gov/pubmed/21571086.

Morita-Yamamuro, C., T. Tsutsui, A. Tanaka, and J. Yamaguchi (2004). "Knock-out of the plastid ribosomal protein S21 causes impaired photosynthesis and sugar-response during germination and seedling development in Arabidopsis thaliana". In: *Plant Cell Physiol* 45.6, pp. 781–8. ISSN: 0032-0781 (Print) 0032-0781 (Linking). URL: https://www.ncbi.nlm.nih.gov/pubmed/15215513.

Mullet, J.E. (1988). "Chloroplast Development and Gene Expression". In: *Annual Review of Plant Physiology and Plant Molecular Biology* 39, pp. 475–502.

Mulo, Paula, Saijaliisa Pursiheimo, Cai-Xia Hou, Tyystj, Taina rvi, and Eva-Mari Aro (2003). "Multiple effects of antibiotics on chloroplast and nuclear gene expression". In: *Functional Plant Biology* 30.11, pp. 1097–1103. DOI: http://dx.doi.org/10.1071/FP03149. URL: http://www.publish.csiro.au/paper/FP03149.

Myouga, F., R. Motohashi, T. Kuromori, N. Nagata, and K. Shinozaki (2006). "An Arabidopsis chloroplast-targeted Hsp101 homologue, APG6, has an essential role in chloroplast development as well as heat-stress response". In: *Plant J* 48.2, pp. 249–60. ISSN: 0960-7412 (Print) 0960-7412 (Linking). DOI: 10.1111/j.1365-313X.2006.02873.x. URL: https://www.ncbi.nlm.nih.gov/pubmed/16995899.

Nargund, A. M., M. W. Pellegrino, C. J. Fiorese, B. M. Baker, and C. M. Haynes (2012). "Mitochondrial import efficiency of ATFS-1 regulates mitochondrial UPR activation". In: *Science* 337.6094, pp. 587–90. ISSN: 1095-9203 (Electronic) 0036-8075 (Linking). DOI: 10.1126/science.1223560. URL: http://www.ncbi.nlm.nih.gov/pubmed/22700657.

Nemeth, K., K. Salchert, P. Putnoky, R. Bhalerao, Z. Koncz-Kalman, B. Stankovic-Stangeland, L. Bako, J. Mathur, L. Okresz, S. Stabel, P. Geigenberger, M. Stitt, G. P. Redei, J. Schell, and C. Koncz (1998). "Pleiotropic control of glucose and hormone responses by PRL1, a nuclear WD protein, in Arabidopsis". In: *Genes Dev* 12.19,

pp. 3059–73. ISSN: 0890-9369 (Print) 0890-9369 (Linking). URL: https://www.ncbi.nlm.nih.gov/pubmed/9765207.

Nishimura, K. and K. J. Van Wijk (2015). "Organization, function and substrates of the essential Clp protease system in plastids". In: *Biochim Biophys Acta* 1847.9, pp. 915–30. ISSN: 0006-3002 (Print) 0006-3002 (Linking). DOI: 10.1016/j.bbabio.2014.11.012. URL: https://www.ncbi.nlm.nih.gov/pubmed/25482260.

Nishimura, K., Y. Asakura, G. Friso, J. Kim, S. H. Oh, H. Rutschow, L. Ponnala, and K. J. van Wijk (2013). "ClpS1 is a conserved substrate selector for the chloroplast Clp protease system in Arabidopsis". In: *Plant Cell* 25.6, pp. 2276–301. ISSN: 1532-298X (Electronic) 1040-4651 (Linking). DOI: 10.1105/tpc.113.112557. URL: https://www.ncbi.nlm.nih.gov/pubmed/23898032.

Nishimura, K., J. Apitz, G. Friso, J. Kim, L. Ponnala, B. Grimm, and K. J. van Wijk (2015). "Discovery of a Unique Clp Component, ClpF, in Chloroplasts: A Proposed Binary ClpF-ClpS1 Adaptor Complex Functions in Substrate Recognition and Delivery". In: *Plant Cell* 27.10, pp. 2677–91. ISSN: 1532-298X (Electronic) 1040-4651 (Linking). DOI: 10.1105/tpc.15.00574. URL: https://www.ncbi.nlm.nih.gov/pubmed/26419670.

Nishimura, K., Y. Kato, and W. Sakamoto (2016). "Chloroplast Proteases: Updates on Proteolysis within and across Suborganellar Compartments". In: *Plant Physiol* 171.4, pp. 2280–93. ISSN: 1532-2548 (Electronic) 0032-0889 (Linking). DOI: 10.1104/pp.16.00330. URL: https://www.ncbi.nlm.nih.gov/pubmed/27288365.

Nishimura, K., Y. Kato, and W. Sakamoto (2017). "Essentials of Proteolytic Machineries in Chloroplasts". In: *Mol Plant* 10.1, pp. 4–19. ISSN: 1752-9867 (Electronic) 1674-2052 (Linking). DOI: 10.1016/j.molp.2016.08.005. URL: https://www.ncbi.nlm.nih.gov/pubmed/27585878.

Niyogi, K. K. (1999). "PHOTOPROTECTION REVISITED: Genetic and Molecular Approaches". In: *Annu Rev Plant Physiol Plant Mol Biol* 50, pp. 333–359. ISSN: 1040-2519 (Print) 1040-2519 (Linking). DOI: 10.1146/annurev.arplant.50.1.333. URL: https://www.ncbi.nlm.nih.gov/pubmed/15012213.

Nordhues, A., S. M. Miller, T. Muhlhaus, and M. Schroda (2010). "New insights into the roles of molecular chaperones in Chlamydomonas and Volvox". In: *Int Rev Cell Mol Biol* 285, pp. 75–113. ISSN: 1937-6448 (Print) 1937-6448 (Linking). DOI: 10.1016/B978-0-12-381047-2.00002-5. URL: https://www.ncbi.nlm.nih.gov/pubmed/21035098.

Olinares, P. D., J. Kim, J. I. Davis, and K. J. van Wijk (2011a). "Subunit stoichiometry, evolution, and functional implications of an asymmetric plant plastid ClpP/R protease complex in Arabidopsis". In: *Plant Cell* 23.6, pp. 2348–61. ISSN: 1532-298X (Electronic) 1040-4651 (Linking). DOI: 10.1105/tpc.111.086454. URL: https://www.ncbi.nlm.nih.gov/pubmed/21712416.

Olinares, P. D., J. Kim, and K. J. van Wijk (2011b). "The Clp protease system; a central component of the chloroplast protease network". In: *Biochim Biophys Acta* 1807.8,

pp. 999–1011. ISSN: 0006-3002 (Print) 0006-3002 (Linking). DOI: 10.1016/j.bbabio.2010.12.003. URL: https://www.ncbi.nlm.nih.gov/pubmed/21167127.

Paetzold, H., S. Garms, S. Bartram, J. Wieczorek, E. M. Uros-Gracia, M. Rodriguez-Concepcion, W. Boland, D. Strack, B. Hause, and M. H. Walter (2010). "The isogene 1-deoxy-D-xylulose 5-phosphate synthase 2 controls isoprenoid profiles, precursor pathway allocation, and density of tomato trichomes". In: *Mol Plant* 3.5, pp. 904–16. ISSN: 1674-2052 (Print) 1674-2052 (Linking). DOI: 10.1093/mp/ssq032. URL: https://www.ncbi.nlm.nih.gov/pubmed/20591838.

Park, S. and S. R. Rodermel (2004). "Mutations in ClpC2/Hsp100 suppress the requirement for FtsH in thylakoid membrane biogenesis". In: *Proc Natl Acad Sci U S A* 101.34, pp. 12765–70. ISSN: 0027-8424 (Print) 0027-8424 (Linking). DOI: 10.1073/pnas.0402764101. URL: https://www.ncbi.nlm.nih.gov/pubmed/15304652.

Peltier, J. B., D. R. Ripoll, G. Friso, A. Rudella, Y. Cai, J. Ytterberg, L. Giacomelli, J. Pillardy, and K. J. van Wijk (2004). "Clp protease complexes from photosynthetic and non-photosynthetic plastids and mitochondria of plants, their predicted three-dimensional structures, and functional implications". In: *J Biol Chem* 279.6, pp. 4768–81. ISSN: 0021-9258 (Print) 0021-9258 (Linking). DOI: 10.1074/jbc.M309212200. URL: https://www.ncbi.nlm.nih.gov/pubmed/14593120.

Perello, C., M. Rodriguez-Concepcion, and P. Pulido (2014). "Quantification of plant resistance to isoprenoid biosynthesis inhibitors". In: *Methods Mol Biol* 1153, pp. 273–83. ISSN: 1940-6029 (Electronic) 1064-3745 (Linking). DOI: 10.1007/978-1-4939-0606-2_20. URL: https://www.ncbi.nlm.nih.gov/pubmed/24777805.

Perello, C., E. Llamas, V. Burlat, M. Ortiz-Alcaide, M. A. Phillips, P. Pulido, and M. Rodriguez-Concepcion (2016). "Differential Subplastidial Localization and Turnover of Enzymes Involved in Isoprenoid Biosynthesis in Chloroplasts". In: *PLoS One* 11.2, e0150539. ISSN: 1932-6203 (Electronic) 1932-6203 (Linking). DOI: 10.1371/journal.pone.0150539. URL: http://www.ncbi.nlm.nih.gov/pubmed/26919668.

Phillips, M. A., P. Leon, A. Boronat, and M. Rodriguez-Concepcion (2008). "The plastidial MEP pathway: unified nomenclature and resources". In: *Trends Plant Sci* 13.12, pp. 619–23. ISSN: 1360-1385 (Print) 1360-1385 (Linking). DOI: 10.1016/j.tplants.2008.09.003. URL: https://www.ncbi.nlm.nih.gov/pubmed/18948055.

Pokhilko, A., J. Bou-Torrent, P. Pulido, M. Rodriguez-Concepcion, and O. Ebenhoh (2015). "Mathematical modelling of the diurnal regulation of the MEP pathway in Arabidopsis". In: *New Phytol* 206.3, pp. 1075–85. ISSN: 1469-8137 (Electronic) 0028-646X (Linking). DOI: 10.1111/nph.13258. URL: https://www.ncbi.nlm.nih.gov/pubmed/25598499.

Powikrowska, M., A. Khrouchtchova, H. J. Martens, A. Zygadlo-Nielsen, J. Melonek, A. Schulz, K. Krupinska, S. Rodermel, and P. E. Jensen (2014). "SVR4 (suppressor of variegation 4) and SVR4-like: two proteins with a role in proper organization of the chloroplast genetic machinery". In: *Physiol Plant* 150.3, pp. 477–92. ISSN: 1399-3054 (Electronic) 0031-9317 (Linking). DOI: 10.1111/ppl.12108. URL: https://www.ncbi.nlm.nih.gov/pubmed/24111559.

Pulido, P., C. Perello, and M. Rodriguez-Concepcion (2012). "New insights into plant isoprenoid metabolism". In: *Mol Plant* 5.5, pp. 964–7. ISSN: 1752-9867 (Electronic) 1674-2052 (Linking). DOI: 10.1093/mp/sss088. URL: https://www.ncbi.nlm.nih.gov/pubmed/22972017.

Pulido, P., G. Toledo-Ortiz, M. A. Phillips, L. P. Wright, and M. Rodriguez-Concepcion (2013). "Arabidopsis J-protein J20 delivers the first enzyme of the plastidial isoprenoid pathway to protein quality control". In: *Plant Cell* 25.10, pp. 4183–94. ISSN: 1532-298X (Electronic) 1040-4651 (Linking). DOI: 10.1105/tpc.113.113001. URL: http://www.ncbi.nlm.nih.gov/pubmed/24104567.

Pulido, P., E. Llamas, B. Llorente, S. Ventura, L. P. Wright, and M. Rodriguez-Concepcion (2016). "Specific Hsp100 Chaperones Determine the Fate of the First Enzyme of the Plastidial Isoprenoid Pathway for Either Refolding or Degradation by the Stromal Clp Protease in Arabidopsis". In: *PLoS Genet* 12.1, e1005824. ISSN: 1553-7404 (Electronic) 1553-7390 (Linking). DOI: 10.1371/journal.pgen.1005824. URL: http://www.ncbi.nlm.nih.gov/pubmed/26815787.

Putarjunan, A., X. Liu, T. Nolan, F. Yu, and S. Rodermel (2013). "Understanding chloroplast biogenesis using second-site suppressors of immutans and var2". In: *Photosynth Res* 116.2-3, pp. 437–53. ISSN: 1573-5079 (Electronic) 0166-8595 (Linking). DOI: 10.1007/s11120-013-9855-9. URL: http://www.ncbi.nlm.nih.gov/pubmed/23703455.

Qi, Y., U. Armbruster, C. Schmitz-Linneweber, E. Delannoy, A. F. de Longevialle, T. Ruhle, I. Small, P. Jahns, and D. Leister (2012). "Arabidopsis CSP41 proteins form multimeric complexes that bind and stabilize distinct plastid transcripts". In: *J Exp Bot* 63.3, pp. 1251–70. ISSN: 1460-2431 (Electronic) 0022-0957 (Linking). DOI: 10.1093/jxb/err347. URL: https://www.ncbi.nlm.nih.gov/pubmed/22090436.

Qi, Y., J. Zhao, R. An, J. Zhang, S. Liang, J. Shao, X. Liu, L. An, and F. Yu (2016). "Mutations in circularly permuted GTPase family genes AtNOA1/RIF1/SVR10 and BPG2 suppress var2-mediated leaf variegation in Arabidopsis thaliana". In: *Photosynth Res* 127.3, pp. 355–67. ISSN: 1573-5079 (Electronic) 0166-8595 (Linking). DOI: 10.1007/s11120-015-0195-9. URL: https://www.ncbi.nlm.nih.gov/pubmed/26435530.

Raines, C. A. (2003). "The Calvin cycle revisited". In: *Photosynth Res* 75.1, pp. 1–10. ISSN: 1573-5079 (Electronic) 0166-8595 (Linking). DOI: 10.1023/A:1022421515027. URL: https://www.ncbi.nlm.nih.gov/pubmed/16245089.

Raines, C. A., J. C. Lloyd, N. M. Willingham, S. Potts, and T. A. Dyer (1992). "cDNA and gene sequences of wheat chloroplast sedoheptulose-1,7-bisphosphatase reveal homology with fructose-1,6-bisphosphatases". In: *Eur J Biochem* 205.3, pp. 1053–9. ISSN: 0014-2956 (Print) 0014-2956 (Linking). URL: https://www.ncbi.nlm.nih.gov/pubmed/1374332.

Ramel, F., S. Birtic, C. Ginies, L. Soubigou-Taconnat, C. Triantaphylides, and M. Havaux (2012). "Carotenoid oxidation products are stress signals that mediate gene responses to singlet oxygen in plants". In: *Proc Natl Acad Sci U S A* 109.14, pp. 5535–40. ISSN: 1091-6490 (Electronic) 0027-8424 (Linking). DOI: 10.1073/pnas.1115982109. URL: https://www.ncbi.nlm.nih.gov/pubmed/22431637.

Ramundo, S. and J. D. Rochaix (2014). "Chloroplast unfolded protein response, a new plastid stress signaling pathway?" In: *Plant Signal Behav* 9.10, e972874. ISSN: 1559-2324 (Electronic) 1559-2316 (Linking). DOI: 10.4161/15592316.2014.972874. URL: http://www.ncbi.nlm.nih.gov/pubmed/25482768.

Rasmussen, S., P. Barah, M. C. Suarez-Rodriguez, S. Bressendorff, P. Friis, P. Costantino, A. M. Bones, H. B. Nielsen, and J. Mundy (2013). "Transcriptome responses to combinations of stresses in Arabidopsis". In: *Plant Physiol* 161.4, pp. 1783–94. ISSN: 1532-2548 (Electronic) 0032-0889 (Linking). DOI: 10.1104/pp.112.210773. URL: https://www.ncbi.nlm.nih.gov/pubmed/23447525.

Reyes-Prieto, A., A. P. Weber, and D. Bhattacharya (2007). "The origin and establishment of the plastid in algae and plants". In: *Annu Rev Genet* 41, pp. 147–68. ISSN: 0066-4197 (Print) 0066-4197 (Linking). DOI: 10.1146/annurev.genet.41.110306.130134. URL: https://www.ncbi.nlm.nih.gov/pubmed/17600460.

Rigas, S., G. Daras, D. Tsitsekian, A. Alatzas, and P. Hatzopoulos (2014). "Evolution and significance of the Lon gene family in Arabidopsis organelle biogenesis and energy metabolism". In: *Front Plant Sci* 5, p. 145. ISSN: 1664-462X (Linking). DOI: 10.3389/fpls.2014.00145. URL: https://www.ncbi.nlm.nih.gov/pubmed/24782883.

Rodriguez-Concepcion, M. and A. Boronat (2002). "Elucidation of the methylerythritol phosphate pathway for isoprenoid biosynthesis in bacteria and plastids. A metabolic milestone achieved through genomics". In: *Plant Physiol* 130.3, pp. 1079–89. ISSN: 0032-0889 (Print) 0032-0889 (Linking). DOI: 10.1104/pp.007138. URL: https://www.ncbi.nlm.nih.gov/pubmed/12427975.

Rodriguez-Concepcion, M. and A. Boronat (2015). "Breaking new ground in the regulation of the early steps of plant isoprenoid biosynthesis". In: *Curr Opin Plant Biol* 25, pp. 17–22. ISSN: 1879-0356 (Electronic) 1369-5266 (Linking). DOI: 10.1016/j.pbi.2015.04.001. URL: https://www.ncbi.nlm.nih.gov/pubmed/25909859.

Rodriguez-Concepcion, M., O. Fores, J. F. Martinez-Garcia, V. Gonzalez, M. A. Phillips, A. Ferrer, and A. Boronat (2004). "Distinct light-mediated pathways regulate the

biosynthesis and exchange of isoprenoid precursors during Arabidopsis seedling development". In: *Plant Cell* 16.1, pp. 144–56. ISSN: 1040-4651 (Print) 1040-4651 (Linking). DOI: 10.1105/tpc.016204. URL: https://www.ncbi.nlm.nih.gov/pubmed/14660801.

Rodriguez-Villalon, A., E. Gas, and M. Rodriguez-Concepcion (2009). "Phytoene synthase activity controls the biosynthesis of carotenoids and the supply of their metabolic precursors in dark-grown Arabidopsis seedlings". In: *Plant J* 60.3, pp. 424–35. ISSN: 1365-313X (Electronic) 0960-7412 (Linking). DOI: 10.1111/j.1365-313X.2009.03966.x. URL: https://www.ncbi.nlm.nih.gov/pubmed/19594711.

Rodríguez-Concepción, M. (2006). "Early Steps in Isoprenoid Biosynthesis: Multilevel Regulation of the Supply of Common Precursors in Plant Cells". In: *Phytochemistry Reviews* 5.1, pp. 1–15. ISSN: 1572-980X. DOI: 10.1007/s11101-005-3130-4. URL: http://dx.doi.org/10.1007/s11101-005-3130-4.

Romani, I., L. Tadini, F. Rossi, S. Masiero, M. Pribil, P. Jahns, M. Kater, D. Leister, and P. Pesaresi (2012). "Versatile roles of Arabidopsis plastid ribosomal proteins in plant growth and development". In: *Plant J* 72.6, pp. 922–34. ISSN: 1365-313X (Electronic) 0960-7412 (Linking). DOI: 10.1111/tpj.12000. URL: https://www.ncbi.nlm.nih.gov/pubmed/22900828.

Rosenzweig, R., S. Moradi, A. Zarrine-Afsar, J. R. Glover, and L. E. Kay (2013). "Unraveling the mechanism of protein disaggregation through a ClpB-DnaK interaction". In: *Science* 339.6123, pp. 1080–3. ISSN: 1095-9203 (Electronic) 0036-8075 (Linking). DOI: 10.1126/science.1233066. URL: https://www.ncbi.nlm.nih.gov/pubmed/23393091.

Ruckle, M. E., S. M. DeMarco, and R. M. Larkin (2007). "Plastid signals remodel light signaling networks and are essential for efficient chloroplast biogenesis in Arabidopsis". In: *Plant Cell* 19.12, pp. 3944–60. ISSN: 1040-4651 (Print) 1040-4651 (Linking). DOI: 10.1105/tpc.107.054312. URL: https://www.ncbi.nlm.nih.gov/pubmed/18065688.

Rudella, A., G. Friso, J. M. Alonso, J. R. Ecker, and K. J. van Wijk (2006). "Downregulation of ClpR2 leads to reduced accumulation of the ClpPRS protease complex and defects in chloroplast biogenesis in Arabidopsis". In: *Plant Cell* 18.7, pp. 1704–21. ISSN: 1040-4651 (Print) 1040-4651 (Linking). DOI: 10.1105/tpc.106.042861. URL: https://www.ncbi.nlm.nih.gov/pubmed/16766689.

Ruiz-Sola, M. A. and M. Rodriguez-Concepcion (2012). "Carotenoid biosynthesis in Arabidopsis: a colorful pathway". In: *Arabidopsis Book* 10, e0158. ISSN: 1543-8120 (Electronic) 1543-8120 (Linking). DOI: 10.1199/tab.0158. URL: https://www.ncbi.nlm.nih.gov/pubmed/22582030.

Ruiz-Sola, M. A., D. Coman, G. Beck, M. V. Barja, M. Colinas, A. Graf, R. Welsch, P. Rutimann, P. Buhlmann, L. Bigler, W. Gruissem, M. Rodriguez-Concepcion,

and E. Vranova (2016). "Arabidopsis GERANYLGERANYL DIPHOSPHATE SYNTHASE 11 is a hub isozyme required for the production of most photosynthesis-related isoprenoids". In: *New Phytol* 209.1, pp. 252–64. ISSN: 1469-8137 (Electronic) 0028-646X (Linking). DOI: 10.1111/nph.13580. URL: https://www.ncbi.nlm.nih.gov/pubmed/26224411.

Saini, G., R. Meskauskiene, W. Pijacka, P. Roszak, L. L. Sjogren, A. K. Clarke, M. Straus, and K. Apel (2011). "'happy on norflurazon' (hon) mutations implicate perturbance of plastid homeostasis with activating stress acclimatization and changing nuclear gene expression in norflurazon-treated seedlings". In: *Plant J* 65.5, pp. 690–702. ISSN: 1365-313X (Electronic) 0960-7412 (Linking). DOI: 10.1111/j.1365-313X.2010.04454.x. URL: http://www.ncbi.nlm.nih.gov/pubmed/21208309.

Sakamoto, W., S. Y. Miyagishima, and P. Jarvis (2008). "Chloroplast biogenesis: control of plastid development, protein import, division and inheritance". In: *Arabidopsis Book* 6, e0110. ISSN: 1543-8120 (Linking). DOI: 10.1199/tab.0110. URL: https://www.ncbi.nlm.nih.gov/pubmed/22303235.

Saladie, M., L. P. Wright, J. Garcia-Mas, M. Rodriguez-Concepcion, and M. A. Phillips (2014). "The 2-C-methylerythritol 4-phosphate pathway in melon is regulated by specialized isoforms for the first and last steps". In: *J Exp Bot* 65.17, pp. 5077–92. ISSN: 1460-2431 (Electronic) 0022-0957 (Linking). DOI: 10.1093/jxb/eru275. URL: https://www.ncbi.nlm.nih.gov/pubmed/25013119.

Sauret-Gueto, S., P. Botella-Pavia, U. Flores-Perez, J. F. Martinez-Garcia, C. San Roman, P. Leon, A. Boronat, and M. Rodriguez-Concepcion (2006). "Plastid cues posttranscriptionally regulate the accumulation of key enzymes of the methylerythritol phosphate pathway in Arabidopsis". In: *Plant Physiol* 141.1, pp. 75–84. ISSN: 0032-0889 (Print) 0032-0889 (Linking). DOI: 10.1104/pp.106.079855. URL: http://www.ncbi.nlm.nih.gov/pubmed/16531478.

Schmitz-Linneweber, C. and I. Small (2008). "Pentatricopeptide repeat proteins: a socket set for organelle gene expression". In: *Trends Plant Sci* 13.12, pp. 663–70. ISSN: 1360-1385 (Print) 1360-1385 (Linking). DOI: 10.1016/j.tplants.2008.10.001. URL: https://www.ncbi.nlm.nih.gov/pubmed/19004664.

Schroda, M. (2004). "The Chlamydomonas genome reveals its secrets: chaperone genes and the potential roles of their gene products in the chloroplast". In: *Photosynth Res* 82.3, pp. 221–40. ISSN: 1573-5079 (Electronic) 0166-8595 (Linking). DOI: 10.1007/s11120-004-2216-y. URL: https://www.ncbi.nlm.nih.gov/pubmed/16143837.

Seemann, M., B. Tse Sum Bui, M. Wolff, M. Miginiac-Maslow, and M. Rohmer (2006). "Isoprenoid biosynthesis in plant chloroplasts via the MEP pathway: direct thylakoid / ferredoxin-dependent photoreduction of GcpE/IspG". In: *FEBS Lett* 580.6, pp. 1547–52. ISSN: 0014-5793 (Print) 0014-5793 (Linking). DOI: 10.1016/j.febslet.2006.01.082. URL: https://www.ncbi.nlm.nih.gov/pubmed/16480720.

Seo, J. and K. J. Lee (2004). "Post-translational modifications and their biological functions: proteomic analysis and systematic approaches". In: *J Biochem Mol Biol* 37.1, pp. 35–44. ISSN: 1225-8687 (Print) 1225-8687 (Linking). URL: https://www.ncbi.nlm.nih.gov/pubmed/14761301.

Seyffer, F., E. Kummer, Y. Oguchi, J. Winkler, M. Kumar, R. Zahn, V. Sourjik, B. Bukau, and A. Mogk (2012). "Hsp70 proteins bind Hsp100 regulatory M domains to activate AAA+ disaggregase at aggregate surfaces". In: *Nat Struct Mol Biol* 19.12, pp. 1347–55. ISSN: 1545-9985 (Electronic) 1545-9985 (Linking). DOI: 10.1038/nsmb.2442. URL: https://www.ncbi.nlm.nih.gov/pubmed/23160352.

Shi, L. X. and S. M. Theg (2010). "A stromal heat shock protein 70 system functions in protein import into chloroplasts in the moss Physcomitrella patens". In: *Plant Cell* 22.1, pp. 205–20. ISSN: 1532-298X (Electronic) 1040-4651 (Linking). DOI: 10.1105/tpc.109.071464. URL: https://www.ncbi.nlm.nih.gov/pubmed/20061551.

Shikanai, T., K. Shimizu, K. Ueda, Y. Nishimura, T. Kuroiwa, and T. Hashimoto (2001). "The chloroplast clpP gene, encoding a proteolytic subunit of ATP- dependent protease, is indispensable for chloroplast development in tobacco". In: *Plant Cell Physiol* 42.3, pp. 264–73. ISSN: 0032-0781 (Print) 0032-0781 (Linking). URL: https://www.ncbi.nlm.nih.gov/pubmed/11266577.

Singh, S. K., J. Rozycki, J. Ortega, T. Ishikawa, J. Lo, A. C. Steven, and M. R. Maurizi (2001). "Functional domains of the ClpA and ClpX molecular chaperones identified by limited proteolysis and deletion analysis". In: *J Biol Chem* 276.31, pp. 29420–9. ISSN: 0021-9258 (Print) 0021-9258 (Linking). DOI: 10.1074/jbc.M103489200. URL: https://www.ncbi.nlm.nih.gov/pubmed/11346657.

Sjogren, L. L. and A. K. Clarke (2011). "Assembly of the chloroplast ATP-dependent Clp protease in Arabidopsis is regulated by the ClpT accessory proteins". In: *Plant Cell* 23.1, pp. 322–32. ISSN: 1532-298X (Electronic) 1040-4651 (Linking). DOI: 10.1105/tpc.110.082321. URL: https://www.ncbi.nlm.nih.gov/pubmed/21266658.

Sjogren, L. L., T. M. MacDonald, S. Sutinen, and A. K. Clarke (2004). "Inactivation of the clpC1 gene encoding a chloroplast Hsp100 molecular chaperone causes growth retardation, leaf chlorosis, lower photosynthetic activity, and a specific reduction in photosystem content". In: *Plant Physiol* 136.4, pp. 4114–26. ISSN: 0032-0889 (Print) 0032-0889 (Linking). DOI: 10.1104/pp.104.053835. URL: https://www.ncbi.nlm.nih.gov/pubmed/15563614.

Sjogren, L. L., T. M. Stanne, B. Zheng, S. Sutinen, and A. K. Clarke (2006). "Structural and functional insights into the chloroplast ATP-dependent Clp protease in Arabidopsis". In: *Plant Cell* 18.10, pp. 2635–49. ISSN: 1040-4651 (Print) 1040-4651 (Linking). DOI: 10.1105/tpc.106.044594. URL: https://www.ncbi.nlm.nih.gov/pubmed/16980539.

Sjogren, L. L., N. Tanabe, P. Lymperopoulos, N. Z. Khan, S. R. Rodermel, H. Aronsson, and A. K. Clarke (2014). "Quantitative analysis of the chloroplast molecular

chaperone ClpC/Hsp93 in Arabidopsis reveals new insights into its localization, interaction with the Clp proteolytic core, and functional importance". In: *J Biol Chem* 289.16, pp. 11318–30. ISSN: 1083-351X (Electronic) 0021-9258 (Linking). DOI: 10.1074/jbc.M113.534552. URL: https://www.ncbi.nlm.nih.gov/pubmed/24599948.

Stanne, T. M., L. L. Sjogren, S. Koussevitzky, and A. K. Clarke (2009). "Identification of new protein substrates for the chloroplast ATP-dependent Clp protease supports its constitutive role in Arabidopsis". In: *Biochem J* 417.1, pp. 257–68. ISSN: 1470-8728 (Electronic) 0264-6021 (Linking). DOI: 10.1042/BJ20081146. URL: https://www.ncbi.nlm.nih.gov/pubmed/18754756.

Steinbacher, S., J. Kaiser, W. Eisenreich, R. Huber, A. Bacher, and F. Rohdich (2003). "Structural basis of fosmidomycin action revealed by the complex with 2-C-methyl-D-erythritol 4-phosphate synthase (IspC). Implications for the catalytic mechanism and anti-malaria drug development". In: *J Biol Chem* 278.20, pp. 18401–7. ISSN: 0021-9258 (Print) 0021-9258 (Linking). DOI: 10.1074/jbc.M300993200. URL: https://www.ncbi.nlm.nih.gov/pubmed/12621040.

Stern, D. B., M. Goldschmidt-Clermont, and M. R. Hanson (2010). "Chloroplast RNA metabolism". In: *Annu Rev Plant Biol* 61, pp. 125–55. ISSN: 1545-2123 (Electronic) 1543-5008 (Linking). DOI: 10.1146/annurev-arplant-042809-112242. URL: https://www.ncbi.nlm.nih.gov/pubmed/20192740.

Su, P. H. and H. M. Li (2008). "Arabidopsis stromal 70-kD heat shock proteins are essential for plant development and important for thermotolerance of germinating seeds". In: *Plant Physiol* 146.3, pp. 1231–41. ISSN: 0032-0889 (Print) 0032-0889 (Linking). DOI: 10.1104/pp.107.114496. URL: https://www.ncbi.nlm.nih.gov/pubmed/18192441.

Su, P. H. and H. M. Li (2010). "Stromal Hsp70 is important for protein translocation into pea and Arabidopsis chloroplasts". In: *Plant Cell* 22.5, pp. 1516–31. ISSN: 1532-298X (Electronic) 1040-4651 (Linking). DOI: 10.1105/tpc.109.071415. URL: https://www.ncbi.nlm.nih.gov/pubmed/20484004.

Sun, X., P. Feng, X. Xu, H. Guo, J. Ma, W. Chi, R. Lin, C. Lu, and L. Zhang (2011). "A chloroplast envelope-bound PHD transcription factor mediates chloroplast signals to the nucleus". In: *Nat Commun* 2, p. 477. ISSN: 2041-1723 (Electronic) 2041-1723 (Linking). DOI: 10.1038/ncomms1486. URL: http://www.ncbi.nlm.nih.gov/pubmed/21934661.

Sung, D. Y., E. Vierling, and C. L. Guy (2001). "Comprehensive expression profile analysis of the Arabidopsis Hsp70 gene family". In: *Plant Physiol* 126.2, pp. 789–800. ISSN: 0032-0889 (Print) 0032-0889 (Linking). URL: https://www.ncbi.nlm.nih.gov/pubmed/11402207.

Susek, R. E., F. M. Ausubel, and J. Chory (1993). "Signal transduction mutants of Arabidopsis uncouple nuclear CAB and RBCS gene expression from chloroplast development". In: *Cell* 74.5, pp. 787–99. ISSN: 0092-8674 (Print) 0092-8674 (Linking). URL: https://www.ncbi.nlm.nih.gov/pubmed/7690685.

Suss, K. H., C. Arkona, R. Manteuffel, and K. Adler (1993). "Calvin cycle multienzyme complexes are bound to chloroplast thylakoid membranes of higher plants in situ". In: *Proc Natl Acad Sci U S A* 90.12, pp. 5514–8. ISSN: 0027-8424 (Print) 0027-8424 (Linking). URL: https://www.ncbi.nlm.nih.gov/pubmed/11607406.

Swiatecka-Hagenbruch, M., C. Emanuel, B. Hedtke, K. Liere, and T. Borner (2008). "Impaired function of the phage-type RNA polymerase RpoTp in transcription of chloroplast genes is compensated by a second phage-type RNA polymerase". In: *Nucleic Acids Res* 36.3, pp. 785–92. ISSN: 1362-4962 (Electronic) 0305-1048 (Linking). DOI: 10.1093/nar/gkm1111. URL: https://www.ncbi.nlm.nih.gov/pubmed/18084023.

Tadini, L., P. Pesaresi, T. Kleine, F. Rossi, A. Guljamow, F. Sommer, T. Muhlhaus, M. Schroda, S. Masiero, M. Pribil, M. Rothbart, B. Hedtke, B. Grimm, and D. Leister (2016). "GUN1 Controls Accumulation of the Plastid Ribosomal Protein S1 at the Protein Level and Interacts with Proteins Involved in Plastid Protein Homeostasis". In: *Plant Physiol* 170.3, pp. 1817–30. ISSN: 1532-2548 (Electronic) 0032-0889 (Linking). DOI: 10.1104/pp.15.02033. URL: https://www.ncbi.nlm.nih.gov/pubmed/26823545.

Takechi, K., Sodmergen, M. Murata, F. Motoyoshi, and W. Sakamoto (2000). "The YELLOW VARIEGATED (VAR2) locus encodes a homologue of FtsH, an ATP-dependent protease in Arabidopsis". In: *Plant Cell Physiol* 41.12, pp. 1334–46. ISSN: 0032-0781 (Print) 0032-0781 (Linking). URL: https://www.ncbi.nlm.nih.gov/pubmed/11134419.

Tiller, N. and R. Bock (2014). "The translational apparatus of plastids and its role in plant development". In: *Mol Plant* 7.7, pp. 1105–20. ISSN: 1752-9867 (Electronic) 1674-2052 (Linking). DOI: 10.1093/mp/ssu022. URL: https://www.ncbi.nlm.nih.gov/pubmed/24589494.

Tiller, N., M. Weingartner, W. Thiele, E. Maximova, M. A. Schottler, and R. Bock (2012). "The plastid-specific ribosomal proteins of Arabidopsis thaliana can be divided into non-essential proteins and genuine ribosomal proteins". In: *Plant J* 69.2, pp. 302–16. ISSN: 1365-313X (Electronic) 0960-7412 (Linking). DOI: 10.1111/j.1365-313X.2011.04791.x. URL: https://www.ncbi.nlm.nih.gov/pubmed/21923745.

Trentini, D. B., M. J. Suskiewicz, A. Heuck, R. Kurzbauer, L. Deszcz, K. Mechtler, and T. Clausen (2016). "Arginine phosphorylation marks proteins for degradation by a Clp protease". In: *Nature* 539.7627, pp. 48–53. ISSN: 1476-4687 (Electronic) 0028-0836 (Linking). DOI: 10.1038/nature20122. URL: https://www.ncbi.nlm.nih.gov/pubmed/27749819.

Trowbridge, A. M., D. Asensio, A. S. Eller, D. A. Way, M. J. Wilkinson, J. P. Schnitzler, R. B. Jackson, and R. K. Monson (2012). "Contribution of various carbon sources toward isoprene biosynthesis in poplar leaves mediated by altered atmospheric

CO2 concentrations". In: *PLoS One* 7.2, e32387. ISSN: 1932-6203 (Electronic) 1932-6203 (Linking). DOI: 10.1371/journal.pone.0032387. URL: https://www.ncbi.nlm.nih.gov/pubmed/22384238.

Tryggvesson, A., F. M. Stahlberg, A. Mogk, K. Zeth, and A. K. Clarke (2012). "Interaction specificity between the chaperone and proteolytic components of the cyanobacterial Clp protease". In: *Biochem J* 446.2, pp. 311–20. ISSN: 1470-8728 (Electronic) 0264-6021 (Linking). DOI: 10.1042/BJ20120649. URL: https://www.ncbi.nlm.nih.gov/pubmed/22657732.

Tsai, J. and M. G. Douglas (1996). "A conserved HPD sequence of the J-domain is necessary for YDJ1 stimulation of Hsp70 ATPase activity at a site distinct from substrate binding". In: *J Biol Chem* 271.16, pp. 9347–54. ISSN: 0021-9258 (Print) 0021-9258 (Linking). URL: https://www.ncbi.nlm.nih.gov/pubmed/8621599.

Tseng, C. C., C. J. Lee, Y. T. Chung, T. Y. Sung, and M. H. Hsieh (2013). "Differential regulation of Arabidopsis plastid gene expression and RNA editing in non-photosynthetic tissues". In: *Plant Mol Biol* 82.4-5, pp. 375–92. ISSN: 1573-5028 (Electronic) 0167-4412 (Linking). DOI: 10.1007/s11103-013-0069-5. URL: https://www.ncbi.nlm.nih.gov/pubmed/23645360.

Van Wijk, K. J. (2015). "Protein maturation and proteolysis in plant plastids, mitochondria, and peroxisomes". In: *Annu Rev Plant Biol* 66, pp. 75–111. ISSN: 1545-2123 (Electronic) 1543-5008 (Linking). DOI: 10.1146/annurev-arplant-043014-115547. URL: https://www.ncbi.nlm.nih.gov/pubmed/25580835.

Vidi, P. A., M. Kanwischer, S. Baginsky, J. R. Austin, G. Csucs, P. Dormann, F. Kessler, and C. Brehelin (2006). "Tocopherol cyclase (VTE1) localization and vitamin E accumulation in chloroplast plastoglobule lipoprotein particles". In: *J Biol Chem* 281.16, pp. 11225–34. ISSN: 0021-9258 (Print) 0021-9258 (Linking). DOI: 10.1074/jbc.M511939200. URL: https://www.ncbi.nlm.nih.gov/pubmed/16414959.

Vidi, P. A., F. Kessler, and C. Brehelin (2007). "Plastoglobules: a new address for targeting recombinant proteins in the chloroplast". In: *BMC Biotechnol* 7, p. 4. ISSN: 1472-6750 (Electronic) 1472-6750 (Linking). DOI: 10.1186/1472-6750-7-4. URL: https://www.ncbi.nlm.nih.gov/pubmed/17214877.

Vranova, E., D. Coman, and W. Gruissem (2012). "Structure and dynamics of the isoprenoid pathway network". In: *Mol Plant* 5.2, pp. 318–33. ISSN: 1752-9867 (Electronic) 1674-2052 (Linking). DOI: 10.1093/mp/sss015. URL: https://www.ncbi.nlm.nih.gov/pubmed/22442388.

Vranova, E., D. Coman, and W. Gruissem (2013). "Network analysis of the MVA and MEP pathways for isoprenoid synthesis". In: *Annu Rev Plant Biol* 64, pp. 665–700. ISSN: 1545-2123 (Electronic) 1543-5008 (Linking). DOI: 10.1146/annurev-arplant-050312-120116. URL: https://www.ncbi.nlm.nih.gov/pubmed/23451776.

Wall, D., M. Zylicz, and C. Georgopoulos (1994). "The NH2-terminal 108 amino acids of the Escherichia coli DnaJ protein stimulate the ATPase activity of DnaK and are

sufficient for lambda replication". In: *J Biol Chem* 269.7, pp. 5446–51. ISSN: 0021-9258 (Print) 0021-9258 (Linking). URL: https://www.ncbi.nlm.nih.gov/pubmed/8106526.

Walley, Justin, Yanmei Xiao, Jin-Zheng Wang, Edward E. Baidoo, Jay D. Keasling, Zhouxin Shen, Steven P. Briggs, and Katayoon Dehesh (2015). "Plastid-produced interorgannellar stress signal MEcPP potentiates induction of the unfolded protein response in endoplasmic reticulum". In: *Proceedings of the National Academy of Sciences* 112.19, pp. 6212–6217. DOI: 10.1073/pnas.1504828112. URL: http://www.pnas.org/content/112/19/6212.abstract.

Wang, S., L. Yin, J. Mano, and K. Tanaka (2015). "Isolation of Chloroplast Inner and Outer Envelope Membranes". In: *Bio-protocol* 5.4, e1405. DOI: DOI:10.21769/BioProtoc.1405.

Winkel, B. S. (2004). "Metabolic channeling in plants". In: *Annu Rev Plant Biol* 55, pp. 85–107. ISSN: 1543-5008 (Print) 1543-5008 (Linking). DOI: 10.1146/annurev.arplant.55.031903.141714. URL: https://www.ncbi.nlm.nih.gov/pubmed/15725058.

Wright, L. P., J. M. Rohwer, A. Ghirardo, A. Hammerbacher, M. Ortiz-Alcaide, B. Raguschke, J. P. Schnitzler, J. Gershenzon, and M. A. Phillips (2014). "Deoxyxylulose 5-Phosphate Synthase Controls Flux through the Methylerythritol 4-Phosphate Pathway in Arabidopsis". In: *Plant Physiol* 165.4, pp. 1488–1504. ISSN: 1532-2548 (Electronic) 0032-0889 (Linking). DOI: 10.1104/pp.114.245191. URL: https://www.ncbi.nlm.nih.gov/pubmed/24987018.

Xiao, Y., T. Savchenko, E. E. Baidoo, W. E. Chehab, D. M. Hayden, V. Tolstikov, J. A. Corwin, D. J. Kliebenstein, J. D. Keasling, and K. Dehesh (2012). "Retrograde signaling by the plastidial metabolite MEcPP regulates expression of nuclear stress-response genes". In: *Cell* 149.7, pp. 1525–35. ISSN: 1097-4172 (Electronic) 0092-8674 (Linking). DOI: 10.1016/j.cell.2012.04.038. URL: https://www.ncbi.nlm.nih.gov/pubmed/22726439.

Yu, F., X. Liu, M. Alsheikh, S. Park, and S. Rodermel (2008). "Mutations in SUPPRESSOR OF VARIEGATION1, a factor required for normal chloroplast translation, suppress var2-mediated leaf variegation in Arabidopsis". In: *Plant Cell* 20.7, pp. 1786–804. ISSN: 1040-4651 (Print) 1040-4651 (Linking). DOI: 10.1105/tpc.107.054965. URL: http://www.ncbi.nlm.nih.gov/pubmed/18599582.

Zambrano, R., M. Jamroz, A. Szczasiuk, J. Pujols, S. Kmiecik, and S. Ventura (2015). "AGGRESCAN3D (A3D): server for prediction of aggregation properties of protein structures". In: *Nucleic Acids Res* 43.W1, W306–13. ISSN: 1362-4962 (Electronic) 0305-1048 (Linking). DOI: 10.1093/nar/gkv359. URL: https://www.ncbi.nlm.nih.gov/pubmed/25883144.

Zeidler, J., J. Schwender, C. Mueller, and H. K. Lichtenthaler (2000). "The non- mevalonate isoprenoid biosynthesis of plants as a test system for drugs against malaria and pathogenic bacteria". In: *Biochem Soc Trans* 28.6, pp. 796–8. ISSN: 0300-5127

(Print) 0300-5127 (Linking). URL: https://www.ncbi.nlm.nih.gov/pubmed/11171212.

Zhang, S., Y. Liu, and B. Yu (2014). "PRL1, an RNA-binding protein, positively regulates the accumulation of miRNAs and siRNAs in Arabidopsis". In: *PLoS Genet* 10.12, e1004841. ISSN: 1553-7404 (Electronic) 1553-7390 (Linking). DOI: 10.1371/journal.pgen.1004841. URL: https://www.ncbi.nlm.nih.gov/pubmed/25474114.

Zheng, B., T. Halperin, O. Hruskova-Heidingsfeldova, Z. Adam, and A. K. Clarke (2002). "Characterization of Chloroplast Clp proteins in Arabidopsis: Localization, tissue specificity and stress responses". In: *Physiol Plant* 114.1, pp. 92–101. ISSN: 1399-3054 (Electronic) 0031-9317 (Linking). URL: https://www.ncbi.nlm.nih.gov/pubmed/11982939.

Zheng, M., X. Liu, S. Liang, S. Fu, Y. Qi, J. Zhao, J. Shao, L. An, and F. Yu (2016). "Chloroplast Translation Initiation Factors Regulate Leaf Variegation and Development". In: *Plant Physiol* 172.2, pp. 1117–1130. ISSN: 1532-2548 (Electronic) 0032-0889 (Linking). DOI: 10.1104/pp.15.02040. URL: https://www.ncbi.nlm.nih.gov/pubmed/27535792.

Zolkiewski, M. (1999). "ClpB cooperates with DnaK, DnaJ, and GrpE in suppressing protein aggregation. A novel multi-chaperone system from Escherichia coli". In: *J Biol Chem* 274.40, pp. 28083–6. ISSN: 0021-9258 (Print) 0021-9258 (Linking). URL: https://www.ncbi.nlm.nih.gov/pubmed/10497158.

Zybailov, B., H. Rutschow, G. Friso, A. Rudella, O. Emanuelsson, Q. Sun, and K. J. van Wijk (2008). "Sorting signals, N-terminal modifications and abundance of the chloroplast proteome". In: *PLoS One* 3.4, e1994. ISSN: 1932-6203 (Electronic) 1932-6203 (Linking). DOI: 10.1371/journal.pone.0001994. URL: https://www.ncbi.nlm.nih.gov/pubmed/18431481.

Zybailov, B., G. Friso, J. Kim, A. Rudella, V. R. Rodriguez, Y. Asakura, Q. Sun, and K. J. van Wijk (2009). "Large scale comparative proteomics of a chloroplast Clp protease mutant reveals folding stress, altered protein homeostasis, and feedback regulation of metabolism". In: *Mol Cell Proteomics* 8.8, pp. 1789–1810. ISSN: 1535-9484 (Electronic) 1535-9476 (Linking). DOI: 10.1074/mcp.M900104-MCP200. URL: https://www.ncbi.nlm.nih.gov/pubmed/19423572.

8. Publications

Published

- Perello C, **Llamas E**, Burlat V, Ortiz-Alcaide M, Phillips MA, Pulido P, Rodriguez -Concepcion M (2016) Differential Subplastidial Localization and Turnover of Enzymes Involved in Isoprenoid Biosynthesis in Chloroplasts. PLOS One. 11 (2):e0150539. doi:10.1371/journal.pone.0150539

- Pulido P, **Llamas E**, Llorente B, Ventura S, Wright LP, Rodriguez-Concepcion M (2016) Specific Hsp100 Chaperones Determine the Fate of the First Enzyme of the Plastidial Isoprenoid Pathway for Either Refolding or Degradation by the Stromal Clp Protease in Arabidopsis. PLOS Genetics. 12 (1):e1005824. doi:10.13 71/journal.pgen.1005824

- Pulido P, **Llamas E**, Rodriguez-Concepcion M (2017) Both Hsp70 chaperone and Clp protease plastidial systems are required for protection against oxidative stress. Plant signaling & behavior. 12 (3):e1290039. doi:10.1080/15592324. 2017.1290039

Under review

- **Llamas E**, Pulido P, Rodriguez-Concepcion M. Interference with plastome gene expression in Arabidopsis triggers an unfolded protein response that promotes accumulation of active isoprenoid biosynthetic enzymes in chloroplasts. PLOS Genetics.

- D'Andrea L, Simon-Moya M, Llorente B, **Llamas E**, Marro M, Loza-Alvarez P, Yang Y, Fish T, Thannhauser T W, Li L, Rodriguez-Concepcion M. A role for the Clp protease in chromoplast differentiation and carotenoid accumulation during tomato fruit ripening. The Plant Journal.